Modern Adaptive Protection and Control Techniques for Enhancing Distribution Grid Resiliency

Tapas Kumar Barik

Dissertation submitted to the Faculty of the

Virginia Polytechnic Institute and State University

in partial fulfillment of the requirements for the degree of

Doctor of Philosophy

in

Electrical Engineering

Virginia A. Centeno, Chair

Jamie DeLaRee Lopez

Chen-Ching Liu

William T. Baumann

Steve C. Southward

May 10, 2021

Blacksburg, Virginia

Keywords: Adaptive protection, Power distribution systems, Islanding, Loss of mains, Protective devices, Critical load shedding, Voltage sensitivities, Optimal relay coordination

Modern Adaptive Protection and Control Techniques for Enhancing Distribution Grid Resiliency

Tapas Kumar Barik

(ABSTRACT)

Power distribution systems have underwent a lot of significant changes in the last two decades. Wide-scale integration of Distributed Energy Resources (DERs) have made the distribution grid more resilient to abnormal conditions and severe weather induced outages. These DERs enhance the reliability of the system to bounce back from an abnormal situation rather quickly. However, the conventional notion of a radial system with unidirectional power flow does not hold true due to the addition of these DERs. Bidirectional power flow has challenged the conventional protection schemes in place. The most notable effects on the protection schemes can be seen in the field of islanding or Loss of Mains(LOM) detection and general fault identification and isolation. Adaptive protection schemes are needed to properly resolve these issues. Although, previous works in this field have dealt with this situation, a more comprehensive approach needs to be taken considering multiple topologies for developing adaptive protection schemes. The most common protective devices widely deployed in the distribution system such as overcurrent relays, reverse power relays at Point of Common Coupling(PCC), fuses, reclosers and feeder breakers need to studied in implementing these schemes.

The work presented in this dissertation deals with simulation based and analytical approaches to tackle the issues of islanding and adaptive protection schemes. First we propose a multi-principle passive islanding detection technique which relies on local PCC measurements, thus reducing the need of additional infrastructure and still ensuring limited Non Detection Zone

(NDZ). The next step to islanding detection would be to sustain a islanded distribution system in order to reduce the restoration time and still supply power to critical loads. Such an approach to maintain generator load balance upon islanding detection is studied next by appropriate shedding of non-critical and low priority critical loads based upon voltage sensitivity analysis. Thereafter, adaptive protection schemes considering limited communication dependency is studied with properly assigning relay settings in directional overcurrent relays (DOCRs), which are one of the most widely deployed protective devices in distribution systems by catering to multiple topologies and contingencies. A simulation based technique is discussed first and then an analytical approach to solve the conventional optimal relay coordination problem using Mixed Integer Linear Programming (MILP) with the usage of multiple setting groups is studied. All these approaches make the distribution more robust and resilient to system faults and ensure proper fault identification and isolation, ensuring overall safety of system.

Modern Adaptive Protection and Control Techniques for Enhancing Distribution Grid Resiliency

Tapas Kumar Barik

(GENERAL AUDIENCE ABSTRACT)

With widespread integration of inverter-based distributed energy resources (DERs) in the distribution grid, the conventional protection and control schemes no longer hold valid. The necessity of an adaptive protection scheme increases as the DER penetration in the system increases. Apart from this, changes in system topology and variability in DER generation, also change the fault current availability in the system in real-time. Hence, the protection schemes should be able to adapt to these variations and modify their settings for proper selectivity and sensitivity towards faults in the system, especially in systems with high penetration of DERs. These protection schemes need to be modified in order to properly identify and isolate faults in the network as well as correctly identify Loss of Mains (LOM) or islanding phenomenon. Special attention is needed to plan the next course of action after the islanding occurence. Additionally, the protective devices in distribution system should be utilized to their maximum capability to create an adaptive and smart protection system. This document elaborately explains the research work pertaining to these areas.

Dedication

To my parents who have provided me strength and motivation in every stage of my life.

Acknowledgments

First and foremost, I would like to express my heartfelt gratitude to my advisor and chair Dr. Virgilio Centeno who provided me with the opportunity to explore topics of my interest and has always pushed me towards excellence. Without his guidance and supervision, this work would not have been possible. His insights on distribution system protection and utility grade protection systems helped me to grasp the basic nuances of this work and grow as a student. His motivation to make me think out of the box yet relate my work such that it can be practical and easily implementable in the power system community has been the source of continuous persistence of my research work.

I would like to thank Dr. Jamie DeLaRee Lopez and Dr. Chen-Ching Liu, who provided a perfect learning environment to set a foundation and strengthen my concepts in basic power system fundamentals which underpinned several parts of this dissertation. I feel really obliged having learnt so many aspects of my field of study during their lectures. I would also like to acknowledge my committee members Dr. William T. Baumann and Dr. Steve C. Southward, for providing insightful comments and suggestions aimed to increase the quality of my work.

Additionally, I would also want to express my gratitude to Dr. Francisco Velez-Cedeno from Dominion Energy Virginia who guided me through the initial phase of my work and whose endless discussions on this topic helped me to transform my work from conception to reality. His expertise in power system protection devices and the current practices in the power utilities led to my initial motivation to pursue this field of work.

I would also like to thank my parents who have been the constant source of inspiration to me, who have never lost their faith in me and always encourage me to pursue excellence in

life, both personal and professional. The virtues instilled in me by them has made me the person I am today. I would also like to thank my brother who had always believed in me and supported me in all my endeavors.

Finally, I would like to extend my thanks to my friends- Piyush, Manish, Sarthak, Kunal, Mayank and Vamsi who have filled my life with innumerable instances of memorable hangouts to cherish. During the course of my stay at Blacksburg, these special people have been my second family far away from home. I really appreciate for all their personal and professional guidance, which steered the course of this work in a positive direction for the past several years

Contents

List of Figures

List of Tables

Chapter 1

Introduction

1.1 Background & Motivation

Power distribution system has underwent a significant number of changes in the last 1-2 decades. The conventional distribution system had a radial structure with unidirectional flow of power supplying electricity from the power utility side to the consumer side. However, with the current wide scale integration of the Distributed Energy Resources (DERs) which may include Diesel Generators(DGs), Inverter-based Distributed Generators (IBDGs), the earlier notion of unidirectional flow of power doesn't hold true anymore as can be explained referring to Fig. 1.1.

For a fault F_1 in the feeder section BC, fault current provided by the DERs situated at buses E, G, H and I needs to be accounted for. This situation changes the fault current level of the system and also calls for the need of additional protective devices which can properly detect and isolate the fault from the consumer side as well. Hence, there is a huge need for modifying the traditional protection schemes to adapt to the changing distribution system scenarios. The two major aspects that needs utmost attention while designing adaptive protection schemes include:

- Islanding or Loss of Mains (LOM) detection.
- Fault detection and isolation.

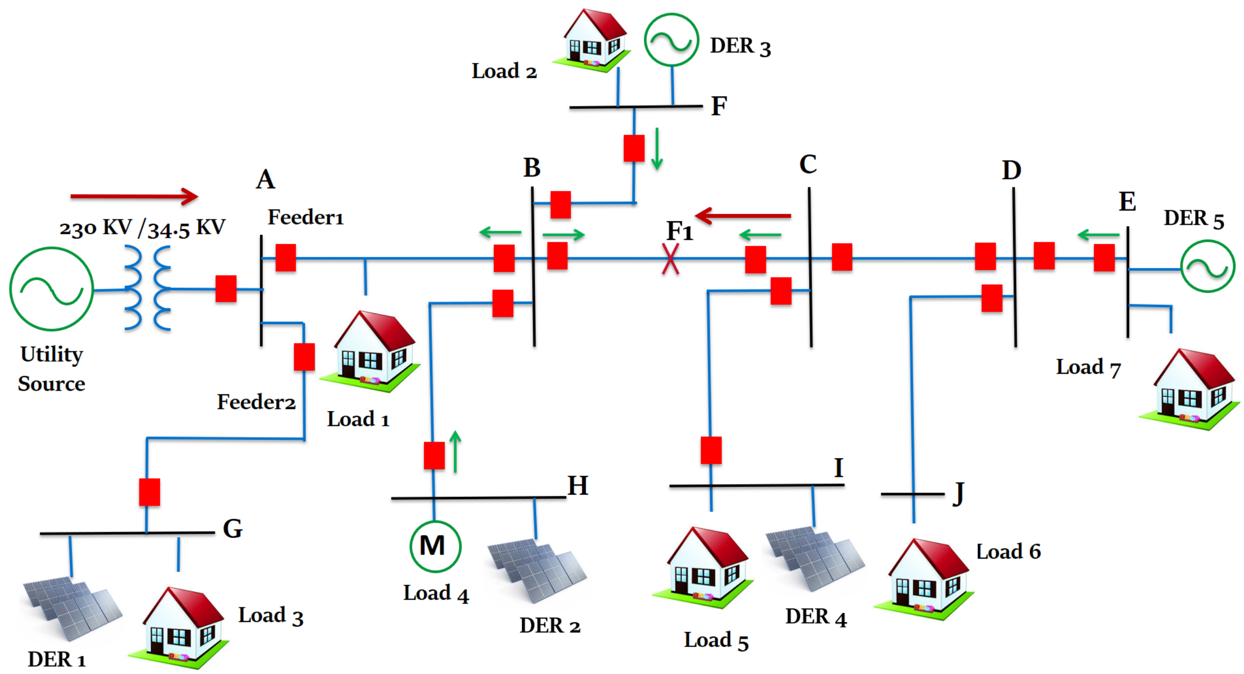

Figure 1.1: Typical distribution system with bi-directional flow of power

These issues need to be dealt with to design an efficient adaptive protection scheme and serve as the center focus of this dissertation. The following subsections deal with the challenges associated with each aspect.

1.1.1 Islanding or Loss of Mains Issues

Islanding [12] refers to a condition where a portion of the power system that contains utility served loads and on site DERs remain energized but is electrically isolated from the rest of the utility system.This condition can occur due to many typical reasons as listed below:

- Disturbance in utility system due to faults or wide fluctuations in frequency/voltage caused by real/reactive power mismatch.
- Intentional/Nuisance tripping of up-line Utility devices (Feeder breaker/ Line Re-

closer).

However, the power utility might have different approaches to handle this issue. These are divided into two categories primarily. The first approach can be intentional islanding where the utility might desire to have the islanded system to self-sustain as in case of Microgrids in order to serve critical loads likes hospitals, important buildings or military bases. The alternate approach refers to unintentional islanding. As the name suggests, the utility doesn't desire the islanded system to self-sustain and hence proper identification of island is of utmost concern as there are certain concerns with unintentional islanding as described below:

- Endangering the safety of utility/non-utility personnel.
- Power quality issues in terms of voltage and frequency.
- Protection scheme mis-coordination due to drastic change in short-circuit current availability.
- Improper grounded island system by the DER posing huge overvoltage issues.
- Out of Step automatic reclosing causing high electrical torque which translates to stress on the mechanical shaft of the rotating equipment.

Hence, in order to properly identify islanding conditions there are several methods commonly used in electric power systems which are broadly classified in various categories such as:

A. Active Methods:

These methods introduce deliberate changes or disturbances to the connected circuit and monitor the response. The principle relies on the fact that, for the same change or disturbance applied, the islanded system will act or respond differently than when the same system is connected with the utility or grid. Common methods [14]-[21] are:

- Slip-mode frequency shift
- Frequency bias
- Sandia frequency shift
- Sandia voltage shift

B. Passive Methods:

These methods only rely upon the local measurements at the location of the protective device and do not modify or introduce any changes in the system. Common passive islanding detection methods[22]-[29] include:

- Under/Over voltage
- Under/Over frequency
- Voltage phase shift
- Fast rate of change of frequency
- Reverse Power (RP) for non-exporting DERs

C. Topology or Communication Based methods:

These methods communicate the status of the upline utility device to the downline protective device and during islanding condition, trips the point of common coupling breaker in order to prevent islanding. The medium of communication might vary from system to system.Some of the most common methods currently implemented in the system include:

- Direct Transfer Trip (DTT)
- Power Line Carrier Communication (PLCC)

- Power line signalling scheme

Figure. 1.2 summarizes the various categories of detection methods as described above.

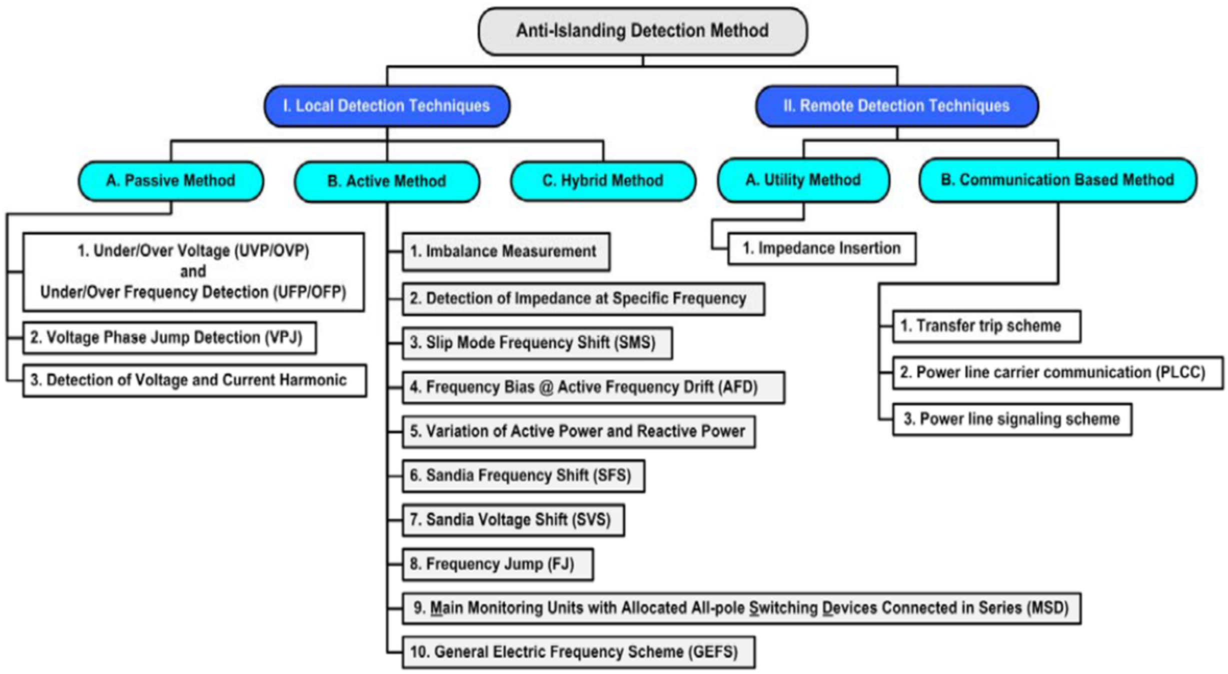

Figure 1.2: Different types of Islanding detection techniques utilized in power utilities

However, the issues faced with the above methods is what motivated the course of the research work outlined in this document. The issues pertaining to the various schemes are listed below:

a) Communication based schemes like the Transfer Trip:

They incur huge infrastructural costs or huge installation costs. On top of that, these schemes depend heavily on the reliability of the communication medium. And finally these schemes are prone to nuisance tripping of up-line utility device (although the probability might be less). But as they only rely upon the status of upline utility device, there is need to use methods which are local and reliable.

b) Dead line reclosing scheme:

This scheme requires additional voltage permissive feature to be included in the device and moreover this scheme actually doesn't detect islanding. It rather prevents out of step reclosing ensuring that the utility doesn't try to synchronize back to the islanded system. If Live line reclosing is allowed, an additional synch check relay element (American National Standards Institute (ANSI) code 25) needs to be included in the recloser adding to cost and complexity.

c) Passive detection scheme:

Normally, issues arise when "local load to generation power ratio" is close to 1.5-2 and thus, the conventional elements do not usually pickup for a small change. Moreover, for cases when reverse power relays are used, they only work effectively for non-exporting DERs. Finally the most important issue of using passive detection methods is their large Non Detection zone (NDZ) which is an indicator of the efficiency of the islanding detection scheme. Hence, smaller the NDZ, better the scheme.

The work in the initial phase of the research outlined in this document tries to tackle these challenges and provide some adaptive protection techniques pertaining to islanding detection and sustenance with minimum dependency on the communication network.

1.1.2 Fault isolation and detection issues

As the percentage of DER penetration in the system increases, the necessity of an adaptive protection scheme increases as the operating scenarios are becoming more complicated, which may cause the short-circuit currents flowing through local relays to vary frequently. Additionally, fault current availability in the system dynamically changes in real-time with changes in operating conditions. These conditions primarily refer to changes in the topology or connection status of DERs in the system. Many prior works have discussed the concept of adaptive protection addressing these issues. Voltage and impedance-based protection schemes were proposed in [54],[55]. Several adaptive overcurrent (OC) protection schemes [56],[57] were proposed to modify the setting values for local relays by utilizing the high-speed communication networks and employing numerous fault analysis techniques.

Most of these methods rely on the proper operation of the control center. The changing topology of the system is monitored at the Distribution Management System (DMS) of the power utility company by acquiring the status of circuit breakers as well as the connection status of DERs. Based on this information, appropriate adaptive settings of the overcurrent relays are calculated and transmitted back to the modern digital relays via communication links. However, in case of severe weather-induced outages, communication networks might not be functional, and hence, a centralized adaptive protection scheme cannot always be deemed reliable. Previous works [57]-[59] have addressed this issue by proposing peer-to-peer communication within protective devices, making the adaptive protection scheme somewhat decentralized. However, considering the present level of communication infrastructure in most of the distribution systems operated by the utilities around the world, these schemes might not be easily implementable shortly.

Digital microprocessor-based relays consist of multiple setting group (SG) functionality, which has been one of the basis to design many adaptive schemes in the past [72],[73]. These setting groups may correspond to multiple operating conditions of the system, ensuring proper selectivity and sensitivity of the relay with only one SG being active at one time. Pertaining to numerous possible topologies of the system, suitable relay settings can be computed offline and stored as a separate, distinct setting group. Subsequently, detecting any change in the topology of the network by the DMS, the corresponding SG can be activated on the relay, thus lessening the amount of information to be transmitted back to the relay. The drawback of this method is that the modern commercial relays only allow a limited number of SGs to be stored in them, which is far lesser than the total number of possible system topologies and hence, needs to be classified. However, these capabilities are not exploited to the fullest and hence, can be utilized to enhance the sensitivity and selectivity of relays towards fault identification and isolation. Multiple versatile settings can be stored to improve relay observability towards faults and hence, these aspects of finding the appropriate setting groups in protective relays in the power distribution system guided the course of the later part of the research work.

1.2 Outline of the Dissertation

Chapter 2 presents a comparative analysis between the performance and feasibility of directional overcurrent (DOC) and reverse power relays to identify faults at the PCC when DERs are present in the distribution circuit. This work uses hardware-in-the-loop (HIL) technology to combine a relay with a custom distribution circuit modelled in RSCAD to test various types of faults at different locations down-line of the distribution substation. The results are showcased along with a comparative study at the end explaining the delineation of the functionalities of both elements

In Chapter 3, a multi-principle passive islanding detection technique based upon the rate of change of voltage (ROCOV) measurements and 3-phase active power mismatch at the PCC is proposed. Such a method is easier to implement, requires no additional infrastructure (for communication) or equipment installation cost, and has a smaller NDZ as compared to individual passive schemes. The effectiveness of the technique is validated on a synthetic distribution model consisting of DERs (both conventional and inverted-based), using commercially available protective relays and performing Hardware-in-the-loop (HIL) testing using the Real-Time Digital Simulator (RTDS). The proposed method is a viable option in reducing the dependency on communication-based schemes.

Chapter 4 discusses the possibility of sustaining a power distribution system upon the occurrence of an island whenever the load inside the island surpasses the total generation available (implying negative Rate of Change of Frequency or ROCOF) by maintaining the power balance with the help of a Critical Load Shedding Module (CLSM). It also discusses about a synchrophasor-based substation topology estimation technique which could potentially aid the CLSM to make informed decisions regarding the status of the feeder breakers, thus aiding in deducing the topology of the system.

Chapter 5 proposes a decentralized Multi-setting adaptive protection technique by utilizing the commonly used protective devices such as DOCRs in the power distribution systems and storing versatile setting groups enabling better observability of the relays towards fault identification and isolation in the absence of extensive communication links.

Chapter 6 proposes a K-medoids clustering technique to properly decide the relay settings of DOCRs in distribution systems catering to multiple topologies using the multi-setting group storage functionality of such modern relays.

Chapter 7 proposes an Mixed Integer Linear Programming (MILP) formulation of the optimal relay coordination problem considering multiple setting groups as well as catering to multiple topologies, thus presenting an analytical approach to decide the various relay settings of DOCRs in distribution systems.

Chapter 8 concludes the dissertation and summarizes the work completed highlighting the main contributions along with remarks. It also discusses the future work as an extension to this research work and recommends several other ideas for expansion of various topics.

Chapter 2

A Comparative Study of the Reliability of Reverse Power and Directional Overcurrent Elements for Distribution Level Fault Identification

2.1 Details of the publication

Co-authors: Kevin M. Phelps, Joseph J. Petti and Francisco Velez-Cedeno.[1]

Reference [10]**:** T. K. Barik, K. M. Phelps, J. J. Petti, and F. Velez-Cedeno, "A comparative study of the reliability of reverse power and directional overcurrent elements for distribution level fault identification," in *2018 Grid of the Future colloquia, Reston,VA*, , 2018.

[1]The co-authors have contributed in the simulation and testing during the HIL setup

2.2 Abstract

The power distribution system is rapidly undergoing changes with increasing penetration of Distributed Energy Resources (DERs) at the consumer end. This changes the earlier notion of unidirectional flow of power i.e. from the utility end to the consumer end. For this reason, conventional protection schemes need to undergo modifications in order to be able to trip DERs in the case of faults upstream of the Point of Common Coupling (PCC). Failure to trip before the open period of the upstream recloser might lead to out of step reclosing. This phenomenon can cause damage to utility served load due to high electromagnetic transients and is also a potential safety hazard for personnel. In order to achieve proper coordination, certain protective functions need to be put in place by the consumer installing the DERs, as required by the utility. Two of such functions are the Directional Overcurrent (DOC) element, ANSI/IEEE code-67, and the Reverse Power element (RP), ANSI/IEEE code-32R. The DOC element is primarily used to detect faults upstream of the PCC and is primarily used for feeder protection. The RP element is used to detect any abnormal reversal of power flow that may result due to sudden generation loss from the utility side or islanding scenarios[1]. This chapter presents a comparative analysis between the performance and feasibility of DOC and RP elements to identify faults at the PCC when DERs are present in the distribution circuit. This work uses hardware-in-the-loop (HIL) technology to combine a relay with a custom distribution circuit modelled in RSCAD software to test various types of faults at different locations down-line of the distribution substation. The results are showcased along with a comparative study at the end explaining the delineation of the functionalities of both elements.

2.3 Introduction

One of the most important aspects of power system planning and operation is the design of proper and reliable protection schemes. Protection scheme design used to be straightforward, as distribution systems were based upon radial power flow from the utility to the consumer. However, the emergence of consumers DERs has created a new challenge for protection engineers. Properly ensuring reliability and preventing mis-operation of the protective equipment is no longer the commonplace task it once was. DERs are sources of energy located on the load side of the Point of Common Coupling (PCC). Parallel connection of DER to the utility warrants certain protection schemes to be installed at the PCC for the safety of various electrical equipment as well as utility/non-utility personnel. Improper protection design might lead to faults not being cleared, which can cause tremendous destructive energy in the form of heat and magnetic forces. This can heavily damage electrical equipment and endanger utility/non-utility personnel safety. Directional protection schemes are integral to achieving such a desired performance. Directional protection enables the utility to better identify the location of the fault than simply overcurrent protection. It is mostly used in the following conditions [2],[3]:

- Multi-source power distribution systems
- Closed loop or parallel-cabled systems
- Isolated neutral systems for the feedback of capacitive currents
- To detect an abnormal direction of flow of active or reactive power

The directional element uses phase angle displacement between the current phasor of a particular phase and the reference variable to determine the directionality (forward or reverse). In other words, the directional element relies upon the direction of a reference variable to determine the direction of current[5]. This reference variable is called the polarization quantity and can be either a voltage or current phasor. The DOC relay, combines directionality with the standard overcurrent element.

The reverse power relay, is also a directional protection element that relies upon both voltage and current values to determine reversal of power. The applications for RP relay are mostly confined to detecting abnormal reversal of power for a Non-exporting DER at the PCC during sudden loss of generation at the utility side or Loss of Mains (LOM) situation[6]-[8]. However, the feasibility of using the RP element to detect faults has always been a question. This chapter answers that question by providing a comparative analysis of the 67 and 32R elements for fault identification. A comprehensive comparison of the two protection techniques was completed by placing various faults at numerous locations in a relatively complex RSCAD model. This RSCAD model was then combined with a relay via Real Time Digital Simulator (RTDS) Hardware-in-the-Loop (HIL) technology.

Section 2.4 discusses about setting up the test bench and building the custom model. Section 2.5 discusses about the testing and actual results obtained, and finally, section 2.6 summarizes the conclusions drawn from the overall study and a brief scope of the future work possible as an extension to this chapter.

2.4 Layout of test Bench Setup

A custom distribution circuit model was created in RSCAD to simulate actual fault conditions, as shown in Fig. 2.1

The system consists of the power utility side modelled as an infinite grid, capable of maintaining constant voltage and frequency. At the distribution substation, two feeders emerge

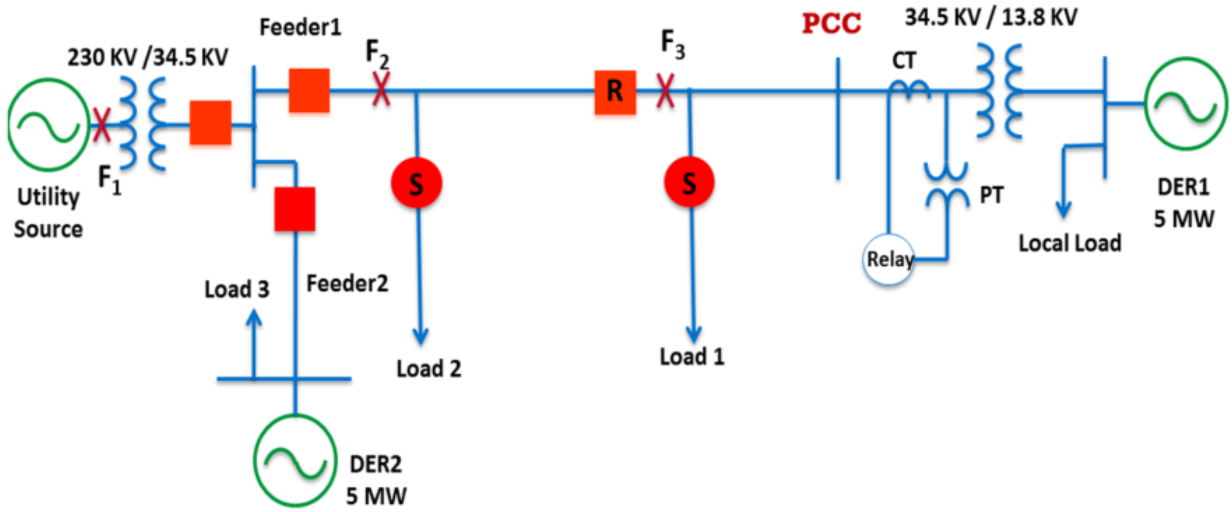

Figure 2.1: Custom distributed energy system model

to supply power to two separate circuits. The parameters of the feeders, line equipment, and transformers were designed with Dominion Energy system(an USA based utility) models as reference in order to replicate practical scenarios and performance. The relay under consideration is situated at the PCC of DER_1, which is connected at the end of Feeder-1 as shown in Fig. 2.1. In order to perform a more comprehensive analysis, two DERs were connected in the system and the performance of the relay in presence or absence of the DER_2 (at the end of Feeder-2) was also studied. Both DERs are modelled as synchronous machines. Faults were placed at various locations, F_1, F_2, and F_3, to carry out the comparative studies, as shown in Fig. 2.1.

By using RTDS HIL technology, a custom made RSCAD model, and a commercial relay, realistic simulations were run for different fault scenarios with different parameters. The RTDS system was connected to a Doble amplifier that generated the required analog signals to emulate the secondary voltages and currents of the potential transformers(PT) and Current transformer(CT) which were sent to a microprocessor relay. The relay then sent the DOC and RP pickup output signals to the RTDS and the results were compared on a single graph within the RSCAD software. This allowed for easy comparison of the two elements, allowing the formulation of the conclusions shown in later sections.

2.5 Results and Discussion

Different types of faults,such as single phase to ground ($1\phi - G$) and 3 phase to ground($3\phi - G$), were placed at the various locations along the feeder as shown in Fig. 2.1. The fault impedance (Z) is also varied in order to simulate bolted faults (Low Z), and high impedance (High Z) faults in order to show how the performance of both the elements would vary under various circumstances. Table 2.1 & 2.2 present the results of this work. Column 1 shows the location and type of fault, while columns 2 and 3 show the DOC and RP elements pick up status, respectively. To illustrate the results, Figs. 2.2 - 2.4 show three specific scenarios that give greater insight into the capability of both elements: High impedance 3-phase to ground fault at F_1 with both DERs in service, bolted 3-phase to ground fault at F_1 with both DERs in service, and high impedance phase to ground fault at F_2 with both DERs in service.

The DOC element picks up for all scenarios as each scenario elicits a current response from the DG above the set pick up level. The RP element is only able to sense the high impedance 3-phase to ground faults. This is because the terminal voltage reduction is not substantial, allowing a significant amount of reverse power to be seen by the relay. The RP element does not pick up for the majority of the scenarios because of two reasons: the voltage drop is too low and the power output is negligible or the fault does not affect all three phases and the 3 phase output power does not substantially change.

Fig. 2.2 sub-figures(a)-(d) show the 3-phase current (in KA), 3-phase voltage (in KV), DER_1

Table 2.1: Performance of DOC and RP elements to faults in various conditions with DER_2 connected

Low Z faults		Directional OC Pickup(67)	Reverse power pickup (32R)
F_1	$3\phi - G$	Yes	No
F_1	$1\phi - G$	Yes	No
F_2	$3\phi - G$	Yes	No
F_2	$1\phi - G$	Yes	No
F_3	$3\phi - G$	Yes	No
F_3	$1\phi - G$	Yes	No
High Z faults		Directional OC Pickup(67)	Reverse power pickup (32R)
F_1	$3\phi - G$	Yes	Yes
F_1	$1\phi - G$	Yes	No
F_2	$3\phi - G$	Yes	Yes
F_2	$1\phi - G$	Yes	No
F_3	$3\phi - G$	Yes	Yes
F_3	$1\phi - G$	Yes	No

Table 2.2: Performance of DOC and RP elements to faults in various conditions without DER_2 connected

Low Z faults		Directional OC Pickup(67)	Reverse power pickup (32R)
F_1	$3\phi - G$	Yes	No
F_1	$1\phi - G$	Yes	No
F_2	$3\phi - G$	Yes	No
F_2	$1\phi - G$	Yes	No
F_3	$3\phi - G$	Yes	No
F_3	$1\phi - G$	Yes	No
High Z faults		Directional OC Pickup(67)	Reverse power pickup (32R)
F_1	$3\phi - G$	Yes	Yes
F_1	$1\phi - G$	Yes	No
F_2	$3\phi - G$	Yes	Yes
F_2	$1\phi - G$	Yes	No
F_3	$3\phi - G$	Yes	Yes
F_3	$1\phi - G$	Yes	No

3-phase real power generation (DG1P in MW) and 3-phase real power flow (RealP in MW) at the PCC, and the relay's pick up outputs (either 0 or 1) respectively. The high impedance fault does not cause the voltage to collapse to 0V so reverse power can be seen by the relay. The current rises due to the fault so adequate power and current is seen by the relay, leading

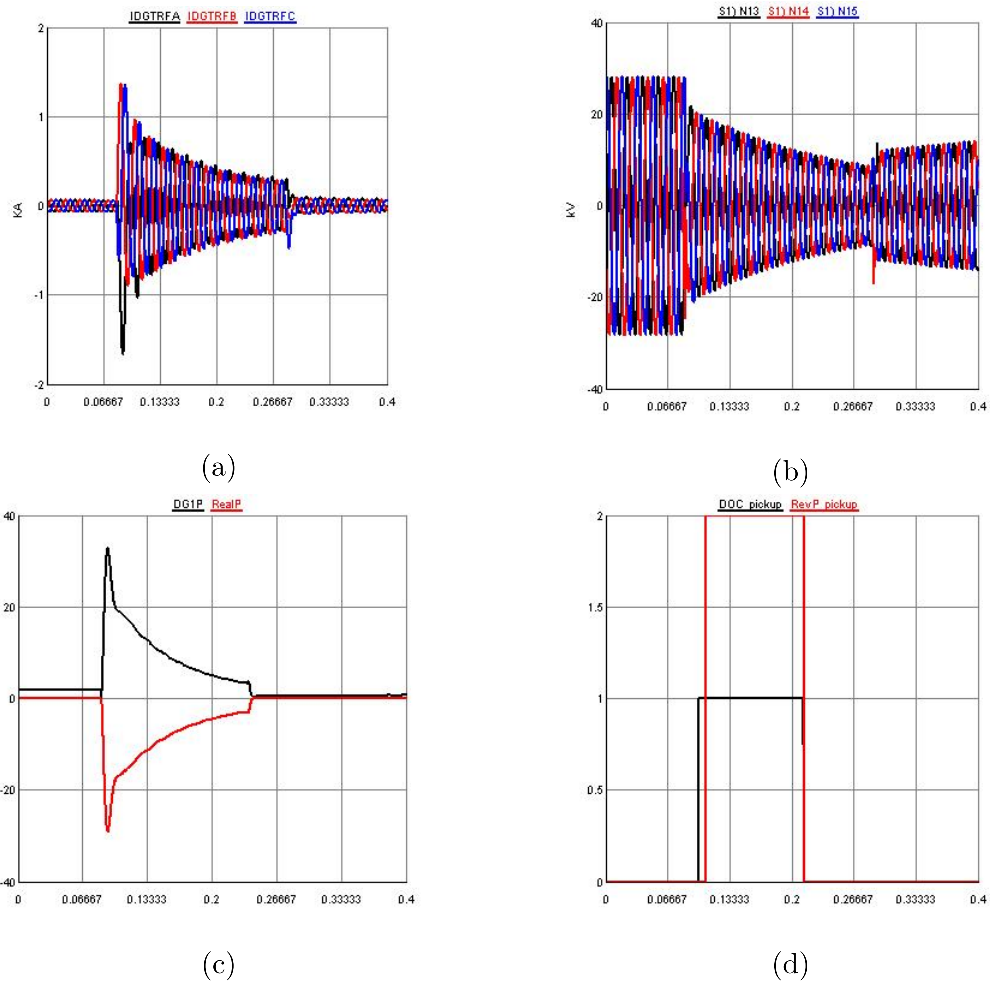

Figure 2.2: High impedance 3-phase to ground fault at F1 with both DERs in service

to both elements picking up.

The same parameters are shown in Fig. 2.3's sub-figures. In this case, the bolted fault causes a sudden steep reduction in voltage, therefore reverse power flowing is negligible even though the current increases greatly. The DOC element picks up due to the large increase in current but the RP element is blinded due to lack of voltage.

Similarily, in case of Fig. 2.4's sub-figures, it can be noticed that the high impedance fault does not cause the voltage to collapse to 0V so reverse power could have been seen by the relay. But, the single phase to ground fault only causes power in one phase to reverse

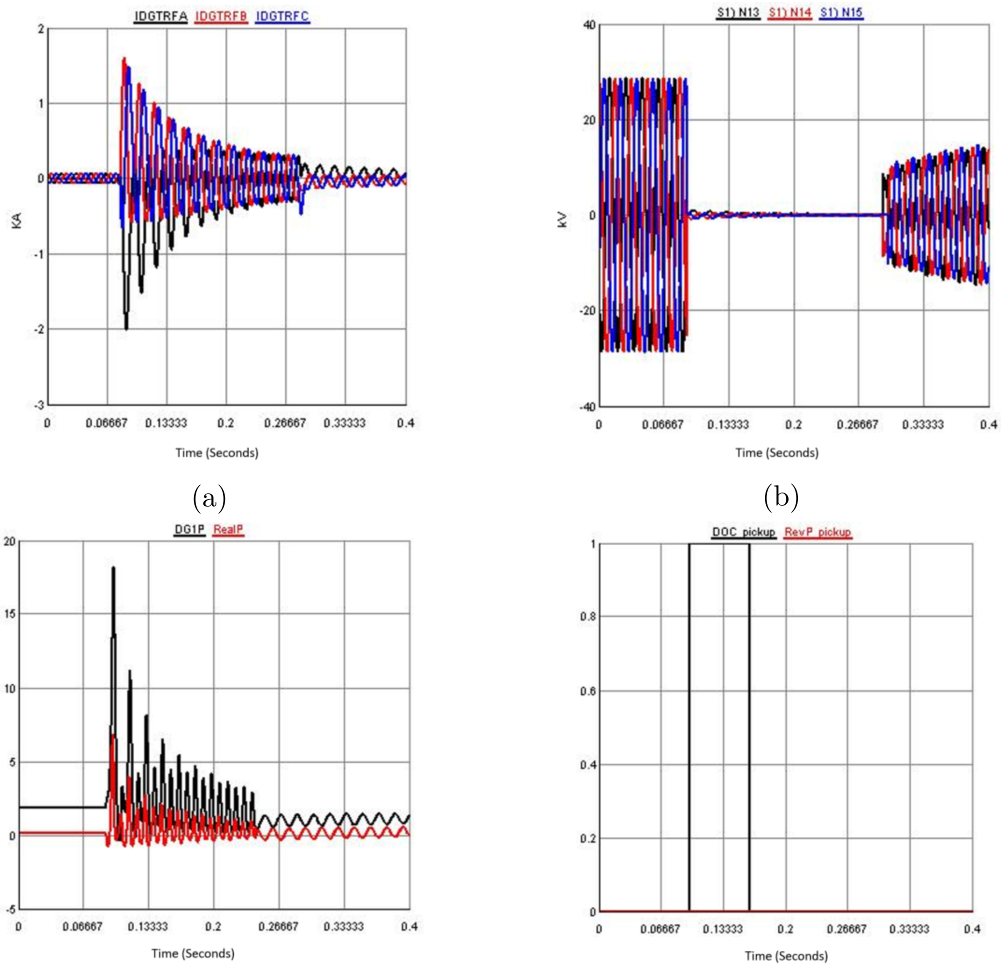

(a) (b) (c) (d)

Figure 2.3: Bolted 3 phase to ground fault at F1 with both DERs in service

directions. Even though the power flow of A phase is the in reverse direction, the overall 3 phase power is still considered to be in the forward direction as the sudden loss of one phase leads to more current being drawn in the other two phases to meet the demand of the loads. Therefore, the RP element does not pick up. However, the DOC element does pick up due to the increased current magnitude.

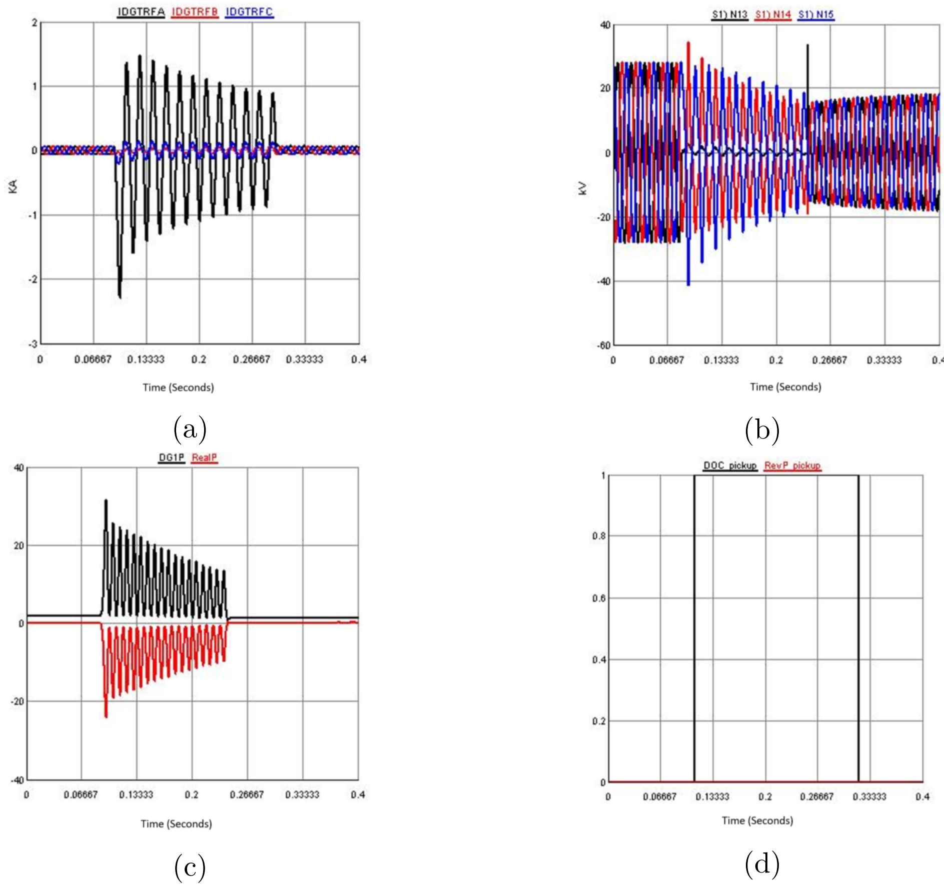

(a) (b) (c) (d)

Figure 2.4: High impedance single phase to ground fault at F2 with both DERs in service

2.6 Conclusion

A comparative analysis was carried out to evaluate the capability of DOC and RP elements to detect various faults. The concept of adaptive feeder protection is increasing in importance as DERs are added to the system and back feeding fault current becomes a large concern. A custom model was built to test consider multiple fault types and locations. The fault impedance and the presence of other DERs were also taken into account, as they play a deciding role in delineating the appropriateness of both the relays. It was found that a proper pickup value of current would guarantee the correct action of a DOC relay. However, because the reverse power relay is dependent on two variables, voltage and current, it was not able to perform accurately in most scenarios. This work shows that low fault impedance will cause the voltage to collapse, which causes a negligible power magnitude. It was also shown that phase to ground faults cause one phase to reverse direction, but the three phase power is not considered in the reverse direction as the other two phases increase power to compensate. It is concluded that reverse power is not a reliable indicator of fault identification, and the DOC element should be considered instead for feeder protection. Research not shown in this work gives the authors reason to believe the RP element can be used for islanding detection in case of LOM situations, which is studied and analyzed in Chapter 3.

Chapter 3

A Multi-principle Passive Islanding Detection Technique for Power Distribution Systems

3.1 Details of the publication

Co-authors: Kevin M. Phelps, Joseph J. Petti and Francisco Velez-Cedeno.[1]

Reference [11]**:** © 2019 IEEE. Reprinted, with permission, from T. K. Barik, K. M. Phelps, J. J. Petti, and F. Velez-Cedeno, "A multi-principle passive islanding detection technique for power distribution systems," in *2019 IEEE Power Energy Society General Meeting (PESGM)*, Aug 2019.

3.2 Abstract

With the recent large-scale integration of distributed energy resources (DERs) in the power distribution system, the conventional notion of a radial system with unidirectional power flow does not hold. Bi-directional power flow has challenged the protection schemes in

[1]The co-authors have contributed in the simulation and testing during the HIL setup

place to detect an islanding event. Numerous passive islanding detection techniques have been proposed in the past. However, the non-detection zone (NDZ) associated with these techniques may be large. The work presented in this chapter advocates the feasibility of a multi-principle passive islanding detection technique based upon the rate of change of voltage measurements and 3-phase active power mismatch at the point of common coupling of the DERs. Such a technique ensures smaller NDZ and easier implementation with no additional cost. The effectiveness of the technique is validated on a synthetic distribution model using commercially available protective relays and performing Hardware-in-the-loop (HIL) testing using the Real Time Digital Simulator (RTDS).

3.3 Introduction

The power distribution system has undergone numerous changes in the past 2-3 decades during which the concept of introducing distributed energy resources (DERs) has gained momentum. The integration of DERs challenges the long-held notion of unidirectional flow of power, i.e., from the utility sources to the consumer. Conventional protection schemes need to undergo modifications to adapt to the changing grid. Loss of mains (LOM) or anti-islanding protection has especially become difficult to implement. Islanding refers to a condition where a portion of the power system that contains utility served loads and on-site DERs remain energized but is electrically isolated from the rest of the utility system [12].
However, the response undertaken by a utility after a section of the distribution system has been islanded, can be classified into two broad categories. The first approach advocates the sustenance of DERs inside a local area such as a microgrid, which has regional controllers to sustain a small island with interior loads. The second and the widely used approach is to disconnect the DERs at their Point of Common Coupling (PCC) within 2 seconds when

islanded [12]. Hence, unintentional islanding detection is a significant aspect of DER protection schemes which has to be highly reliable, or else utility equipment and personnel could come into harm's way.

The works presented in [14]-[21] discusses the usage of active islanding detection methods which rely on the principle of introducing deliberate changes into the system on a continuous basis and monitoring the response of the system which would differ between grid-connected and islanded mode. Such methods are typically used for circuits containing inverter based DERs. However, these methods have certain disadvantages such as introducing power quality issues and higher cost of installation. The authors in [22]-[29] propose various passive detection methods which rely upon measuring local measurements and system parameters to detect LOM event. Such methods are easier to implement, however, have a larger non-detection zone (NDZ) as compared to the active detection methods. A smaller NDZ is usually the indicator of a dependable protection scheme. Communication-based transfer trip schemes are also widely used by utilities for islanding detection. The status of the up-line utility devices such as the feeder breaker or a line recloser upon tripping is transmitted to the breaker at the PCC for disconnecting the respective DER. Such communication-based schemes have a very small NDZ. However, the cost of installation and infrastructure for the implementation of such schemes are huge. Additionally, the effectiveness of such techniques depends upon the reliability of the communication medium being used.

The work presented in this document proposes a multi-principle passive islanding detection technique based upon the rate of change of voltage (ROCOV) measurements and 3-phase active power mismatch upon islanding criteria, which is explained in section 3.4 of the paper. Such a method is easier to implement, requires no additional infrastructure (for communication) or equipment installation cost and has a smaller NDZ as compared to individual passive schemes. The feasibility of the technique is tested on a test bench model consisting of DERs both conventional and inverted-based as described in section 3.5. The percentage of conventional generation has been allocated more than the inverter-based generation to emulate practical scenarios. Section 3.6 discusses the simulations carried out using Real Time Digital Simulator (RTDS) and commercially available relays and the results depicting the efficiency of the technique under numerous scenarios. Finally, section 3.7 summarizes the paper, outlining possible future research.

3.4 Technical Approach

3.4.1 Proposed Methodology

The first principle adopted for the proposed multi-principle technique is based on ROCOV measurements. The voltage profile of an island has a striking difference compared to that of a grid-connected circuit. Usually, when connected to the grid, ROCOV measurement is not significantly large unless a fault or big transient disturbance occurs. Fig. 3.1 shows the voltage response at the PCC of a particular DER under islanding and system fault conditions.

As shown in the figure, the voltage at the PCC during a system fault drops rapidly and hence the ROCOV value is higher. On the other hand, during islanding, the voltage at the PCC would either increase or decrease depending upon the load and generation imbalance. However, the voltage change is not that severe as compared to a fault event, and hence, the ROCOV value is lower. The reason for introducing a contrast between the two signatures of voltage profiles for different scenarios is because an islanding phenomenon has to be differentiated from a fault, including a high impedance fault where ROCOV measurement might not be significant. A successful delineation and indication of the events mentioned above allows the utility to take necessary actions for either case. Currently, utilities adopt

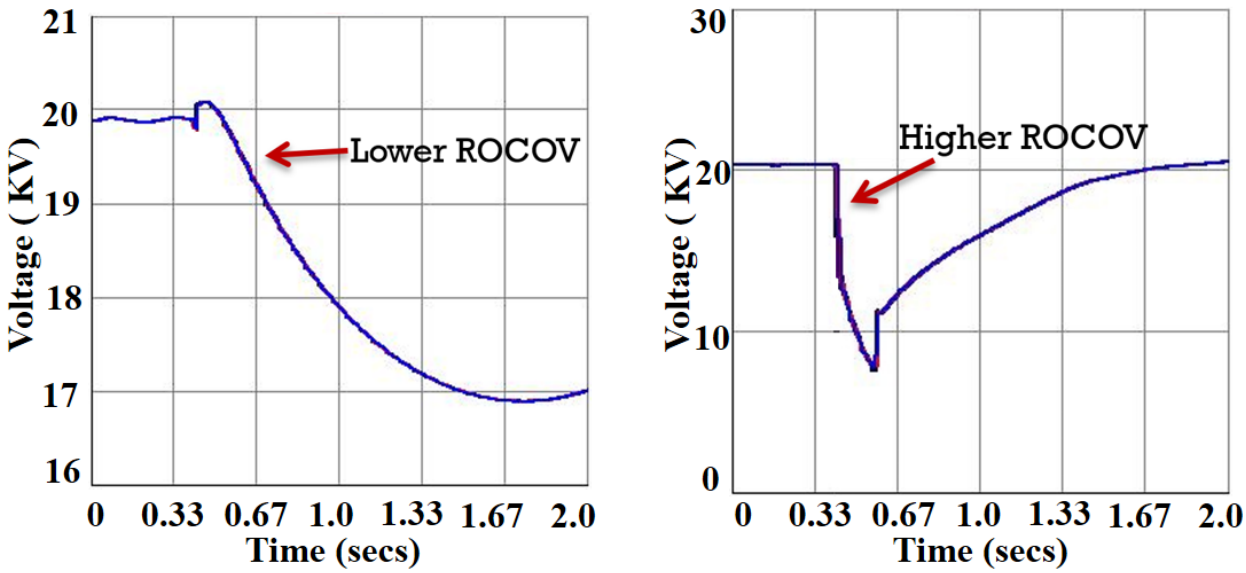

Figure 3.1: The voltage at DER PCC during islanding (left) and a 3 phase fault in the system (right).

complete disconnection of DER at the PCC upon LOM occurrence. However, as per the new IEEE 1547 standards for interconnection of distributed generators, DERs are expected to ride through during faults or other disturbances [12]. The work presented in this paper, apart from identifying islanding occurrence, deals with fault identification especially for high impedance faults (which have a significantly lesser ROCOV as compared to bolted faults). It facilitates the utility to take proper actions for disconnection of DERs during islanding and undertake ride through capable actions for fault or other transient disturbances.

However, the crucial task in differentiating these events is finding proper threshold limits or boundaries for ROCOV values. Fig 3.2 displays the various event regions based upon ROCOV values depicted on a real axis. The boundary between a certain "NEG_HT"(Negative high threshold) and "POS_LT" (Positive low threshold) is defined as the "Normal range". The ROCOV measurements pertaining to common events such as sudden load or generator switching events are included in this range. This buffer region prevents any mis-operation

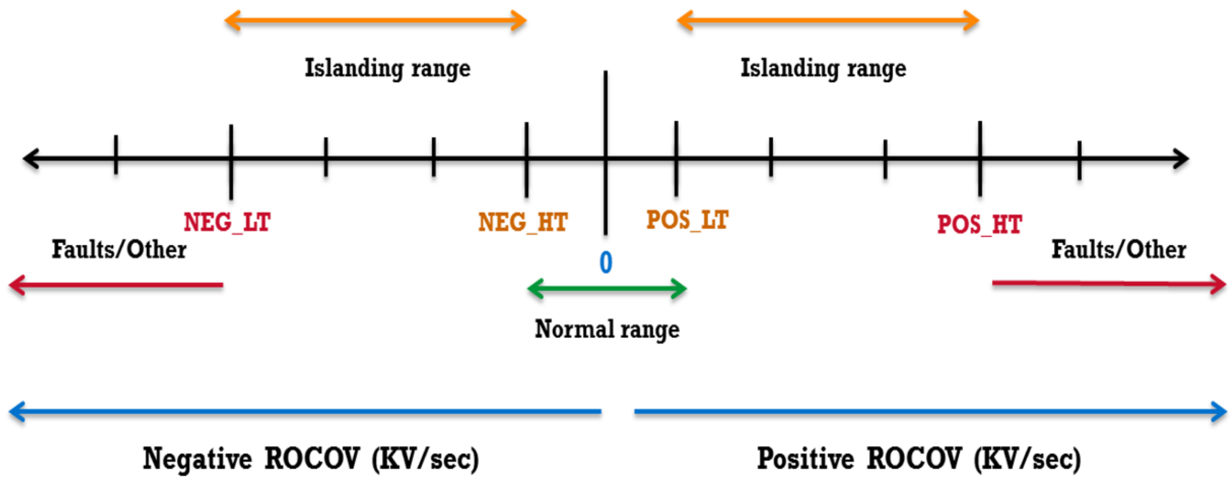

Figure 3.2: ROCOV based range delineation for various events.

of the proposed technique during normal conditions.

The ROCOV values beyond the normal range, however, bounded by “NEG_LT” (Negative low threshold) and “POS_HT” (Positive high threshold) establish the “Islanding range” as denoted in the figure. Finally, the values of ROCOV beyond these ranges are termed to be inside the “Fault/Other” event range. The threshold values are system specific and can be found out by extensive offline simulations. However, simply relying upon the ROCOV measurements might still lead to mis-operation during normal conditions, due to events such as sudden switching of large capacitor banks.

To further reduce the NDZ, 3-phase active power mismatch detection at the PCC upon islanding is also proposed to be used along with the ROCOV based principle in the multi-principle method. The signature of 3-phase active power changes suddenly at the PCC upon islanding. It can be used in conjunction with the ROCOV principle to detect islanding for most of the practical cases. It is important to note that due to this reason, the proposed technique cannot detect islanding event under zero power mismatch scenarios.

The value of power exported or imported at the PCC changes dynamically and hence, the pickup setting and range for 3-phase active power mismatch have to be continuously updated within the relay. The proposed technique suggests two different pickup settings. For DERs meant to import power from utility during normal conditions strictly, relays can be set for a predefined minimum pickup value of export power, thus functioning similarly to a reverse power relay. However, for DERs meant to export power during normal conditions, the pickup setting and pickup range of the relays can be set dynamically. Fig 3.3, shows the pickup setting of 3-phase active power (depicted as moving window Pavg) and the pickup range (illustrated as the shaded box region).

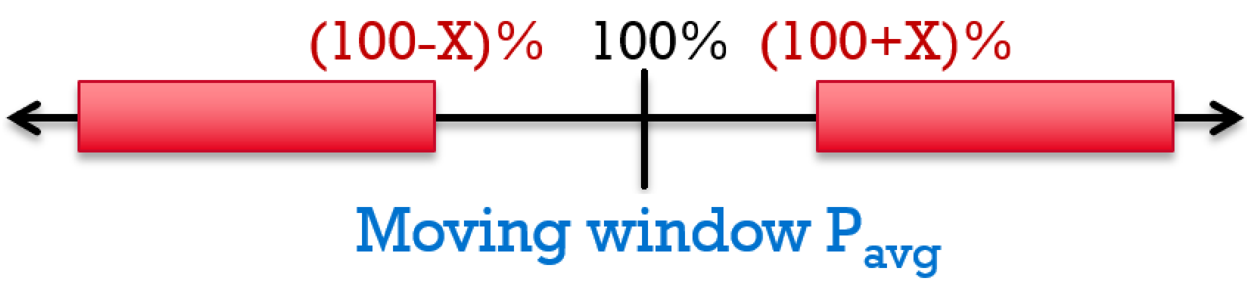

Figure 3.3: Pickup setting and range for 3-phase active power mismatch.

The variable X in Fig 3.3 refers to the percentage of 3-phase active power mismatch (usually a small value such as 10-20%) that cannot be detected by the proposed technique which would be system model specific and similar to ROCOV threshold values, can be found by performing extensive offline simulations.

3.4.2 Algorithm

The two passive detection principles explained in the previous section are used to develop the proposed protection scheme. It should be noted that commercial relays do not directly provide ROCOV values. However, the modern microprocessor-based digital relays can use shift registers and store historic voltage measurements for ROCOV calculation. These relays have varied time intervals (25-100 milliseconds) for storing analog and digital measurements. Assuming a general time interval t, phase voltage measurements are recorded and stored every t milliseconds apart. Fig 3.4 displays the timeline of the measurements where K represents an instant of time (in milliseconds). Two sets of consecutive ROCOV measurements are used to gain a more accurate depiction of the system conditions.

Similarly, as mentioned earlier, instead of tracking a single measurement of 3-phase active power measurement to be set as the pickup setting, a moving window average value is used to correctly detect an islanding event. A buffer of 200ms is provided to ensure that faults and other transient events do not affect the value of the pickup setting of the 3-phase active power. Based on Fig 3.4,

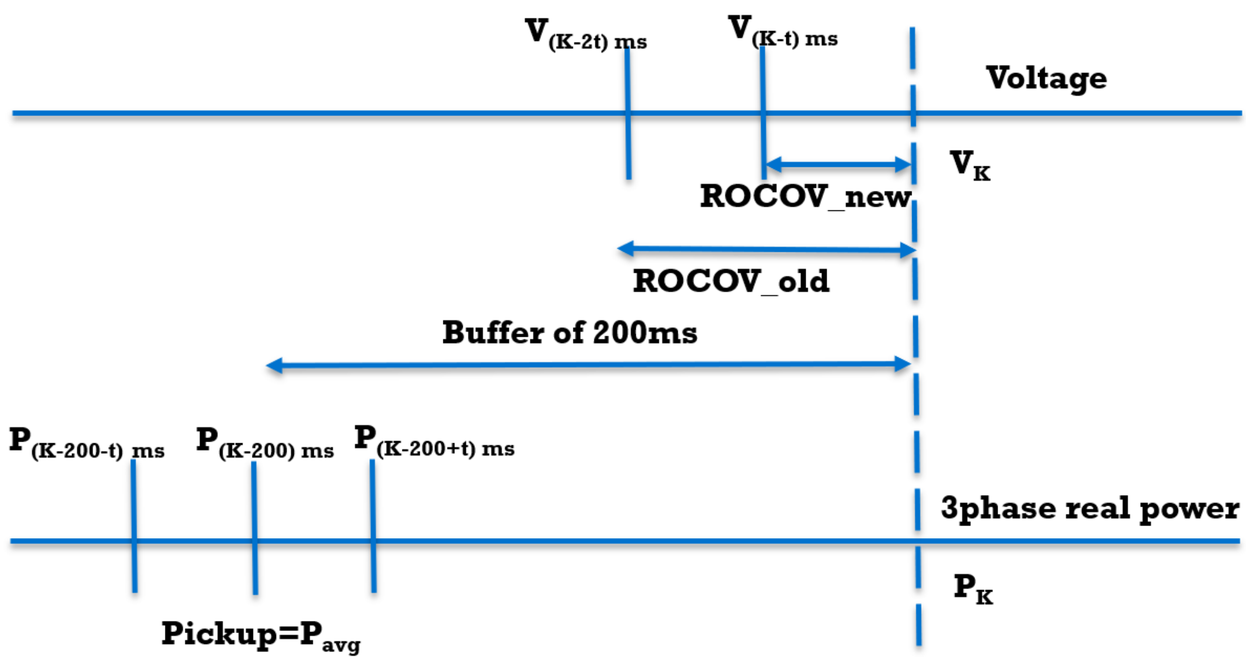

Figure 3.4: Timeline for ROCOV and Power measurements.

$$ROCOV\_new = \frac{V_{(K)} - V_{(K-t)}}{t} \tag{3.1a}$$

$$ROCOV\_old = \frac{V_{(K)} - V_{(K-2t)}}{2t} \tag{3.1b}$$

$$P_{avg} = \frac{P_{(K-200-t)} + P_{(K-200)} + P_{(K-200+t)}}{3}. \tag{3.1c}$$

Where,

V_i = Phase voltage at instant i

P_{avg}= 3 phase active power pickup setting value

Finally, the algorithm devised can be summarized in the form of a flowchart as shown in Fig 3.5.

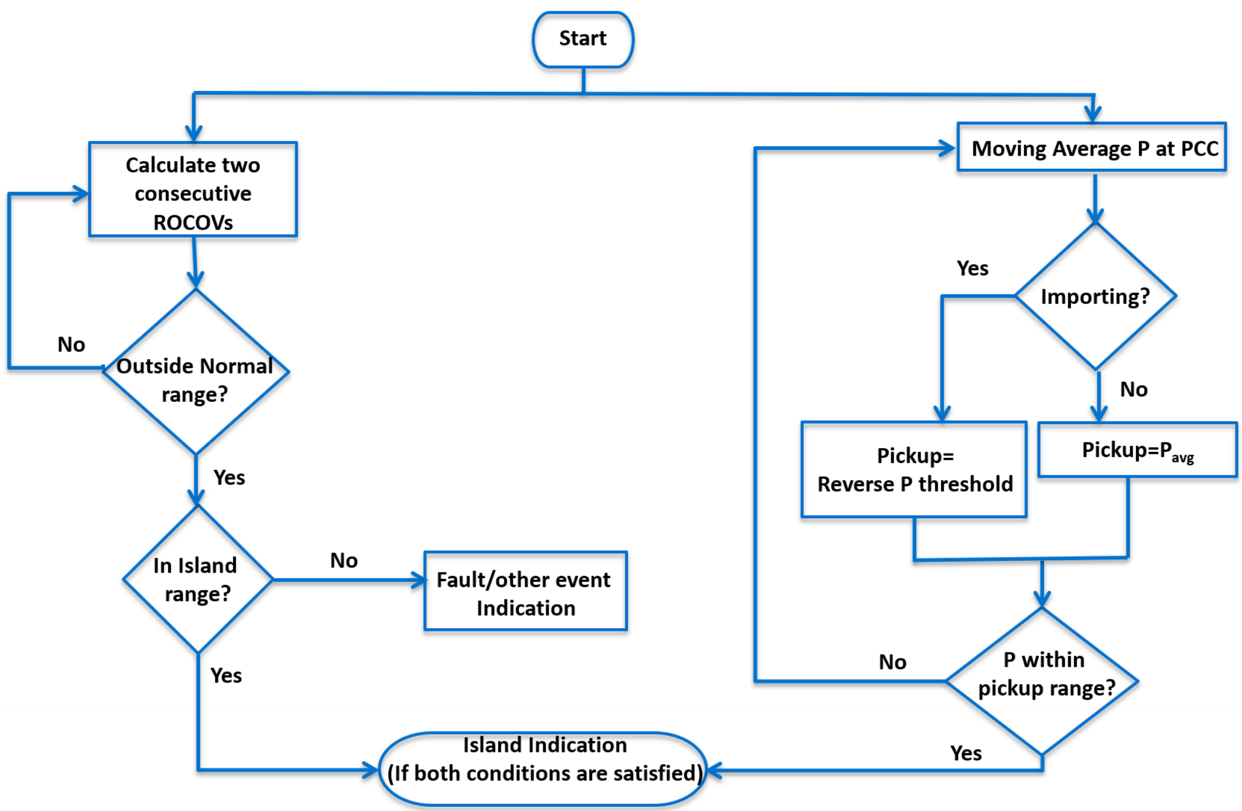

Figure 3.5: Flowchart of the proposed technique.

3.5 Test Bench Setup

3.5.1 Synthetic Distribution Model

For proper testing of the proposed technique, to identify and differentiate between various islanding and fault conditions, a custom modified synthetic distribution model consisting of two feeders, and four DERs was constructed. Fig 3.6 depicts the test bench model proposed for this paper. The proposed technique is tested on the relay located at the PCC of DER_1 as shown in Fig 3.6. The technical parameters for the feeders and laterals, various line equipment, transformer and loads are designed based upon standard Dominion Energy (a USA-based electric utility) distribution system models.

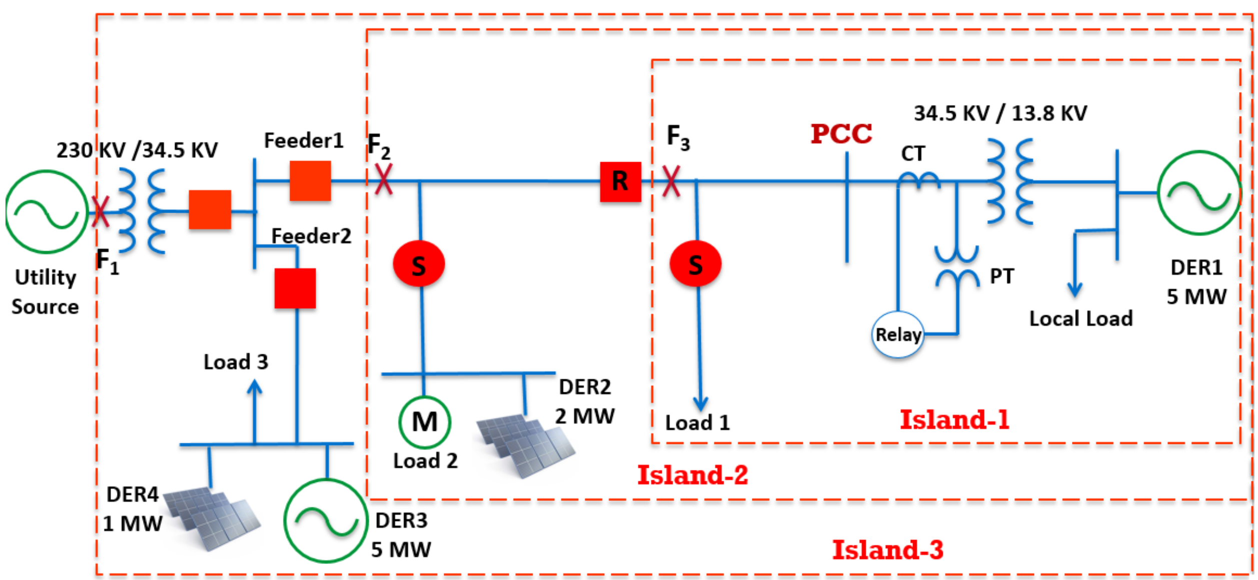

Figure 3.6: Test bench model.

To consider the performance of the technique in the presence of dynamic loads, a motor load (Load 2 in the figure) of approximately 20% of the total distribution system load has been added to the model. Such an arrangement allows multiple islanding scenarios depending upon the disconnection of either the line recloser or the feeder1 breaker or the transformer low voltage side breaker at the distribution substation represented by the formation of Island-1, Island-2, and Island-3 respectively in the figure. As mentioned earlier, the proposed technique integrates inverter-based generation (in this case solar generation) at two different locations on separate feeders denoted as DER_2 and DER_4 along with synchronous generators as DER_1 and DER_3 as shown in Fig 3.6. In this case, inverter-based generation constitute around 25% of the total generation capacity of the distribution system. To test the performance of the technique for numerous fault conditions, various symmetrical and unsymmetrical faults are applied at F_1, F_2 and F_3 locations as depicted in Fig 3.6.

3.5.2 Hardware-in-the-Loop setup

Hardware-in-the-Loop (HIL) technology of the RTDS was used to thoroughly test the feasibility of the proposed technique. Fig 3.7 demonstrates the setup built for carrying out the testing on a commercial relay commonly used in distribution system protection.

The test bench setup model represented in Fig 3.7 was built in RSCAD and executed in RTDS. The PCC voltage and current signals were amplified using an amplifier which was then sent to a commercial feeder protection relay (SEL-751) by Schweitzer Engineering Laboratories (SEL). This relay has got a resolution of 25 ms in its shift registers to store measurements which would result in greater precision in calculating ROCOV and P_{avg} values The feedback from the relays was then communicated back to RTDS.

The proposed algorithm was implemented in the form of a graphical logic as depicted by Figs 3.8-3.10. Fig 3.8 depicts the logic diagram for usage of two consecutive ROCOV values (per phase, phase A in figure) as explained earlier to indicate the possibility of different scenarios. Similarly, the ROCOV values for the other two phases are also used for islanding or fault detection. Fig 3.9 displays the logic diagram to detect 3-phase active power being exported or imported at the PCC and accordingly fix the pickup setting value. The logic also considers the latching of the pickup setting in case an abnormality occurs in the system making the technique more resilient to mis-operations. Finally, Fig 3.10 depicts the logic diagram for island and fault identification incorporating the multi-principle technique.

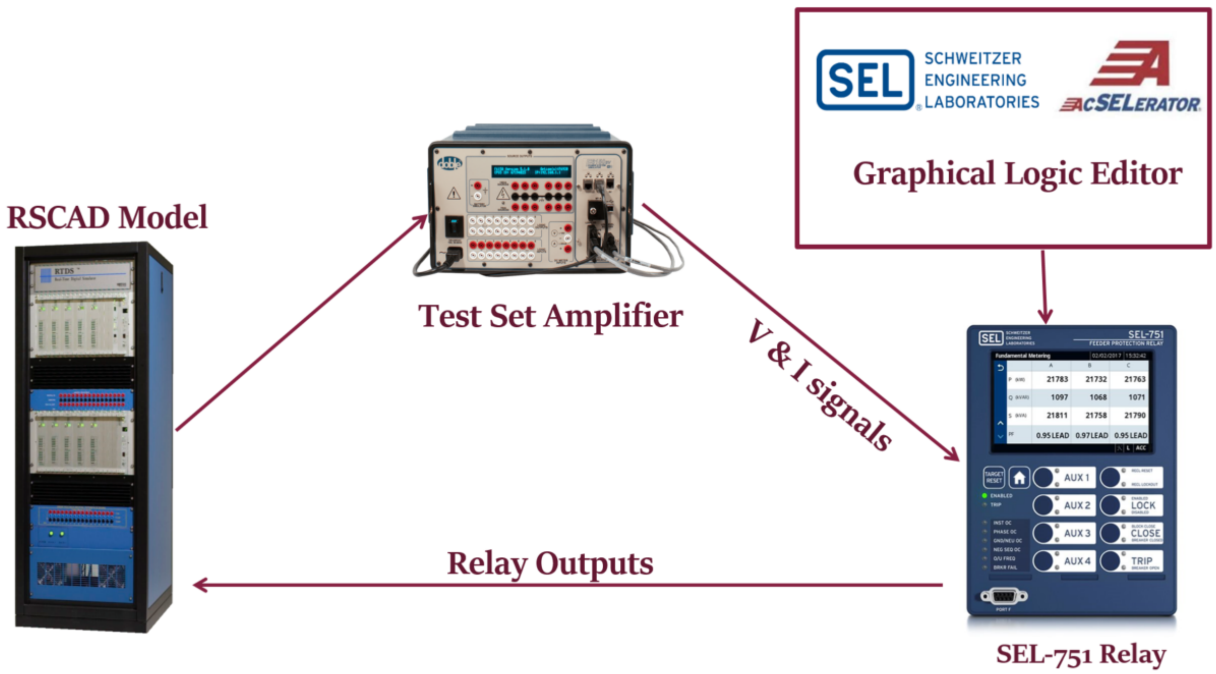

Figure 3.7: Hardware-in-the-loop setup.

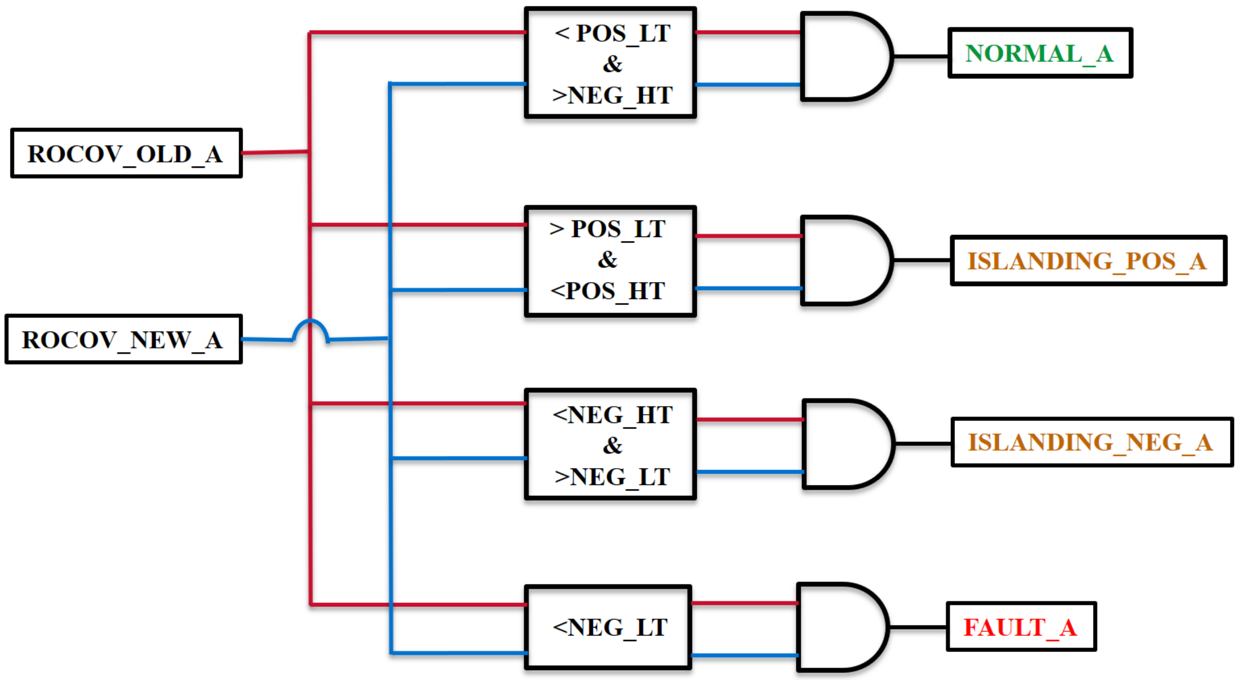

Figure 3.8: The logic diagram for ROCOV based event decision-making.

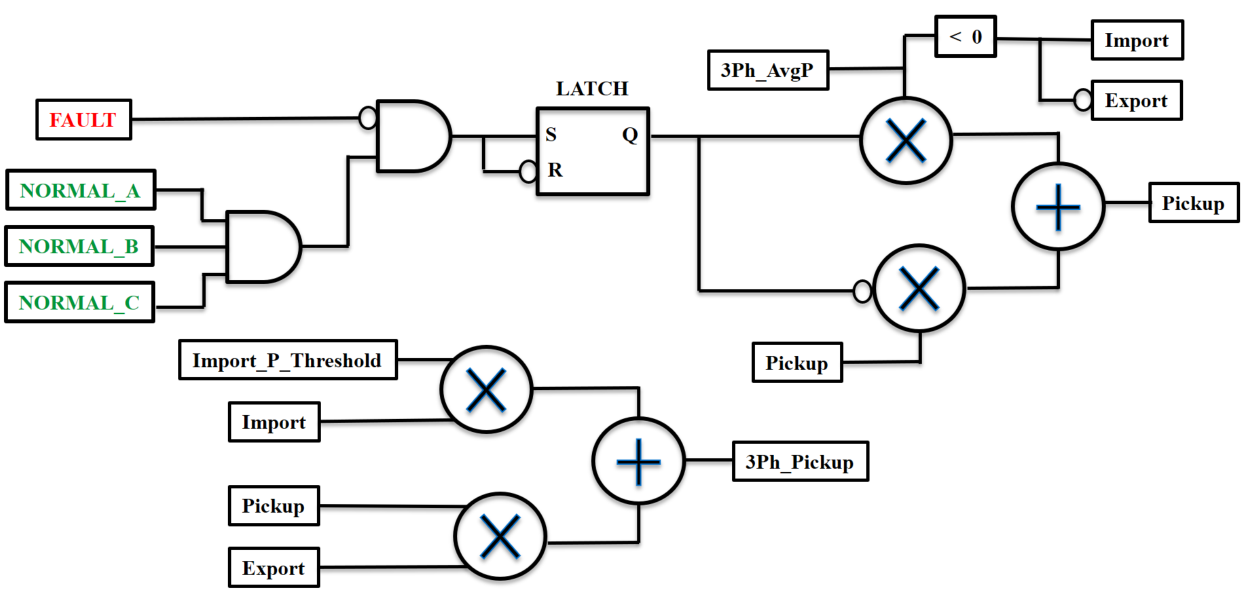

Figure 3.9: The logic diagram for 3-phase active power pickup setting and range.

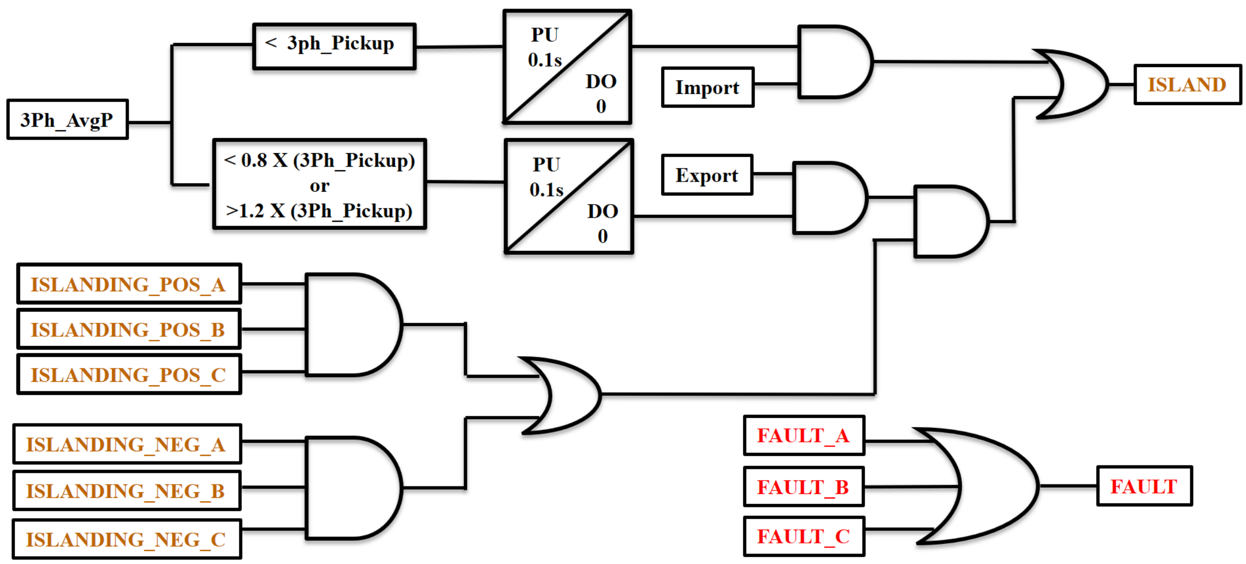

Figure 3.10: The logic diagram for island and fault identification.

3.6 Simulation Results

Using the RTDS HIL setup as explained in the earlier section, several scenarios were tested encompassing the following conditions.

- Possible islanding conditions- Heavy/light system loading in the presence and absence of other DERs.
- Symmetrical/Unsymmetrical faults at various locations (High impedance/Bolted).
- Sudden load injection/rejection.

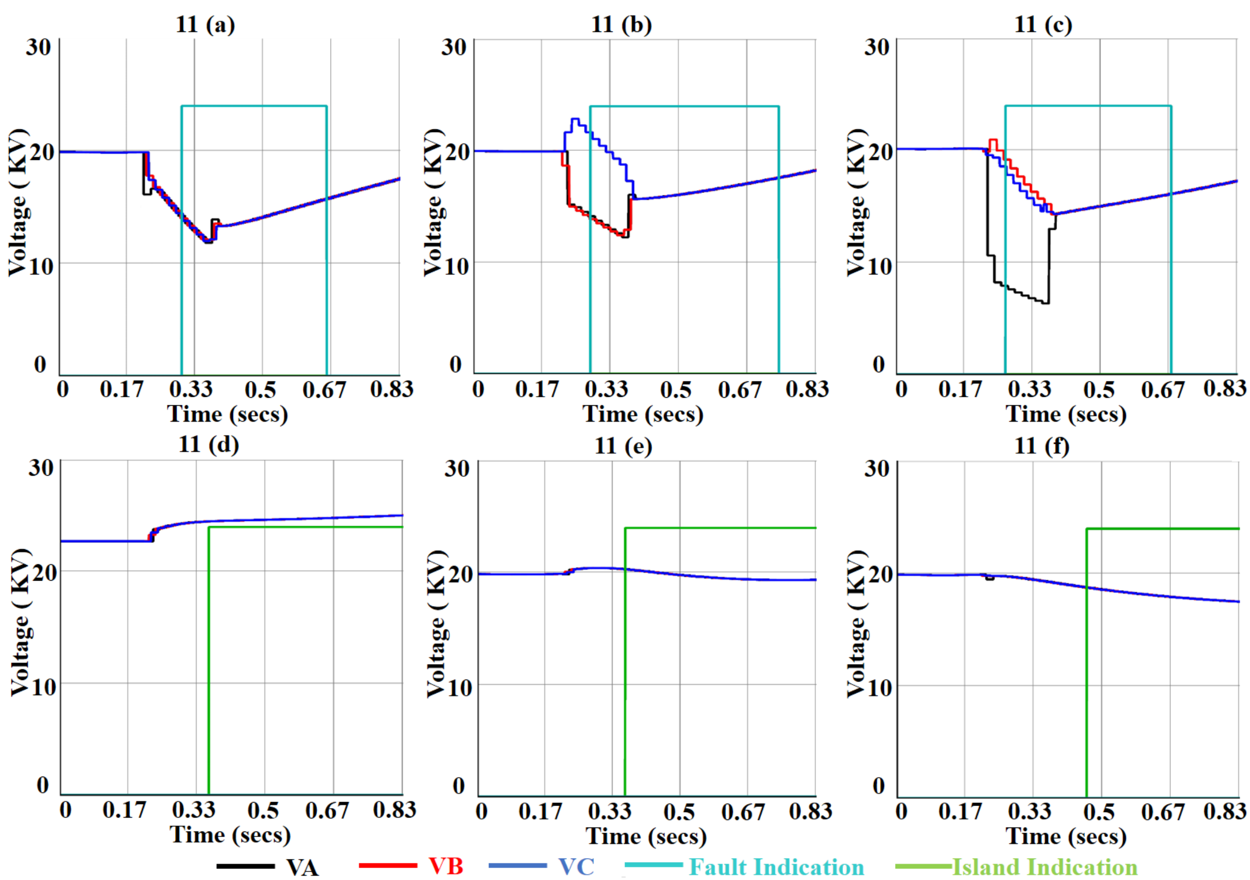

Figure 3.11: Plots for successful identification of various fault and islanding scenarios by the relay at DER_1 PCC

Six of the islanding and fault scenarios are depicted in Fig 3.11. Fig 3.11 (a)-(c) illustrates the occurrence of high impedance three-phase fault at F_1, Line-line fault at F_2 and single phase to ground fault at F_3 respectively. The proposed technique was able to identify fault conditions within 75-100 milliseconds successfully. It should be noted that these response times depend upon the relay being used as explained in the Algorithm part of Section 3.4. To differentiate fault from islanding scenarios, Island 1, 2, 3 were created with the same loading conditions as depicted in Fig 3.11 (d)-(f) respectively. The technique was able to successfully detect islanding occurrence within approximately 200 milliseconds. The logic was able to differentiate between various events as desired for most of the cases. The following table summarizes the result.

Table 3.1: Results for various fault and islanding scenarios

Type of cases	Total No. of cases	Successful indication
Island	12	11
Fault/others	75	72

In the later stages, the effectiveness of the multi-principle technique was also tested on standard Dominion Energy distribution RSCAD models. The proposed technique was able to efficiently identify and differentiate islanding occurrences from system transient disturbances on these practical models.

3.7 Conclusion

The work presented in this chapter details a multi-principle islanding detection technique based on 3-phase active power mismatch and ROCOV measurements. The RTDS HIL setup was used to validate the accuracy of the proposed islanding detection technique. Though the logic can be applied universally, the threshold values and pickup settings will vary for different systems, and extensive offline simulations are needed to determine the appropriate values. The combination of the two passive techniques produced an NDZ smaller than individual schemes. The proposed method is a viable option in reducing the dependency on the communication-based schemes. The multi-principle technique can be further expanded for a system with more percentage of inverter-based distributed generation as their penetration in the system is increasing substantially. Additionally, the possibility of integrating other islanding detection schemes in conjunction or as a backup to the proposed logic can also be researched.

Moreover, measures to sustain and balance power within an islanded distribution system upon islanding occurence can be researched. Methods to quickly balance load-generation power can be implemented to sustain the island as discussed in Chapter 4.

Chapter 4

Dynamic Prioritization of Critical Loads for Sustaining Power Distribution Systems upon Islanding

4.1 Details of the publication

Co-authors: Virgilio.A.Centeno

Reference [31]**:** © 2020 IEEE. Reprinted, with permission, from T. K. Barik and V. A. Centeno, "Dynamic prioritization of critical loads for sustaining power distribution systems upon islanding," in *2020 IEEE Power Energy Society Innovative Smart Grid Technologies Conference (ISGT)*, Feb 2020.

4.2 Abstract

Large-scale integration of distributed energy resources (DERs) in the power distribution system has challenged the conventional notion of a radial system with unidirectional power flow. The bi-directional flow of power from the consumer end raises concern for the protection systems in place to detect islanding phenomenon. However, the current standards/practices do

not allow the DERs in an electric distribution system to stay connected in islanded mode except in a micro-grid mode of operation, which has designated controllers to maintain the stability of an islanded system. The work presented in this chapter proposes the implementation of a technique to assign distinct priority levels to various critical loads in real-time based on voltage sensitivity factor. The proposed module decides the shedding order of these loads in real time depending upon system operating conditions in order to sustain an island from the point of disconnection stabilizing the power balance within the island.

4.3 Introduction

The concept of integrating distributed energy resources (DERs) into the distribution system to increase reliability has challenged the earlier notion of unidirectional flow of power, i.e., from the utility end to the consumer end. For this reason, conventional protection schemes need to undergo modifications to correctly identify and isolate faults. Loss of Mains (LOM) or islanding detection has been difficult due to such modifications. However, the response undertaken by a utility after a section of the distribution system is islanded can be classified into two broad categories. The first approach is to disconnect the DERs at their Point of Common Coupling (PCC) within 2 seconds [13] if it is a part of an island. The second approach, however, is gaining popularity in the recent past, which advocates the sustenance of DERs inside a micro-grid, which has regional controllers to sustain a small island with interior loads. Many prior works have discussed successful detection methods for identifying islands based on active and passive methods [14]-[29]. Prior works have addressed complete disconnection of the micro-grids from the utility, stabilizing the interior system and then later on serving critical loads as a part of distribution system restoration problem [32],[33]. Other papers have discussed sustaining an islanded network by adopting load and generation shedding techniques to maintain power balance after the island has been stabilized [34],[35]. However, the response of these systems during the occurrence of islanding has not been studied in detail and needs to be analyzed. Moreover, many DERs are not a part of a micro-grid operation currently and are simply connected to the distribution system for commercial benefits. Such DERs can be sustained in the event of an islanding phenomenon and need not necessarily be disconnected, as stated in [13].The central idea being that these DERs can form a small grid whose electrical and geographical boundaries can be modified depending upon the point of disconnection.

This chapter discusses the possibility of such an approach of sustaining a power distribution system upon the occurrence of an island whenever the load inside the island surpasses the total generation available (implying negative Rate of Change of Frequency or ROCOF) by maintaining the power balance with the help of a Critical Load Shedding Module (CLSM). The immediate crucial task in sustaining the electrical system island upon its occurrence is to shed the critical loads based upon their criticality factors (which usually are decided offline by the utility) to maintain the power balance inside the island. However, this approach does not consider the fact that various loads having the same offline criticality level may have a varied impact on the power system in real-time. The criticality of these loads needs to be subcategorized into distinct priority levels to ensure correct shedding procedures, which would ensure proper sustainability of the island. Dynamic prioritization of the criticality factors based upon voltage sensitivity factor and QV analysis is adopted for this reason.

Section 4.4 explains the distribution system model and basic assumptions considered for the development of the module. Section 4.5 discusses the technical approach for developing the algorithm of the proposed module. Section 4.6 describes the testing of the CLSM and associated results for various scenarios. Finally, section 4.9 summarizes the work in the paper, outlining the possible scope of future work.

4.4 Distribution System Infrastructure

4.4.1 Minimum system infrastructure requirements

The test bench setup built for testing the performance of CLSM is depicted in Fig. 4.1. A three-phase unbalanced system is built considering numerous static loads to replicate residential loads. Although the system mostly consists of synchronous generators, inverter-based resources are also included in this system, as shown in the Fig. 4.1.

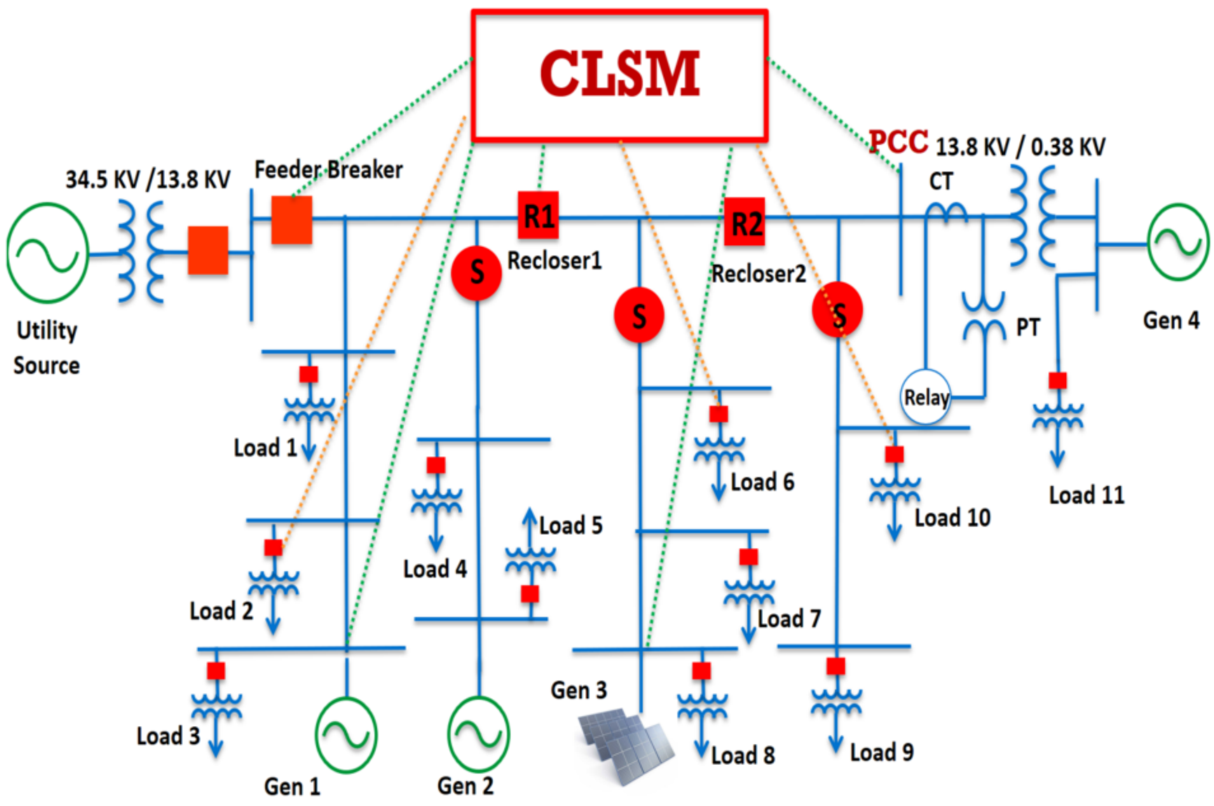

Figure 4.1: Proposed test bench system model.

Each load representation in the figure is an aggregate of various small loads grouped into blocks based on the service transformer location. For all future references in this paper, the high voltage side of any particular service transformer would be termed as a node in the island. Each service transformer serves a bunch of loads. Load break switches (LBS) are usually placed at such nodes, which shed all the loads downline of the corresponding transformer if required, thus enabling control aspect to loads. It should be noted that only such controllable loads (i.e., switched on/off by LBS) are referred in this paper for shedding purposes.

Additionally, advanced metering infrastructure (AMIs) such as smart meters, are usually installed at these nodes. These meters can send out 15-minute average values of voltage, active and reactive power consumption at each node every 15 minutes to the CLSM. Hence, such an approach provides a cost-effective method of installing a lesser number of AMIs needed for the implementation of the technique. The proposed CLSM receives the 15-minute smart meter measurements from each node in the system. These measurements, as discussed in the subsequent section, would be crucial in the dynamic prioritization of the critical loads bearing the same criticality factor otherwise decided offline. The CLSM also receives ROCOF measurements in real-time from the PCC of individual DERs as well as breaker statuses from various utility-owned disconnecting devices on the main primary feeder. These devices can communicate with each other and can be utilized by the proposed CLSM.

4.4.2 Basic assumptions

Some of the basic practical assumptions taken in this approach are as follows:

A) All the controllable loads in the system are categorized offline into four critical levels (where criticality level 1 refers to the most critical and criticality level 4 refers to the least critical loads) based upon their size, importance and financial agreement with the utilities. The offline criticality levels of individual loads are provided in the subsequent testing section.

B) Upon islanding, the Rate of Change of Frequency (ROCOF) measurement at various PCC points is assumed to be nearly the same as the frequency of such a small region as the distribution feeder section would change coherently.
C) The system topology and line parameters from the distribution substation down to each of the service transformers are known well in advance which would be later required in the QV analysis for the dynamic prioritization of critical loads as discussed in the subsequent section.

4.5 Technical Approach

4.5.1 Dynamic Prioritization of critical loads

For load shedding, the most crucial aspect is to shed the appropriate amount of the load at the right instant of time to ensure proper stability of the islanded system. However, the criticality levels of the loads are decided offline by the utility and have to be re-evaluated in real-time to ensure its proper impact on the system. Moreover, loads of the same critical level as decided offline would have varied effects on the system based upon the operating conditions and systems parameters.

Hence, to properly implement a load shedding technique and to prioritize loads of the same offline criticality factors, an approach of incorporating QV analysis has been carried out. QV analysis is widely used in the transmission level to decide the priority and the amount of load to be shed at various locations if required. Fig. 4.2 shows a general QV analysis curve for any node or bus in the system.

This QV graph depicts the relation between the reactive power injection (Q) vs. the voltage (V) at the particular node. It provides an idea of the voltage stability margin with respect

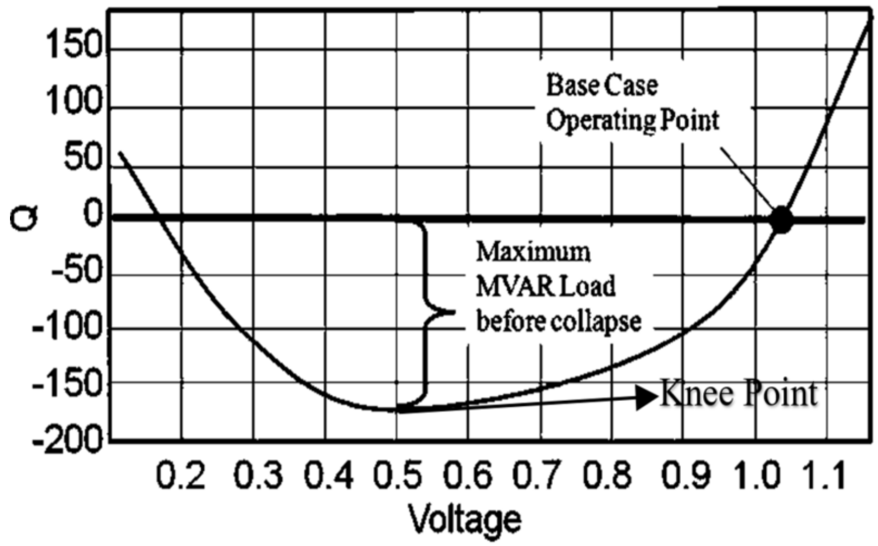

Figure 4.2: QV Analysis Curve at any given node.

to the maximum MVAR load that can be placed at the node before voltage collapse. The slope of the graph (dQ/dV) is termed as the voltage sensitivity of the particular node. It acts as an indicator for the margin of voltage stability of the node concerning the maximum reactive power consumption at that location.

As shown in the figure, a larger positive value of dQ/dV represents stability with a greater margin. As the voltage sensitivity value decreases and approaches zero (Knee point in the figure), the corresponding node approaches the point of voltage collapse. Shedding load at such a node with minimal voltage sensitivity would ensure the stability of other nodes. Thus, voltage sensitivity at different nodes can serve as a deciding factor to prioritize loads with the same offline criticality factors. The AMIs placed at these nodes would be crucial in achieving this goal. The reactive power injection (Q_i) equation at the i^{th} node is depicted as follows:

$$Q_i = \sum_{i=1}^{n} |V_i||V_j||Y_{ij}|sin(\delta_{ij} - \theta_{ij}) \tag{4.1}$$

Where,

n = total number of nodes

V_i = Voltage at node i

$|Y_{ij}|$=Magnitude of the $(i, j)^{th}$ element of the Bus Admittance matrix

θ_{ij}= Angle of the $(i, j)^{th}$ element of the Bus Admittance matrix

δ_{ij}= Voltage phase angle difference between node i and j

Differentiating Eqn. 4.1 with respect to voltage magnitude V_i, the voltage sensitivity (dQi/dVi) at the i^{th} node is calculated as follows:

$$\frac{dQ_i}{dV_i} = |V_i||Y_{ii}|sin(-\theta_{ii}) + \frac{Q_i}{|V_i|} \tag{4.2}$$

As can be seen from Eqn. 4.2, the voltage and reactive power injection at the steady-state of each node can be obtained from the AMIs. The bus admittance matrix elements are already known to the user based upon system topology and line parameters. The voltage sensitivity of each node is calculated every 15 minutes upon the arrival of measurements from the AMIs. The priority level of these critical loads are then decided dynamically, with the nodes having minimum voltage sensitivities considered to be least critical and can be shed sooner to ensure the stability of the system. The CLSM would be updated with the modified online priority levels, as explained above. Hence, the various loads of same offline priority level are now ranked into unique discrete priority levels incorporating voltage sensitivities at various nodes aiding in proper a modified sequence for shedding of loads upon islanding.

4.5.2 Algorithm

The methodology to carry out the general shedding procedure has been outlined below.
Step 1: Based upon the steady-state Q and V measurements from the smart meters and QV analysis of each node as described earlier, the ranking of the same critical level loads are updated every 15 minutes in the CLSM.
Step 2: Islanding phenomenon is confirmed by checking the disconnecting switch status as well as re-affirmed using the ROCOV measurements from at least 2/3rd of the PCC locations continuously based on a methodology as described in [9] for added reliability.
Step 3: Once the islanding is confirmed, the system topology is re-evaluated based upon the point of disconnection, and hence the cumulative inertia constant (H_{total}) of the remaining generators in the island is calculated and used for calculation of the total active power mismatch ($\Delta P_{mismatch}$) in the island as per the modified swing Eqn. 4.3 :

$$\frac{2H_{total}}{f_0}\frac{df}{dt} = \Delta P_{mismatch} \tag{4.3}$$

Where,

f_0= nominal frequency (50 or 60 Hz)

df/dt = ROCOF of the island retrieved from the smallest generator PCC.

In this work, negative ROCOF (when total load demand inside the island surpasses the total generation available) is considered as the focus is mainly on developing a load shedding module. Actions required for positive ROCOF scenarios would be covered as a part of future work.
Step 4: If ROCOF is negative, it indicates the overall load demand of the island is greater than the generation. Hence, load shedding is required. Firstly, the number of controllable

loads based upon the islanding region formed is decided. Secondly, the non-critical loads are shed based upon the prioritization scheme as explained earlier. This proves beneficial in case the total active power of the non-critical loads ($P_{NL_{total}}$) is greater than the $\Delta P_{mismatch}$. However, if the $\Delta P_{mismatch}$ is greater than the $P_{NL_{total}}$, then the shedding procedure of critical loads is initiated starting with the lowest ranked critical loads as evaluated with the help of QV analysis prioritization technique explained earlier. In this work, the wait interval between consecutive load shedding actions is fixed at 100 milliseconds. It should be noted that the wait interval can also be varied based upon the severity of the power mismatch calculated from the ROCOV values at the instant of islanding occurrence.

4.6 Simulation & testing

4.6.1 Simulink Model

The test bench model explained earlier is built in MATLAB/Simulink to evaluate the performance of the algorithm mentioned above. The line and machine parameters were obtained from standard distribution system parameters of the Dominion Energy system (US based electric utility). Improvements and validation of the model were made to emulate a distribution feeder along with the minimum infrastructure as explained earlier. The model and the technique was evaluated for multiple scenarios which encompass short-term islanding condition caused due to a minor system fault upon disconnection of appropriate utility remote controlled switch (feeder breaker or line reclosers).

4.6.2 Testing & Results

The performance of the CLSM upon islanding was evaluated for two scenarios. It should be noted that at any given point of time, a single disconnection is carried out leading to the formation of a single island and not multiple islands. In the first scenario, an island is formed upon tripping of the feeder breaker. In this case, all the 4 DERs and 11 loads are included in the islanded system. The voltage sensitivity factors of the various nodes were calculated as shown in Table 4.1. Based upon these factors, the loads have been assigned discrete and unique criticality defining the shedding order in case of islanding occurrence.

Table 4.1: Proposed relay settings for relays at Node-671

Load No.	Offline Criticality	Voltage Sensitivity	Real-time Criticality	Shedding order
1	4	0.01629	4.2	3
2	3	1.035	3.1	7
3	1	0.8705	1	11
4	2	0.738	2.1	10
5	4	0.01219	4.3	2
6	3	0.8128	3.2	6
7	3	0.5752	3.3	5
8	4	0.009743	4.4	1
9	2	0.2952	2.3	8
10	2	0.0.5903	2.2	9
11	4	0.02441	4.1	4

The simulation is executed, and the feeder breaker is tripped at t=1.5 secs to simulate islanding phenomenon. Fig. 4.3 displays the response of the CLSM upon islanding occurrence along with waiting intervals between consecutive shedding events.In this case, as ROCOF was negative, CLSM started shedding loads as per the shedding order depicted above. However, based upon the power mismatch, only six loads were shed to meet the requirement.

The frequency profile of the islanded system (in terms of generator frequencies) without and with the CLSM can be compared, as shown in Fig. 4.4 & 4.5, respectively. The voltage profile of the islanded system (in terms of generator terminal voltages) in the presence of

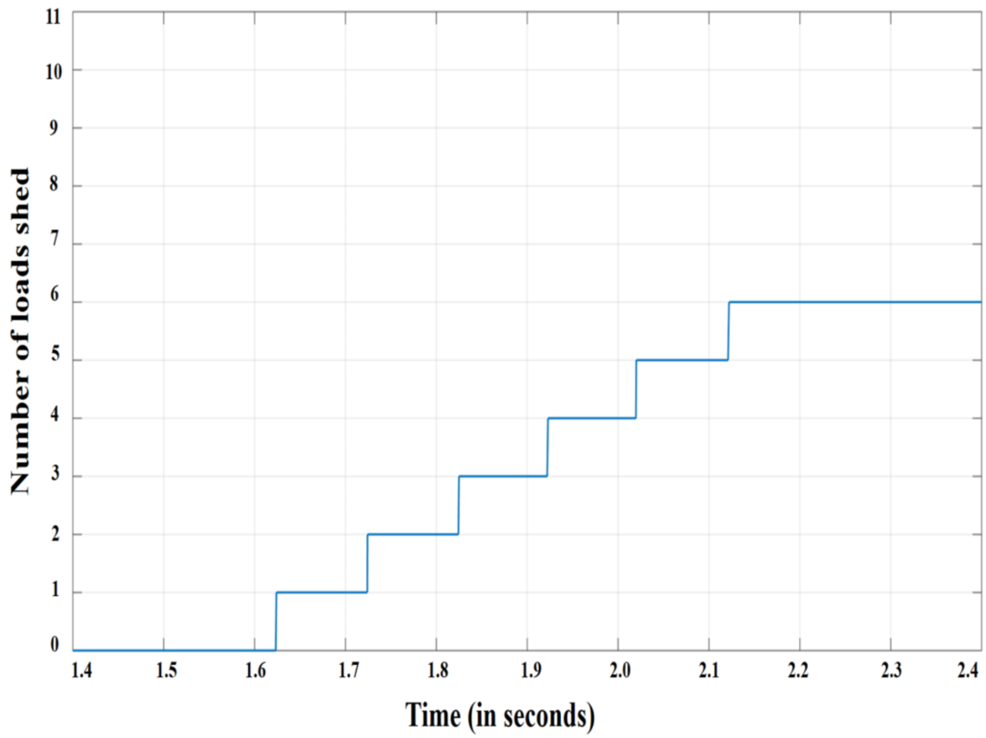

Figure 4.3: Number of loads shed incrementally as per wait interval.

CLSM is displayed in Fig. 4.6.

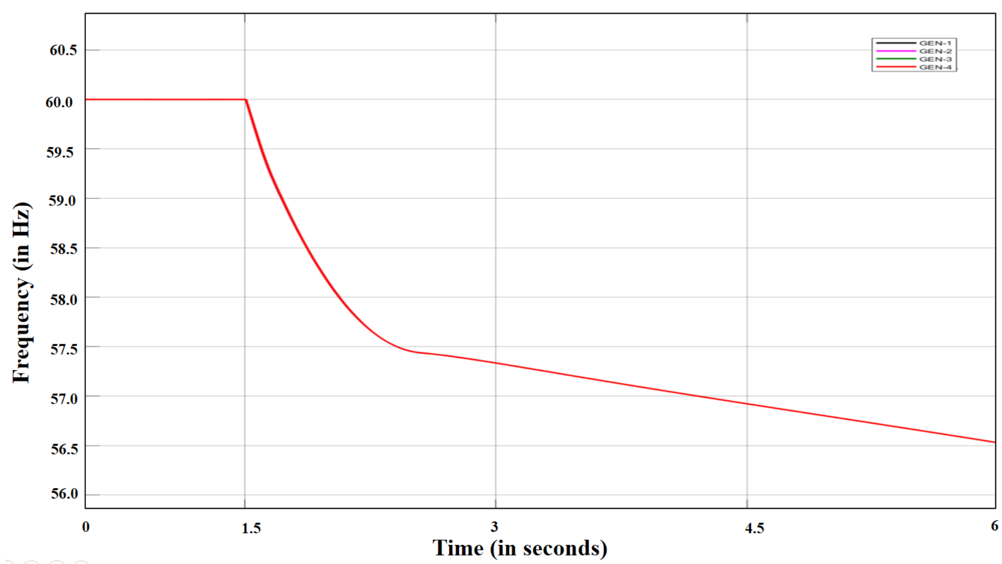

Figure 4.4: PCC Frequency profile in the absence of CLSM for scenario 1.

Hence, it can be seen that the CLSM performed as desired and aids in sustaining an island

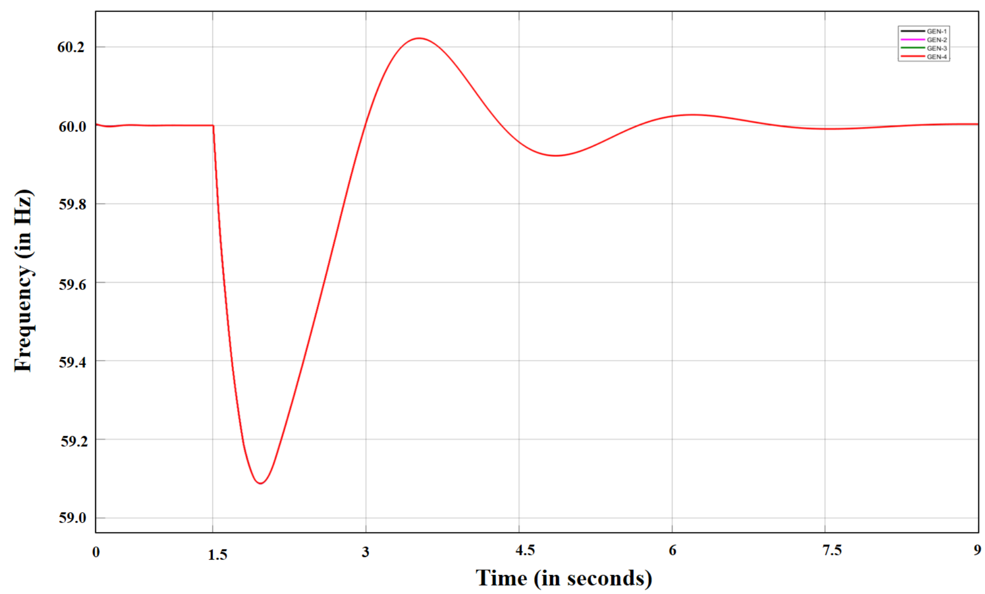

Figure 4.5: PCC frequency profile in the presence of CLSM for scenario 1.

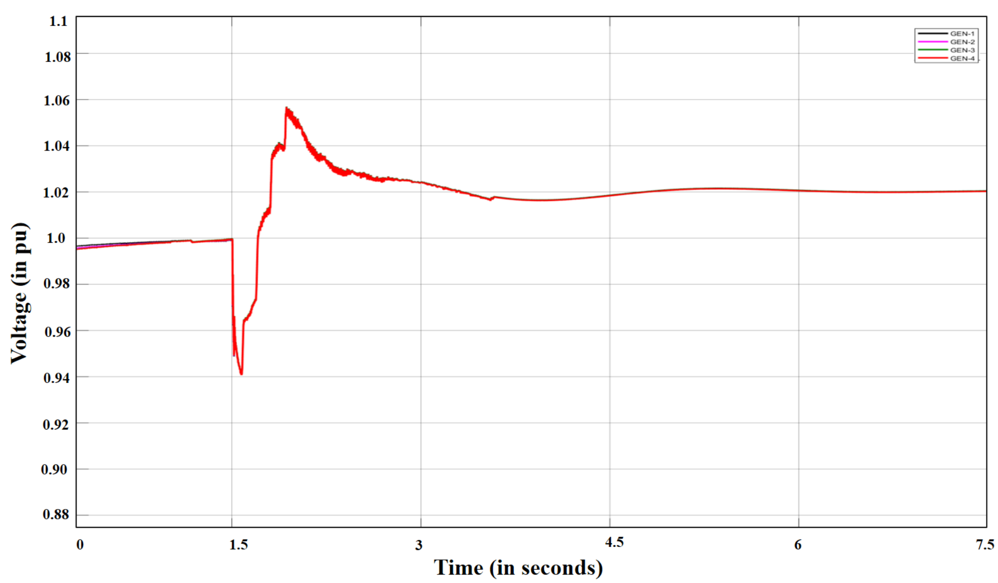

Figure 4.6: PCC Voltage profile in the presence of CLSM for scenario 1.

upon its occurrence.As seen from the above graphs, in the absence of CLSM, the islanded system reaches the under frequency relay pickup setting, 57 HZ (usually 95% of 60 HZ) in about 4 seconds. However, in the presence of CLSM and timely load shedding actions, the islanded system was able to recover the frequency in 4.5 seconds.

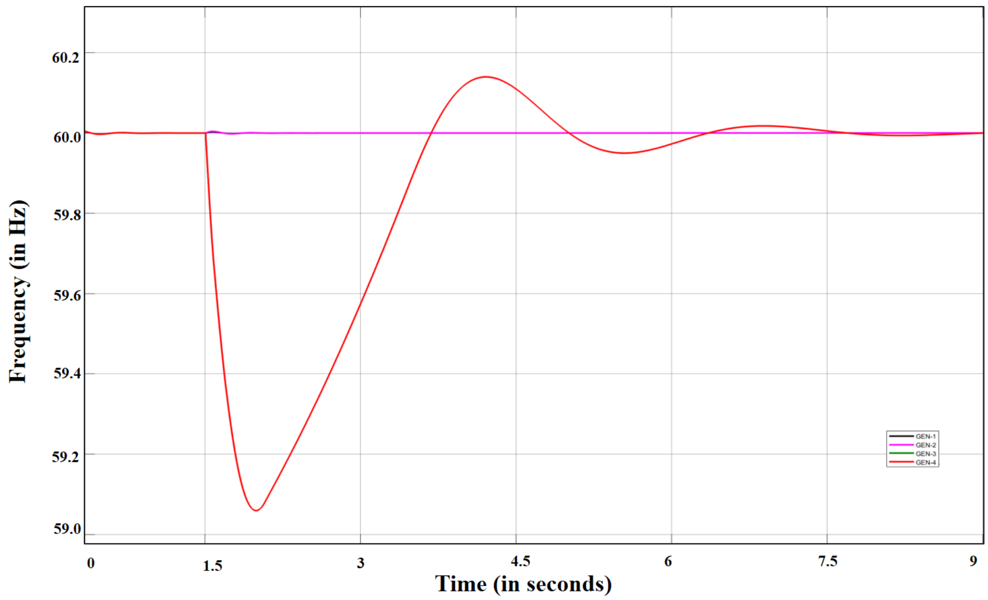

Figure 4.7: PCC Frequency profile in the presence of CLSM for scenario 2.

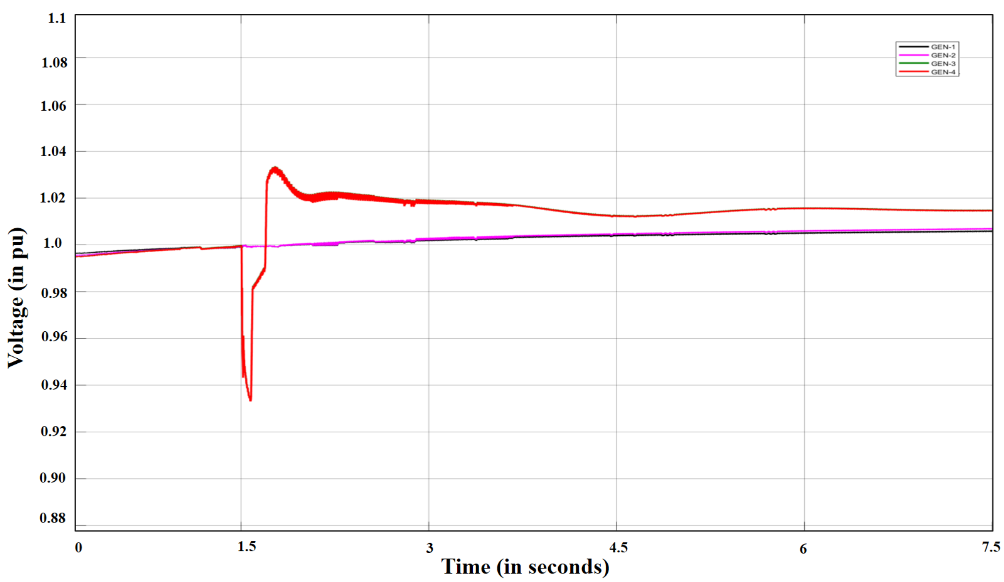

Figure 4.8: PCC Voltage profile in the presence of CLSM for scenario 2.

Additionally, the voltage profile at the PCC was around 1.02 p.u. Similarly, islanding scenario-2 was simulated by tripping line recloser-1 alone. Fig. 4.7 & 4.8 display the frequency and voltage profiles of the islanded system in the presence of CLSM for scenario 2, respectively. A total number of 4 loads (out of 6 loads in this case) were shed to achieve the desired response by the CLSM.

Although the above mentioned scenarios depicted intentional/nuisance tripping of the prptective devices which led to islanding of certain parts or the entirety of the distribution system, the response of the CLSM was also observed during fault scenarios too. Fig. 4.9 depicts the PCC voltage profiles of a particular situation where a 3 phase fault condition at the substation bus leads to the islanding occurence by including the multiple recloser attempts of the feeder breaker/recloser. In this scenario, the permanent 3 phase to ground fault was applied at 0.5s which led to the dip in the voltage profile of the system. The feeder breaker observes the fault condition and trips within 200 ms (around 0.7s as depicted in the figure). The whole distribution system is now islanded and the voltage profile starts recovering due to the performance of CLSM which starts shedding the loads. However, as per standard distribution grade reclosers, the feeder breaker/recloser attempted to reclose around 0.5s of the first trip(around 1.2s as shown in the figure). This leads to the sudden dip in the voltage profile again due to the presence of the permanent fault. The recloser senses this situation and trips again for the final time and islands the distribution system permanently. The CLSM was able to recover the system back to stability which can be also observed from the PCC frequency profile of the system as shown in Fig. 4.10 Hence, it can be seen that the CLSM performed as desired and aids in sustaining an island upon its occurrence.

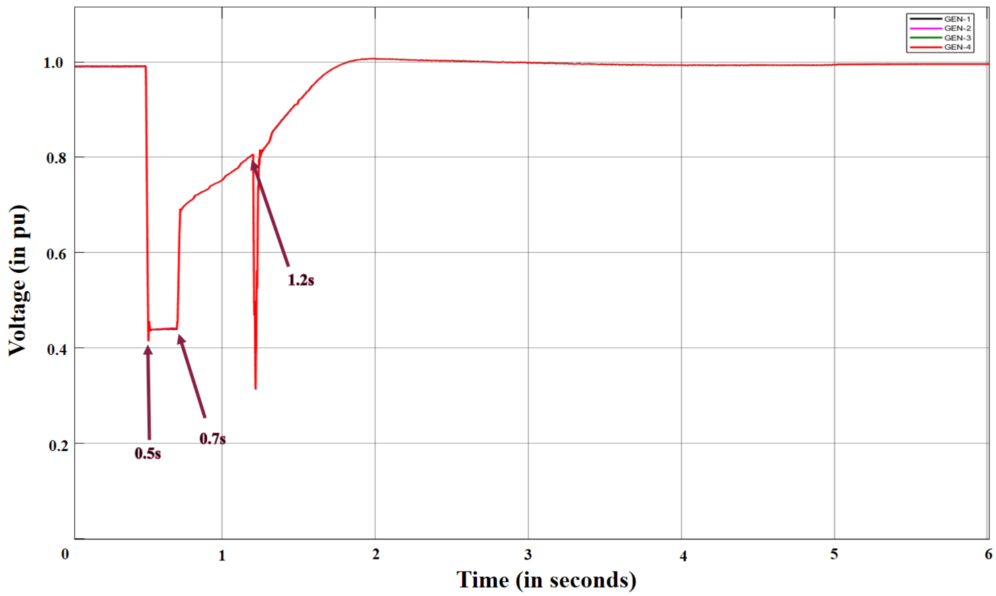

Figure 4.9: PCC voltage profile for a 3phase to ground bus fault at the substation.

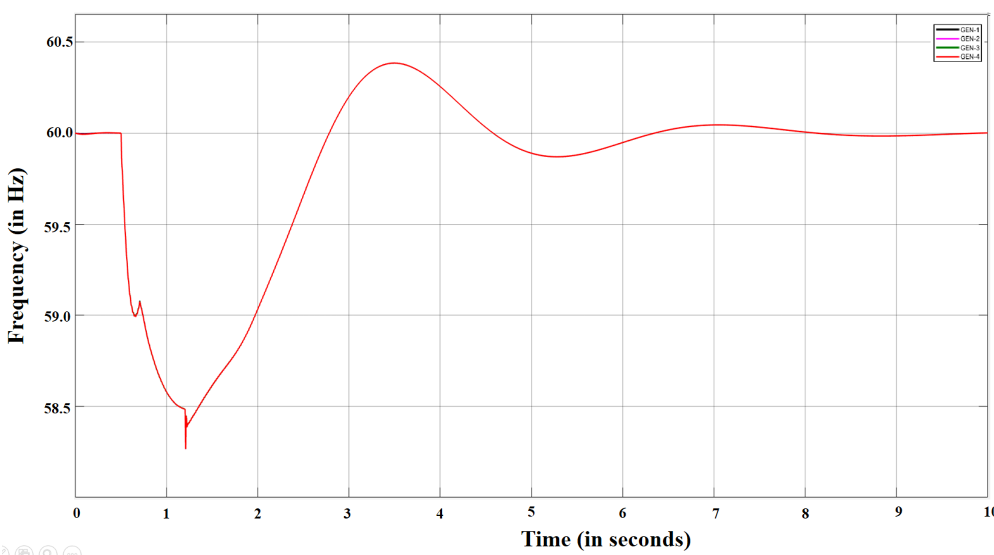

Figure 4.10: PCC frequency profile for a 3phase to ground bus fault at the substation.

4.7 Real-time assessment of Load shedding times incorporating LVRT contrtaints

Although the criticality levels were decided dynamically in real time based on QV analysis, the impact or severity of the islanding occurence couldn't be captured in the earlier sections. The shedding order depicted in Table 4.1 doesn't mention the wait times between consecutive shedding of loads which would heavily rely upon the load-generation power mismatch that occurs upon islanding. One of the clear indicators to determine or gauge this severity would be the voltage profile of the system, especially the ROCOV measurements at crucial nodes such as PCC in the system as discussed in Chapter 3. The recent IEEE-1547 DER interconnection standards[12] specify certain operating procedures for DERs during abnormal conditions based upon low voltage ride through curves. Adhering to these limits can ensure healthiness of the DERs yet providing reactive power support to the system under stress, thus alleviating the overall voltage profile of the system. The standard LVRT curve[2] for category II type DER [12] is illustrated in fig. 4.11

Adhering to the limits yet modifying the LVRT curve, a simplified curve was created for deciding different ranges of the ROCOV regions as depicted by areas 1-4 highlighted in Fig. 4.12. It can be deduced that if the ROCOV measurements at various PCC locations of the system fall under region 1 (referring to more steep ROCOV), the shedding times of the various loads needs to be quicker in order to ensure faster recovery of the system and to prevent unnecessary tripping of the DERs. On the other hand, if the ROCOV measurements at various PCC locations of the system fall under region 4 (referring to relatively less steep ROCOV), the shedding times of the various loads can be relaxed and allow more wait times between consecutive shedding of loads. Such an assessment can be made only with the PCC measuremnets which are usually equipped with high speed communication infrastructure

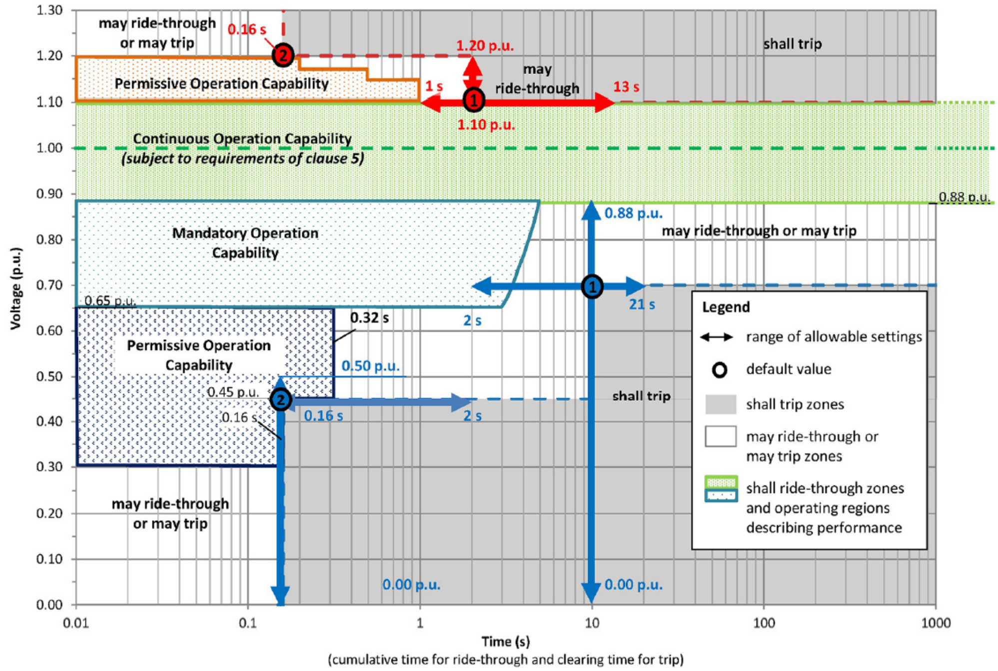

Figure 4.11: DER response to abnormal voltages and voltage ride-through requirements for DER of abnormal operating performance Category-II

(such as fiber optics in most instances). This high speed data can be sent to the CLSM module in real time to assess the shedding wait time intervals of critical loads, thus taking into consideration the severity of the islanding occurence in real-time. Based on Fig. 4.12, the various ROCOV ranges delineating the four regions were calculated and depicted in Table. 4.2 . A heuristic approach based upon multiple simulations of the system was carried out to decide the appropriate shedding wait time interval between consecutive load shedding and provided in table.

Table 4.2: Proposed load shedding wait intervals based upon various ROCOV regions

Region index	Absolute ROCOV range(pu/sec)	Shedding wait time(in ms)
1	>3.625	70
2	>1.34375 & <3.625	150
3	>0.115 & <1.34375	250
4	<0.115	400

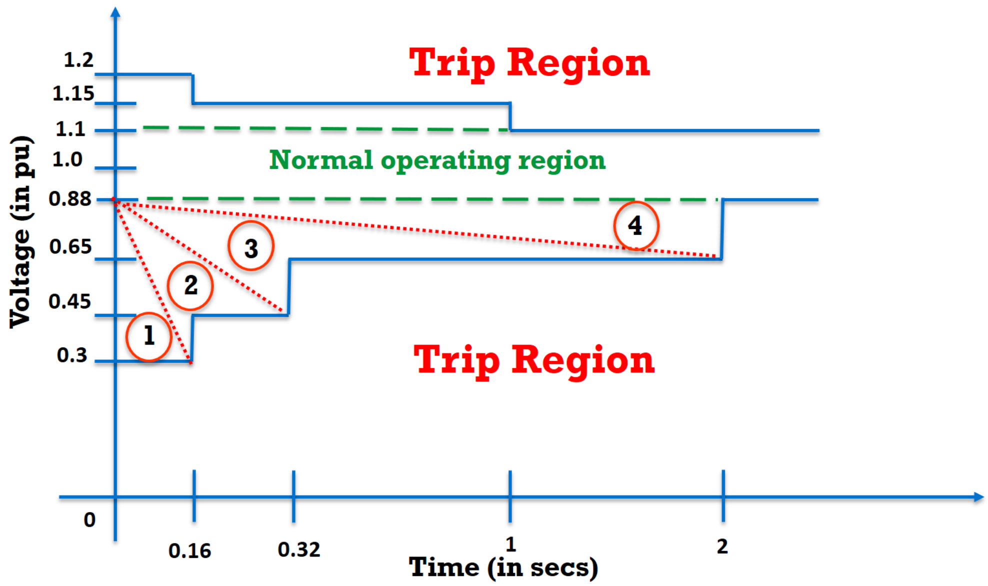

Figure 4.12: Simplified Voltage Ride Through curve for DER of abnormal operating performance Category II

4.7.1 Testing with LVRT constraints

The model as depicted in Fig. 4.1 was executed by modifying the loading conditions and various ROCOV ranges were simulated upon islanding. One such scenario is discussed below, where the ROCOV measurements of the various PCC was found to be around 3.84 pu/sec (hence, lying in region 4 of table) upon islanding the whole distribution system i.e. by opening the main feeder breaker at the substation level. Fig. 4.13- 4.14 shows the frequency of the system as well as the profile of the loads shed if a constant shed time of 150 ms was adopted as explained in earlier sections. It can be seen that only 5 loads were shed with a longer wait time which led to instability of the system and thus the CLSM was not able to perform as intended. However, Fig. 4.15- 4.16 shows the frequency of the system as well as the profile of the loads shed after incorporating the LVRT constraints and adopting a shed time of 70 ms (as outlined in Table. 4.2). In this case a total number of 7 loads were shed quicker than the previous scenario and hence the system was able to recover quickly as can be visualized from Fig. 4.15.

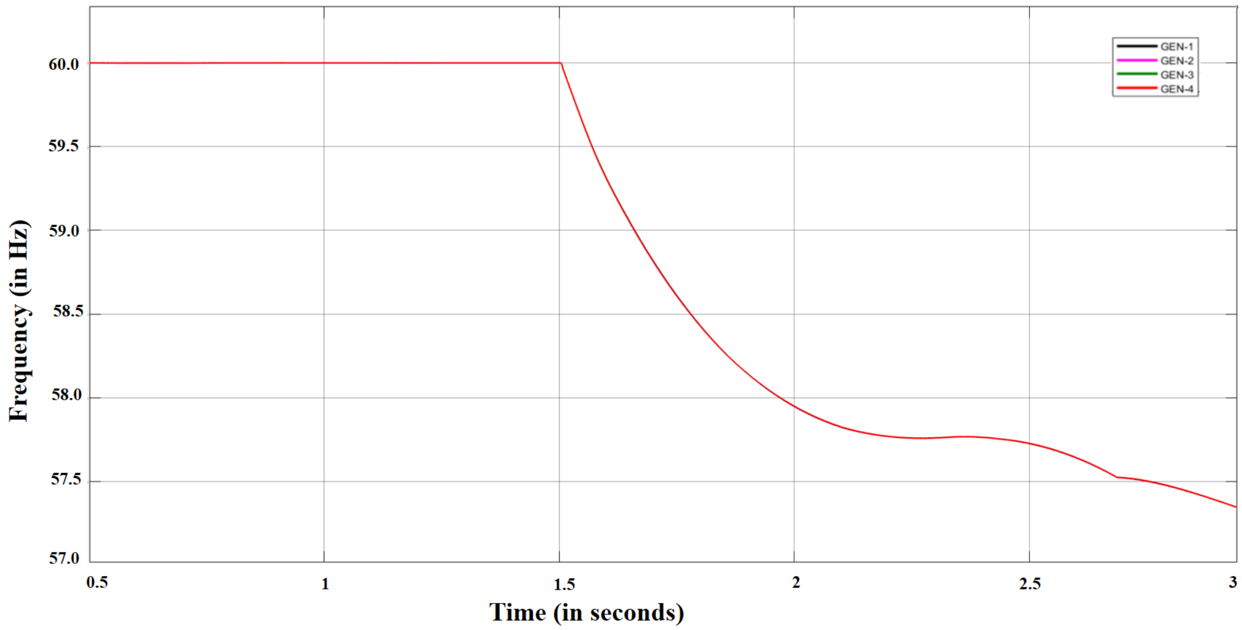

Figure 4.13: Frequency profile of the PCC with a CLSM shedding wait interval of 150ms for Region 4

Hence, a combination of QV analysis to decide the real time criticality level of critical loads along with incorporating LVRT constraints to decide shedding wait time interval for assessing the severity of the islanding occurence can help the CLSM to recover the system sooner than expected. Additionally, in order to aid the CLSM, substation topology status information can be transmitted from the utility side to the CLSM module. With advent of synchrophasor technology, synchrophasor measurements can aid in knowing substation topology and inferring whether a particular feeder breaker has been opened. The following section talks about one such approach.

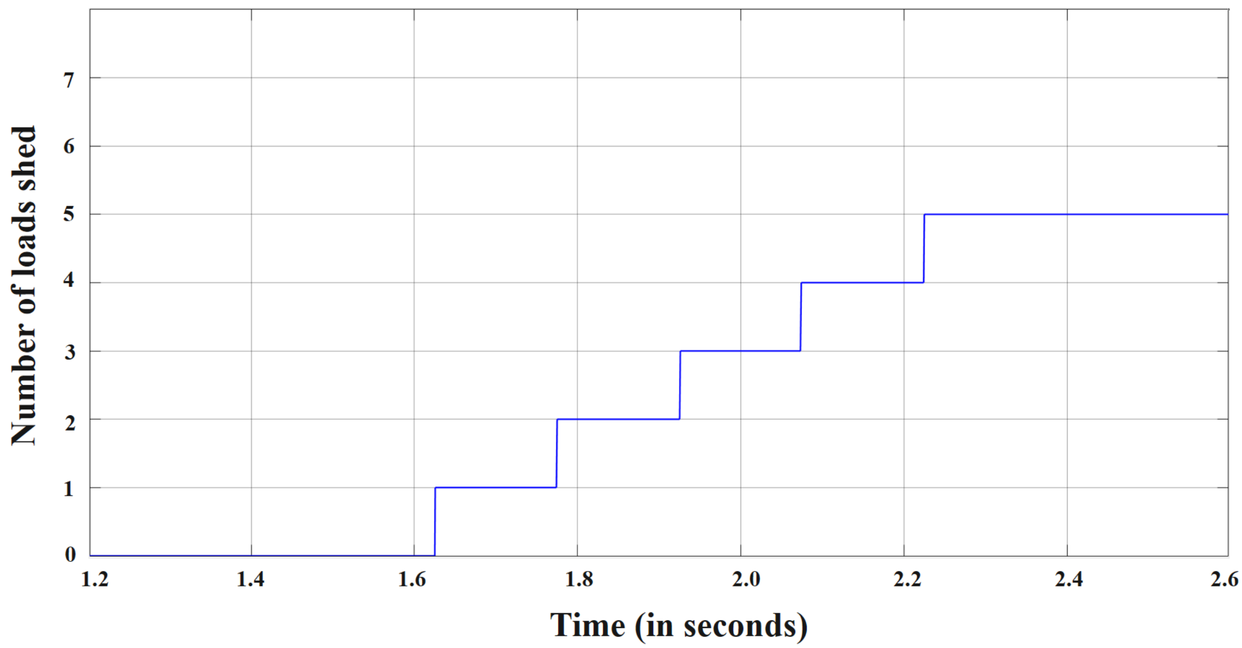

Figure 4.14: Time profile of the number of loads shed with a CLSM shedding wait interval of 150ms for Region 4

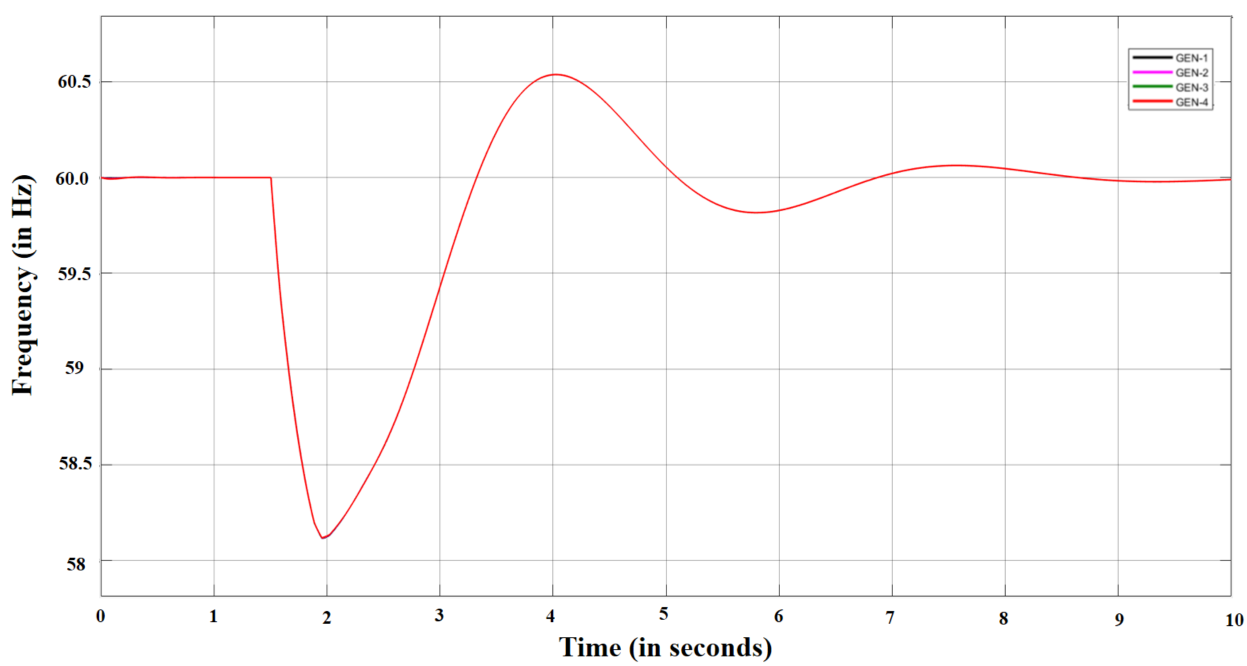

Figure 4.15: Frequency profile of the PCC with a CLSM shedding wait interval of 70ms for Region 4

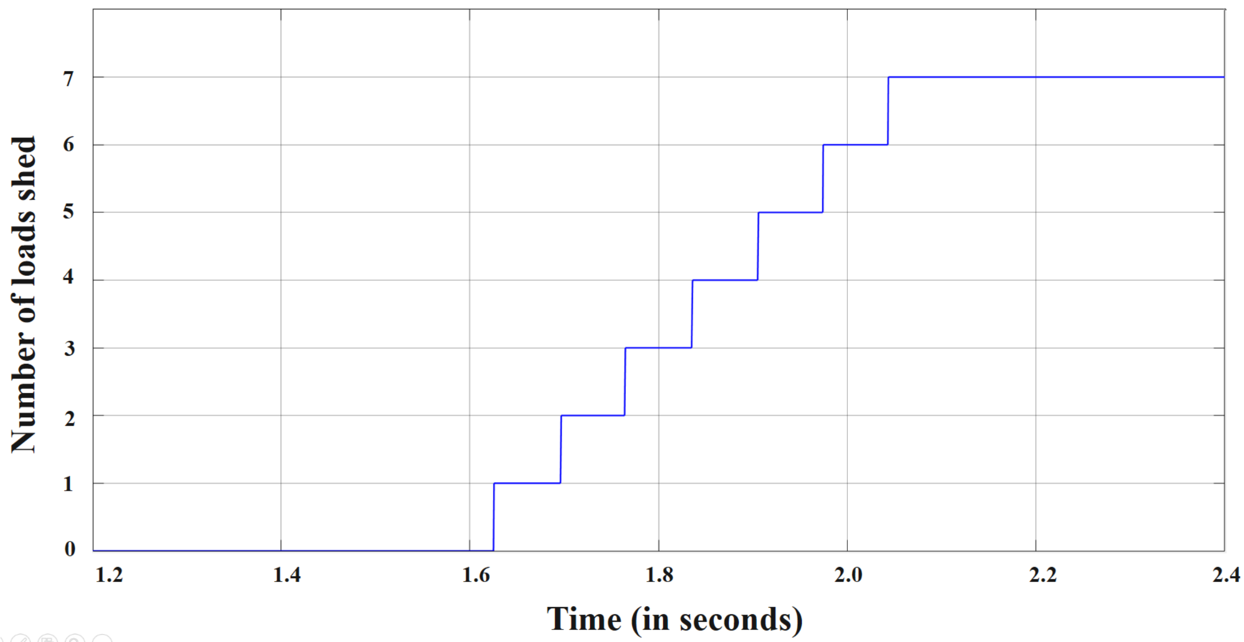

Figure 4.16: Time profile of the number of loads shed with a CLSM shedding wait interval of 70ms for Region 4

4.8 Synchrophasor-based substation topology estimation

4.8.1 Details of the publication

Co-authors: Andreas Schmitt, Kevin D. Jones and Virgilio A. Centeno.[1]

Reference [42]: © 2017 IEEE. Reprinted, with permission, from T. K. Barik, A. Schmitt, K. D. Jones, and V. Centeno, "Empirical determination of voltage phasor angle deviation threshold for synchrophasor-based substation topology estimation," in *2017 North American Power Symposium (NAPS)*, Sept 2017.

[1]The co-authors have contributed in the simulation and testing phase

4.8.2 Background

Accurate knowledge of the topology of a power system is paramount for proper operation of the electric grid. Many analytics, such as optimal power flow and state estimation require the topology of the network to obtain accurate results [44]. Additionally, when the system topology changes from the previous state, the accuracy of any algorithm such as state estimation and in particular Linear State Estimation [43] will suffer until updated with the new system topology. Islanding detection and sustenance techniques as described in earlier sections might get useful information from topology estimation analytics. The methods currently available for topology estimation often make use of time stamped breaker status data. The Topology processor suggested in [45] is capable of processing the topology for those parts of the system which have experienced changes compared to the previous execution cycle. However, as time stamped breaker status is not widely implemented in many current power grids, some of this data may not be available. In the cases where breaker status telemetry is available, the measurements are still subject to errors such as latching or other measurement errors. Thus, these techniques need to be augmented to allow for increased capabilities and use.

Many synchrophasor data measurement systems may use Supervisory Control and Data Acquisition (SCADA) measurements to supplement breaker status data. However, due to the latency issues associated with the SCADA system, these methods are ineffective. The delay incorporated using the SCADA system does not provide a clear picture of each and every frame under consideration especially during switching conditions. Alternatively, phasor measurement units (PMU) themselves can provide breaker telemetry, which can then be used to determine the connectivity of the system. However, the availability of this type of data in synchrophasor data systems is limited to only a few organizations. Where it does exist, it may also be incomplete.

The method described in this section relies upon the concept of equi-potentiality between two nodes inside a particular substation. It states that in an electric power system, the voltage phasor measurements of two nodes that are connected via a breaker (or several breakers across a single voltage level) in a substation should be at equal potential. This is possible due to the minimal impedance between both nodes. Therefore, given voltage phasor measurements on either sides of a switching device it is possible to infer the connectivity between the two nodes. If the difference of two measurements is within a reasonable range, we can assume that the two nodes are connected. However, what is then defined as a reasonable range is a function of network structure and system conditions. Furthermore, the ability to detect this value is also subject to measurement errors. This section develops a methodology for verifying the hypothesis that a reasonable threshold exists and subsequently develops a methodology to empirically determine such a threshold through offline power flow analysis. The resultant values can be used as settings to inform an advanced topology estimation algorithm for CLSM which only rely on synchrophasor data.

4.8.3 Methodology

The methodology presented uses an empirical approach to determine the voltage angle deviation threshold value. The method initially analyzes a bus-branch model of the system to provide a more generic comprehensive analysis to procedurally calculate the angle deviation threshold value in absence of inherent substation topology information. This approach runs a series of power flow analysis where each simulation reconfigures the topology of a bus-branch model at the substation level for possible breaker status configuration converting into standard node-breaker topologies of multiple node-breaker pairs as shown in Fig. 4.17.

It is important to note that this model is introduced with the intention to implement the

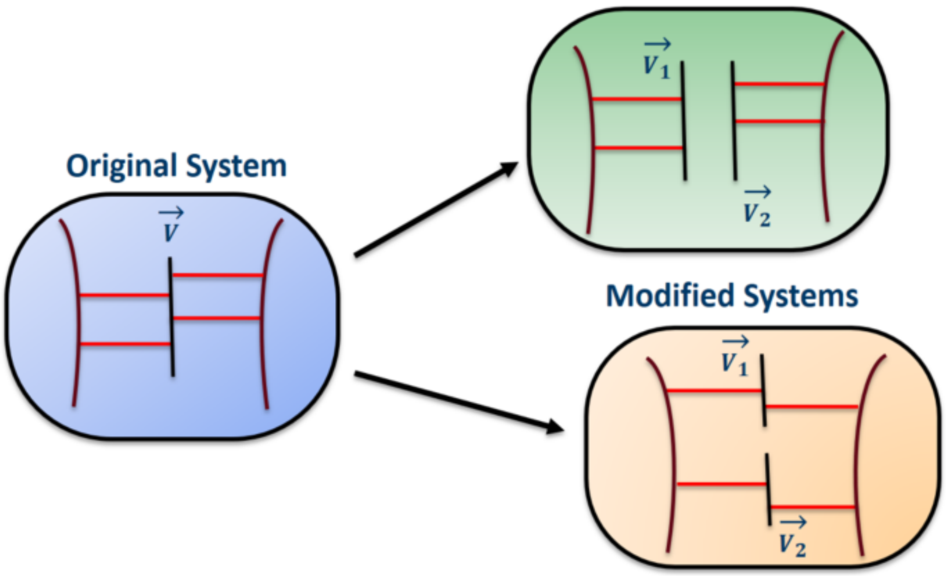

Figure 4.17: Generic Bus Branch model transformation

methodology for practical applications and also to see how the phasor deviation threshold changes in view of practical substation topologies. These designated schemes are Breaker-and-a-half, Double breaker-double bus, Ring bus, and finally single breaker and single bus schemes as shown below in fig. 4.18(a)-(d).

From the power flow analysis, an array of voltage phasor deviations (both angle and magnitude) between disconnected nodes within a substation is created. The resulting data set can then be used to statistically determine the threshold value for a given node-breaker pair. Once the list of all possible disconnected buses inside the substation under consideration is generated along with the difference in voltage phasors (both angle and magnitude) after each power flow, a statistical approach was used to determine the angular deviation threshold. For this study an angular deviation threshold was calculated by studying the cumulative distribution function which would correspond to near about 95% or more probability (which can be user defined in different scenarios) of an angular deviation occurrence greater than the threshold value. The voltage angle deviation threshold calculated in this way allows for the

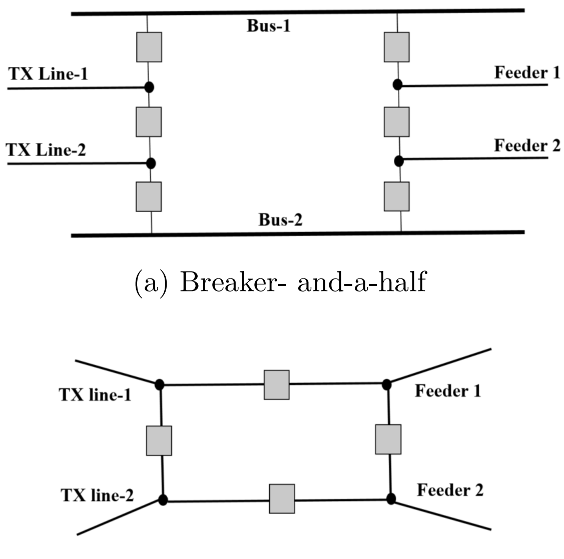

(a) Breaker- and-a-half

(b) Double breaker-double bus

(c) Ring bus

(d) Single breaker single bus

Figure 4.18: Standard node-breaker topologies in substations

selection of a threshold value that is often a statistically significant number, while remaining a realistic value. Ideally, the lower the threshold value is, the more accurate the topology estimation will be. However, due to measurement and noise errors selecting a threshold value that is too small will lead to incorrectly classified connections. Therefore, a probability of 0.95 was selected based upon experience when calculating the threshold value.

4.8.4 Implementation

The methodology was applied to standard node-breaker topology versions of the IEEE 118-Bus system as shown in Fig. 4.19.

Each bus was randomly converted and designed as one of the four standard topologies as discussed earlier. Represented as a histogram, the resulting voltage angle deviations from the complete analysis of the standard node-breaker model are shown in Fig. 4.20. The cumulative distribution function (CDF) of voltage angle deviation between disconnected nodes

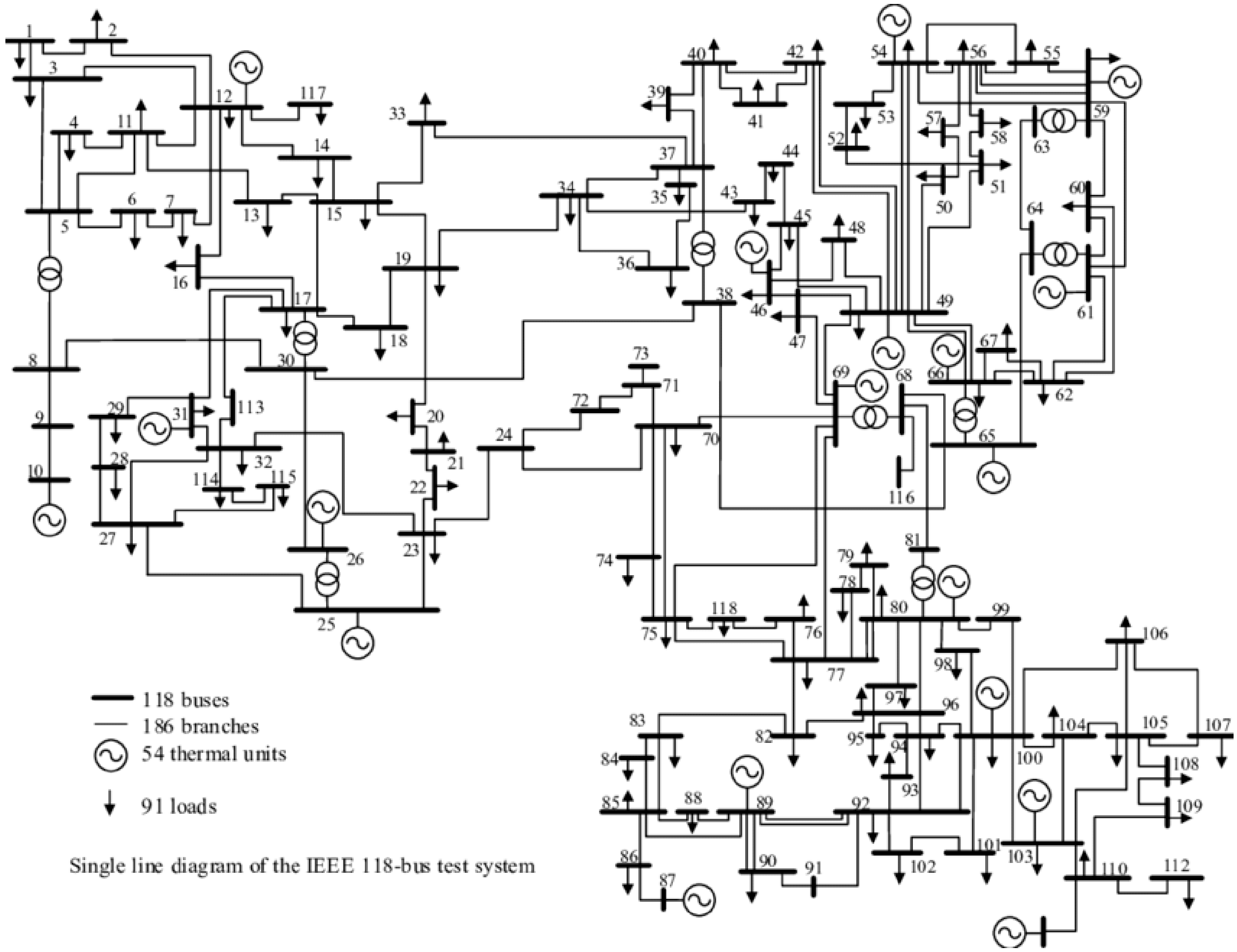

Figure 4.19: IEEE 118 bus test system

is represented in Fig. 4.21. Analysis of this model resulted in a voltage angle deviation threshold of 1.01 degrees for the overall system. This value is associated with a 95% or more probability of an angular deviation occurrence greater than the threshold value. Furthermore, analysis was done to investigate various values of angular deviation threshold for each standard substation topology scheme individually.

It should be noted that the results are system specific and may vary across different parts of the grid. This shows that the characteristics in terms of substation topology being studied will have an impact on the threshold for the system and the threshold value for each system must be found individually analyzing the system under study to obtain accurate results.

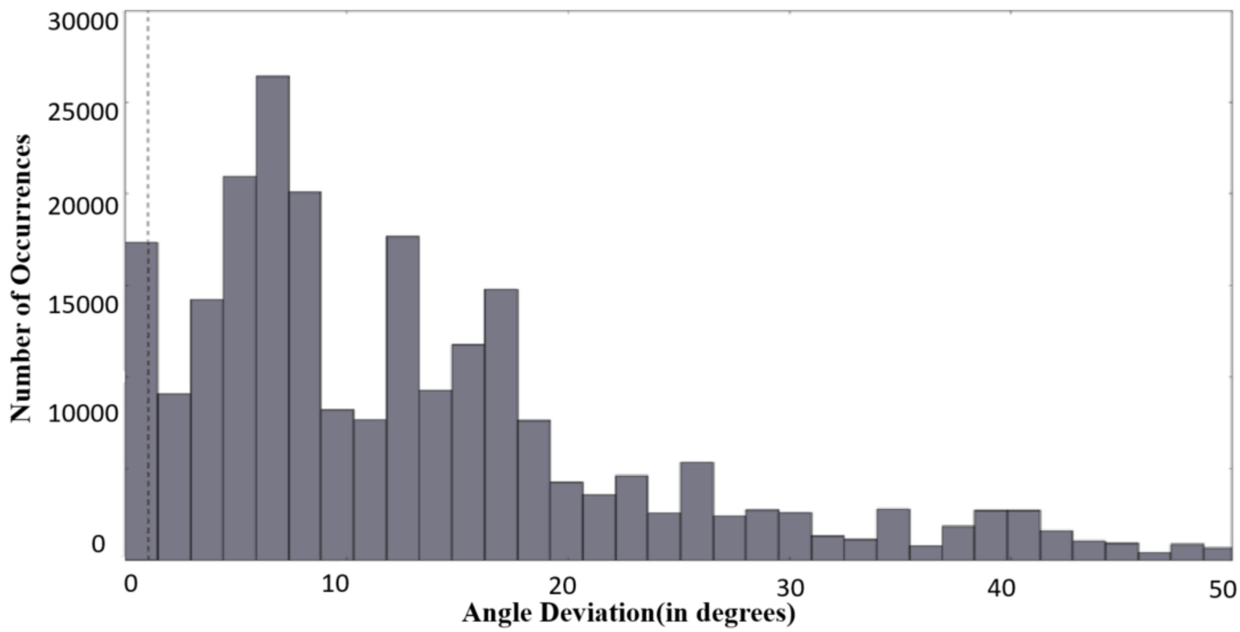

Figure 4.20: Histogram of all the simulated voltage deviations

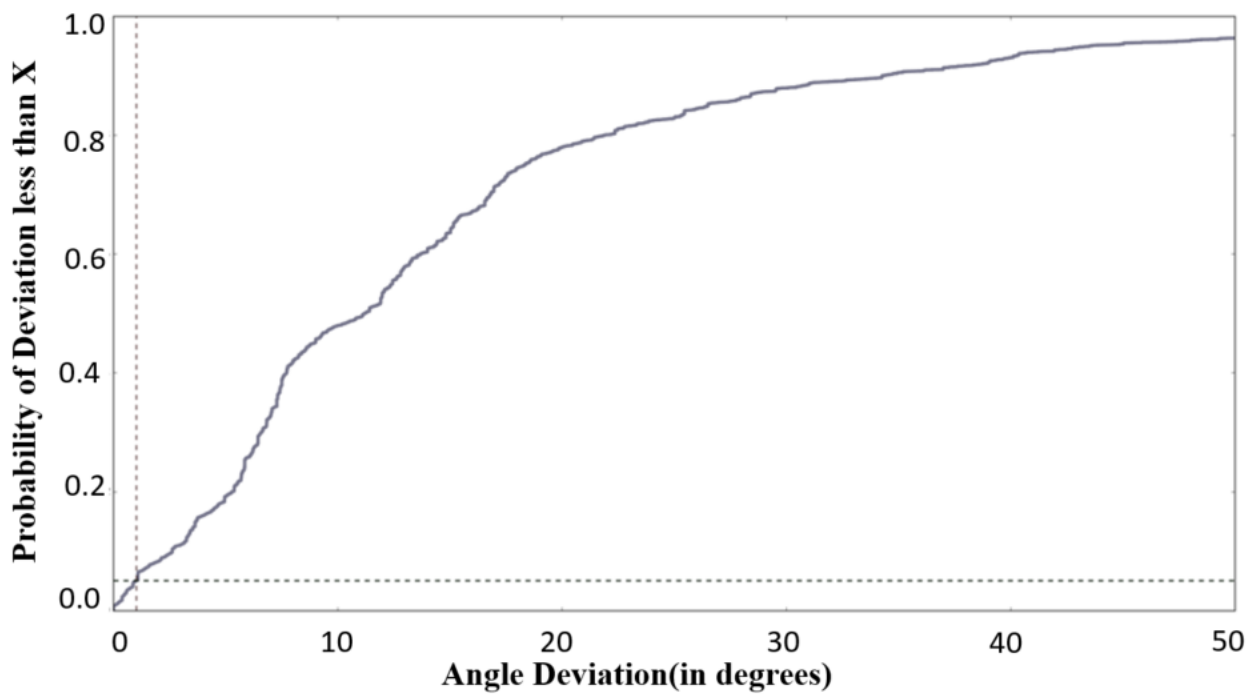

Figure 4.21: CDF of the simulated voltage deviations

Thereafter, the angle deviation threshold was tested for accuracy with over 30,000 randomly generated configurations of the IEEE 118 bus test system. Table 4.3 shows the performance of the methodology.

Table 4.3: Performance of the proposed method against randomly generated configurations

Total no. of cases	30481
Total no. of correct estimated cases	28286
% accuracy	92.8%

Hence, it was corroborated that in the absence of comprehensive breaker status telemetry, synchrophasor measurements themselves can be used as an alternative to breaker status data and can also be used for supplementing breaker status telemetry when it does exist. It was established that nodes which are connected within a substation will have voltage phasor values very close to one another, particularly with respect to phase angle. Therefore, an angular deviation threshold value was empirically found, below which two nodes can be deemed as connected, and thus voltage phasor measurements can be used to check the connectivity between two nodes relying upon such a threshold value. The methodology presented in this section demonstrated how to calculate this threshold for phase angle deviation depending upon substation topology. This method can also be used in conjunction with the Three Phase Linear State Estimator [43] and other synchrophasor-only state estimation techniques, in place of or supplemental to breaker status data to improve its robustness subjected to topological errors.

4.9 Conclusion

A Critical Load Shedding Module (CLSM) was proposed to sustain a section of the distribution system upon islanding in real-time. The minimum infrastructure required to achieve this functionality was studied and presented. The study was done with the consideration of making the technique practically implementable with minimum cost addition. The methodology and algorithm to carry out load and generation shedding were devised. These are based upon analyzing voltage sensitivities to assign priority levels of the critical loads in real-time to prevent voltage and frequency collapse during islanding. The proposed test bench setup was built in MATLAB/Simulink and was validated. The performance of CLSM was evaluated for multiple islanding scenarios based upon the disconnection of appropriate utility devices. It was observed that the CLSM was able to sustain an island upon its occurrence within 3-4 seconds. Thereafter, low voltage ride through constraints were incorporated to decide the load shediing wait interval. This technique caters to the severity of the islanding occurence and hence facilitates smoother recovery of the system. In conclusion, this module would ensure lesser outages of the load, along with serving the maximum amount of load within the service restoration period. Thereafter, a synchrophasor based substation topology estimation technique was also proposed to aid the CLSM to gather the topological knowledge of the system. This would ensure faster detection of islanding phenomenon by the CLSM upon disconnection of the whole distribution grid from the power utility. As an extension to this research, a comprehensive load and generation shedding module for catering both positive and negative ROCOF scenarios can be researched in the future.

Chapter 5

Decentralized Multi-setting Adaptive Distribution Protection Scheme for Directional Overcurrent Relays

5.1 Details of the publication

Co-authors: Virgilio.A.Centeno

Reference [52]: © 2020 IEEE. Reprinted, with permission, from T. K. Barik and V. A. Centeno, "Decentralized multi-setting adaptive distribution protection scheme for directional overcurrent relays," in *2020 IEEE Kansas Power and Energy Conference (KPEC)*, July 2020.

5.2 Abstract

Widespread integration of distributed energy resources (DERs) in the power distribution system has left the conventional protection schemes ineffective in adequately identifying and isolating a fault. Hence, modern protection schemes should be able to adapt to these variations and modify the protective device's settings to ensure effective protection coordination. Although prior works have addressed this issue using extensive communication-

based methods (centralized or peer-to-peer), the actual implementation of these methods is economically less viable shortly considering the present infrastructure. However, with the advent of modern digital relays, protection schemes can be made adaptive yet keeping them decentralized and hence, easily implementable and deployable. The work proposed in this document aspires to achieve this goal by utilizing the commonly used protective devices such as directional overcurrent relays in the power distribution systems by storing versatile setting groups enabling better observability of the relays towards fault identification and isolation in the absence of extensive communication links.

5.3 Introduction

Modern power distribution systems have undergone numerous changes over the last two decades with the wide-scale incorporation of Distributed Energy Resources (DERs) [12]. Although it has increased the resiliency of the distribution system, it has also posed a multitude of challenges to the conventional protection schemes in place. Traditional distribution systems used to be radial with the unidirectional flow of power, and hence, protection coordination among distribution protection devices was relatively more straightforward. However, with large-scale integration of DERs, conventional protection schemes need to be adaptive in nature to ensure proper selectivity and sensitivity towards fault identification and isolation. Additionally, as the percentage of DER penetration in the system increases, the necessity of an adaptive protection scheme increases as the operating scenarios are becoming more complicated, which may cause the short-circuit currents flowing through local relays to vary frequently [53]. Apart from this, fault current availability in the system dynamically changes in real-time with changes in operating conditions. These conditions primarily refer to changes in the topology or connection status of DERs in the system. Many prior works have discussed the concept of adaptive protection addressing these issues. Voltage and impedance-based protection schemes were proposed in [54],[55]. Several adaptive overcurrent (OC) protection schemes [56],[57] were proposed to modify the setting values for local relays by utilizing the high-speed communication networks and employing numerous fault analysis techniques.

Most of these methods rely on the proper operation of the control center. The changing topology of the system is monitored at the Distribution Management System (DMS) by acquiring the status of circuit breakers as well as the connection status of DERs. Based on this information, appropriate adaptive settings of the overcurrent relays are calculated and transmitted back to the modern digital relays via communication links. However, in case of severe weather-induced outages, communication networks might not be functional, and hence, a centralized adaptive protection scheme cannot always be deemed reliable. Previous works [57]-[59] have addressed this issue by proposing peer-to-peer communication within protective devices, making the adaptive protection scheme somewhat decentralized. However, considering the present level of communication infrastructure in most of the distribution systems operated by the utilities around the world, these schemes might not be easily implementable shortly.

Modern digital relays commonly used in distribution system protection have multiple setting group storage as well as programmable logic incorporation functionalities in them. However, these capabilities are not exploited to the fullest and hence, can be utilized to enhance the sensitivity and selectivity of relays towards fault identification and isolation. Multiple versatile settings can be stored to improve relay observability towards faults. The work presented in this chapter puts forth three major improvements over the traditional protection schemes: i) The technique proposes storing of versatile setting groups inside the relays which can mimic the peer-to-peer communication scenario without actual usage of extensive communication links between various distribution system nodes, thus making the proposed scheme easily implementable and deployable;

ii) The proposed relay settings makes the primary protection logic more robust in case of loss of trip signal generated by the primary protection relay;

iii) The proposed scheme also reduces the area of power outage as a part of improved secondary backup protection, ensuring a greater number of loads which can be served with uninterrupted power.

Section 5.4 firstly explains the traditional distribution system protection layout followed by the proposed relay settings to be stored in the relays considered for the development of the adaptive protection scheme. Section 5.5 discusses the operating principles and applications of the proposed scheme. Section 5.6 describes the testing of the proposed methodology and associated results for multiple scenarios on a modified IEEE 13 node test feeder system. Finally, section 5.7 summarizes the work in the paper, outlining the possible scope of future work.

5.4 Distribution System Protection Layout

5.4.1 Conventional distribution system protection layout

Fig. 5.1 shows a typical distribution grid with DER injections at various locations making the system radial yet allowing bi-directional power flow. The feeder is equipped with a feeder breaker near the substation and may consist of downline re-closers, as shown at the different nodes. In contrast, fuses are typically placed on the single or double phase secondary feeders and laterals. Nowadays, each protected 3-phase line segment between two nodes is protected, usually with a re-closer controlled by a digital directional overcurrent relay (DOCR) (ANSI/IEEE 67 Phase/Ground element). Each protected line has a near-end (closer to the utility source end) and a far-end (closer to the consumer side) DOCR as we move downline (highlighted as red boxes in the figure). However, these DOCRs conventionally trip for their assigned forward direction faults (highlighted for node B relays in Fig. 5.1 as an example).

Although the work proposed in this paper advocates for a decentralized protection scheme, which does not require communication links or channels across the whole line length, it should be noted, that the relays on the same node are usually housed in the same junction box and hence can communicate easily with negligible delays. For example, although the relays on node B (B_1, B_2, B_3, B_4) are deployed to clear faults for separate lines, they are housed near node B and hence can communicate with each other. Therefore, the term decentralized refers to the technique being local at each node rather than being local for every relay, thus eliminating the need for extensive communication links between two nodes in the distribution system.

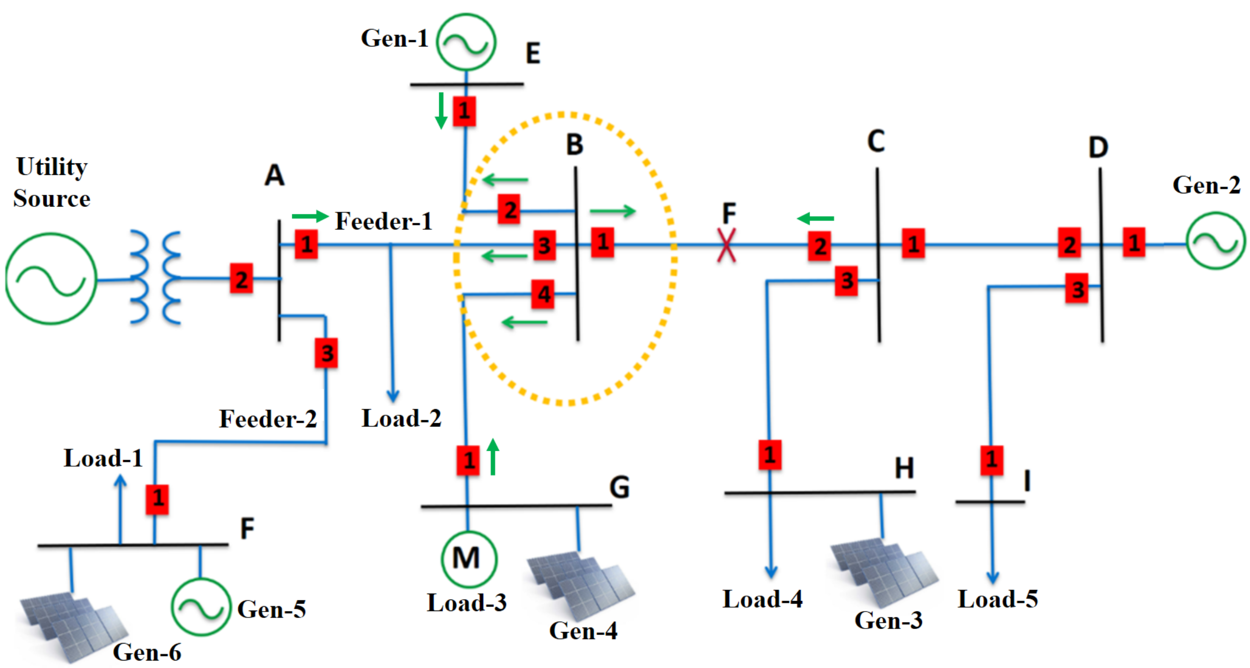

Figure 5.1: A typical distribution system protection scheme layout.

5.4.2 Traditional DOCR settings

A typical DOCR consists of two elements. The first element is the directional element, which detects the direction of current based upon the relative angle between current and voltage signals fed to the relay with voltage signal acting as the polarizing quantity[60]. The second element is the time overcurrent element, which has two values to be set, which are the Pickup current (I_p) value and Time Dial Setting (TDS). Ip is the minimum current value for which the relay operates. TDS defines the operating time (t) of the relay for each fault current value (I_f) as seen by the relay) and is given as a curve t vs M, where M refers to multiples of pickup current as is calculated as per eqn. 5.1,

$$M = \frac{I_f}{I_p}. \tag{5.1}$$

These relays adhere to inverse overcurrent characteristics necessary to ensure protection coordination concerned with the bi-directional nature of the power flow in distribution systems. The relay operating time is a non-linear function of both TDS and I_p as shown in Fig. 5.2 [60].

The time characteristics of overcurrent relay are generally non-linear and can be approximated [61] as per eqn. 5.2:

$$t = \frac{\alpha * TDS}{M^{\beta} - 1}. \tag{5.2}$$

Where, α, β are constants for IEC standard time overcurrent characteristics for various types of overcurrent relays as shown in Table. 5.1. For this work, Normal Inverse overcurrent relays are used, which have parameters, α=0.14 and β= 0.02 [11].

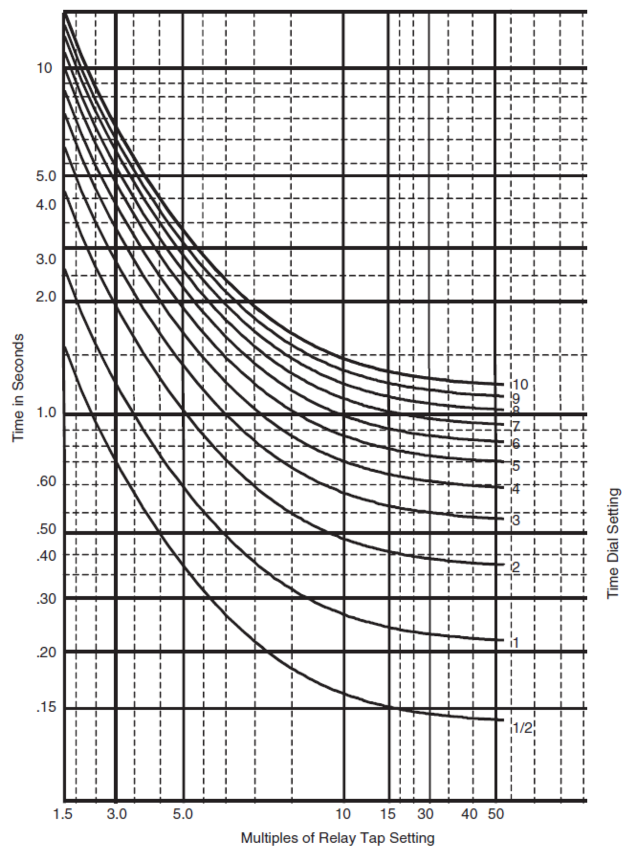

Figure 5.2: Time delay overcurrent relay characteristics.

Table 5.1: Constants for IEC standard time overcurrent characteristics

Type of Characteristics	α	β
Normal Inverse	0.14	0.02
Very Inverse	13.5	1
Extremely Inverse	80	2

The pickup current value for a relay is dependent on the maximum fault current (I_{fmax}) the relay can observe as well as the load current (I_{load}) passing through it in normal conditions [15]. The pickup current value has to be a trade-off between both these values. Generally, the pickup current for this work is calculated as:

$$I_p = \frac{1}{2}\left[\frac{I_{fmax}}{3} + 2I_{load}\right]. \tag{5.3}$$

Such an approach ensures proper dependability and security characteristics for the relay by setting the value of pickup current between I_{fmax} and I_{load} with considerable margins from either extreme. Proper protection coordination is achieved by selecting the appropriate time-current curves of these devices based on prior offline short circuit analysis of the system. The TDS of the relays are set for achieving proper protection time coordination. Firstly, the nearest relay acting as a primary protection device would clear any fault in the system. However, if it fails then, the fault should be cleared by a secondary relay acting as backup protection after a certain coordinated time interval (CTI) which is ensured by setting up different TDS for the various relays based on the overcurrent relay characteristics [60]. It should be noted that the pickup current value for a relay is depended both on the maximum fault current (I_{fmax}) it can observe as well as the load current (I_{load}) passing through the relay in normal conditions. In this work, pickup currents are calculated taking a trade-off between both these quantities as observed by the various relays to ensure proper dependability and security characteristics of the proposed adaptive protection scheme.

5.4.3 Proposed versatile DOCR Settings

The proposed DOCR adaptive protection scheme advocates for storing two sets of settings for each DOCR as presented below.

A. Forward protection settings (FPS):

The forward protection settings consist of P_f, D_f, TDS_f

Where,

P_f = Pickup current in the forward direction.

D_f = Directional element pickup binary variable, which is 1 in the forward direction and 0 in the reverse direction.

TDS_f = Time dial setting of the relay set for protection coordination for faults in the forward direction.

The forward direction refers to the direction which the relays must observe to trip for fault clearing. For example, referring to the Fig. 5.1, the forward direction of relay B_1 would be downline, observing towards line BC. Similarly, the forward direction of relay B_3 would be upstream, observing towards line BA. The relay is provided with these settings to trip as intended, similar to the conventional DOCR protection scheme. Once P_f and D_f settings are picked up, the relay generates a Forward Fault indication (FFI) as a binary variable bit, which can be communicated with the adjacent relays on the same node.

B. Reverse protection settings (RPS):

The reverse protection settings consist of P_r, D_r, TDS_r.

Where,

P_r = Pickup current in the reverse direction

D_r = Directional element pickup binary variable, which is 1 in the reverse direction and 0 in the forward direction.

TDS_r = Time dial setting of the relay set for protection coordination for faults in the reverse direction.

The reverse direction refers to the opposite of the forward direction, as explained earlier. For example, referring to Fig. 5.1, the reverse direction of relay B_1 would be upstream, and the reverse direction of relay B_3 would be downline. The reason for adding these additional settings is to check whether a fault would be picked up by the other end relay of the protected line or not. In other words, for example, the RPS of relay B_3 would be set in such a way that it would be picked up if FFI of relay A_1 is 1. In such an approach, the relay B_3 would sense if A_1 picked up for a fault F (as shown in Fig. 5.1), even in the absence of peer-to-peer communication.

However, in some particular cases, the RPS of a relay can be set equal to the FPS of the relay on the other end of the line in case there are no taps or laterals injecting current in between the protected lines. These settings, in a way, can be utilized to aid the primary protection relays and even act as intermediate secondary backup protection for fault clearing if required. Once P_r and D_r settings are picked up, the relay generates a Reverse Fault indication (RFI) as a binary variable bit, which can be communicated with the adjacent relays on the same node. It should be noted that these relay settings need to be calculated individually, based upon extensive offline short circuit analysis of the distribution model, to ensure proper sensitivity and selectivity of relay operations. These settings would be stored in the DOCRs and can be updated during periodical relay maintenance phases.

5.4.4 Time coordination criteria

The TDS of the relays are set appropriately to provide proper time coordination for fault clearing. We can define three sets of relays for clearing any fault.

1) *Set* P: refers to the primary set of the relays responsible for primary protection for a particular fault clearing. For example, referring to Fig. 5.1, if we consider a fault F on line BC, the relays B_1 and C_2 would act as primary protection and would constitute *Set* P_F.

2) *Set* S: refers to the secondary set of the relays responsible for secondary backup protection for fault clearing. Usually, these are the adjacent relays on the same node of the primary set of relays. For example, *Set* S_{B_1} for relay $B_1 \in P_F$ would consist of relays B_2, B_3, B_4.

3) *Set* T: refers to the tertiary set of the relays responsible for tertiary backup protection for fault clearing. Usually, these are the relays which provide the secondary backup protection in the conventional schemes. For example, *Set* T_{B_1} for relay $B_1 \in P_F$ would be relays A_1, E_1, G_1.

Similar S_{C_2} and T_{C_2} sets would be formed for relay $C_2 \in P_F$ from the consumer end side, respectively. Hence, for fault clearing TDS of the relays should be adjusted as follows:

$$(TDS_{p_i})_f < (TDS_{s_i})_r < (TDS_{t_i})_f. \tag{5.4}$$

Where,

p_i refers to the i^{th} relay in $Set\ P_F$, acting as the primary protection for a particular fault F.
s_i refers to any relay in $Set\ S_{p_i}$, acting as secondary backup protection for fault clearing corresponding to relay p_i.
t_i refers to any relay in $Set\ T_{p_i}$, acting as tertiary backup protection for fault clearing corresponding to relay p_i.

5.5 Operating Principle

5.5.1 Enhanced Primary Protection Logic

In case of a fault F in between nodes B and C, the relay B_1 and C_2 should pick up and act as primary protection and open the breakers at their respective ends. Considering protection coordination from the substation side, due to the addition of the new RPS, B_2, B_3, B_4 would also sense a fault in the reverse direction. Hence, $FFI_{B_1} = 1$ and $RFI_{B_i} = 1$, where, $i = 2, 3, 4$. This added functionality increases the robustness of the primary protection scheme. In the case of loss of a particular signal, the other relays can make an informed decision to correctly detect a fault and isolate it properly. For example, in case of loss of signal from B_1, which fails to trip the appropriate breaker, based upon the informed decision by collecting the RFI signals from adjacent relays, the same breaker could now be tripped promptly, thus making the primary protection logic more effective. The technique can be made even more robust in case of a loss of more than one signal. However, a lower bound on the number of signals required needs to be provided to ensure the correct identification of faults similar to a voting scheme.

5.5.2 Improved Backup Protection Logic

The TDS of the DOCRs are adjusted accordingly to ensure proper time coordination between relays, as explained earlier in section 5.4.4. In case the breaker associated with B_1 fails to operate, the adjacent relays on node B would trip the breakers at their ends due to the proposed time coordination settings, thus acting as the intermediate secondary backup protection. Furthermore, in case any of these breakers at the location of the secondary set of relays fail to trip, the tertiary set of relays would trip their respective breakers after a particular CTI. The added advantage of such a technique is that fault isolation is performed with better accuracy, and backup protection would result in the outage of a smaller area as compared to a much wider area determined in the conventional schemes and is explained clearly in section 5.6.

However, another innovative approach that can be included as a scope for future research would be to focus on modifying the low voltage ride through curve applicable for the different DERs. Recent advancements in the power electronics field can be used to modify the dynamic region of the Low Voltage Ride Through (LVRT) curve to ensure proper protection coordination without violating the IEEE-1547 DER interconnection standards for LVRT curves [12]. Protection coordination would have to be fast enough, and the fault needs to be cleared before the LVRT constraints trip the DER during low voltage conditions. A proper trade-off between the two objectives would ensure proper fault detection and isolation without tripping the DERs.

5.6 Simulation & Testing

5.6.1 Simulink Model

The proposed methodology was validated on a modified IEEE 13 node test feeder system with DER integration modeled in MATLAB/Simulink. Three diesel generator DERs of 10 MW, 3 MW, and 5 MW were included in the distribution system connected to nodes 633, 675, and 680 respectively as shown in Fig. 5.3. Furthermore, two loads emulating as lateral

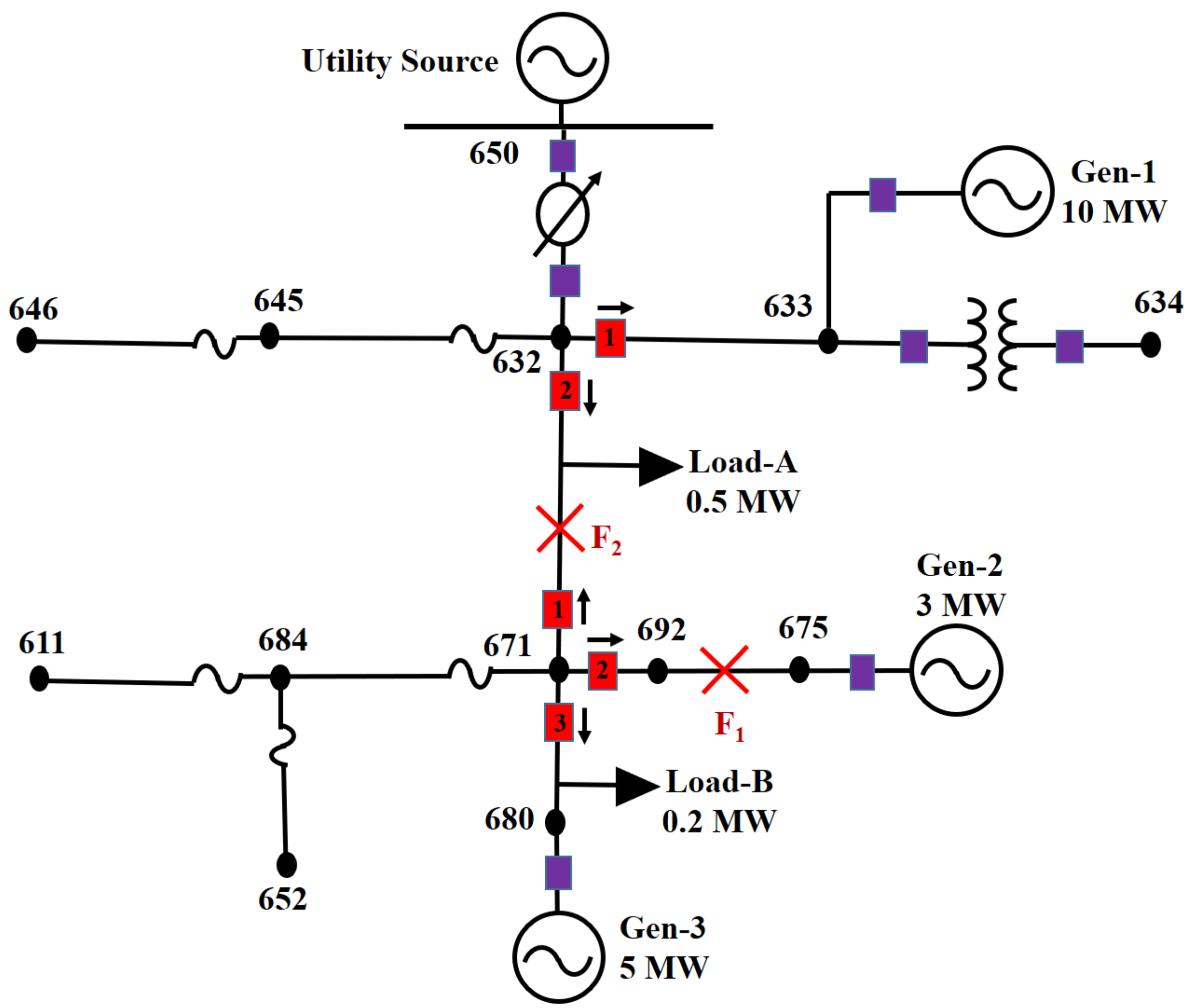

Figure 5.3: Modified IEEE 13 node test feeder system.

taps on a distribution line are introduced in the system. Two 3 phase loads, namely Load-A of 0.5 MW and Load-B of 0.2 MW were added precisely in the middle of the line between nodes 632 and 671 and the line between nodes 671 and 680 respectively as shown in Fig. 5.3. The DOCRs (depicted by red boxes in Fig. 5.3) are placed mostly on the 3-phase primary and secondary feeders with fuses placed on other laterals. The direction of operation of these DOCRs placed in this model is shown in the figure with an arrow beside them. It should be noted that at specific locations of the system, DOCRs might be redundant due to the presence of individual protection schemes of the equipment such as transformers and generators. The individual DERs would have their custom protection schemes located at the point of common coupling in order to protect themselves from system faults if needed. The same holds true for transformer between node 633-634, which would have standard transformer protection schemes to detect any internal as well as external faults. All these individual equipment's protection devices are depicted as purple boxes in Fig. 5.3. This assumption leads to an economical deployment approach of protective relaying in distribution systems.

5.6.2 Testing & Results

The proposed decentralized adaptive protection scheme implemented in the DOCRs located at node 671 is primarily focused in this section. These DOCRs are denoted as $R671_1$, $R671_2$, and $R671_3$ respectively. The FPS and RPS settings of the three relays at this node are set after a comprehensive short circuit analysis of various faults adjacent to these relays. Table 5.2 depicts the proposed relay settings implemented in these relays after the analysis. It should be noted that the RPS of each of these relays is set equal to the FPS of the corresponding relays on the other end of their respective protected lines as described in earlier sections. In other words, RPS of $R671_1$ was set to the FPS of $R632_2$. Additionally, RPS of $R671_2$ and $R671_3$ was set to OC relay settings of Gen-2 relay and Gen-3 relay respectively. However, it should be noted that the TDS values of these three other end relays are set at a higher value of 0.75 to ensure proper protection time coordination.

Table 5.2: Proposed relay settings for relays at Node-671

Proposed Relay Settings	$R671_1$	$R671_2$	$R671_3$
TDS_f	0.5	0.5	0.5
P_f	1200	2500	2500
TDS_r	0.65	0.65	0.65
P_r	2000	800	900

The proposed scheme implemented for the relays at node 671 was tested for 3-phase fault scenarios at various locations. Two of these scenarios are presented in this paper.

Case 1:F1 between node 692 and 675

A 3-phase bolted fault was applied in the middle of the distribution line between node 692 and 675. In this case, primary protection is provided by $R671_2$ from the utility source end and Gen-2 relay from the consumer end constituting the primary relay protection $Set\ P$. However, if $R671_2$ fails to operate its associated breaker, according to the proposed logic, $R671_1$ and $R671_3$ can be used to trip the same breaker.The fault current magnitudes observed by the various relays of node 671 are represented in Fig 5.4.

Comparing the fault currents seen by these DOCRs as shown in Table 5.3 with the RPS settings of $R671_1$ and $R671_3$ from Table 5.2, it can be observed that RFI for both these relays is 1, and is communicated (at the same node) to the breaker to trip, thus adding added robustness to the primary protection scheme. In case the desired breaker does not trip due to any malfunction, secondary backup protection kicks in after some desired time interval depending upon the TDS values set, as discussed earlier. The secondary set of relays in traditional schemes would have been $R632_2$ and Gen-3 relay. However, due to the proposed scheme, secondary $Set\ S$ for $R671_2$ in primary $Set\ P$ contains R6711 and R6713 and the tertiary $Set\ T$ for $R671_2$ in P would consist of $R632_2$ and Gen-3 relay. The fault current

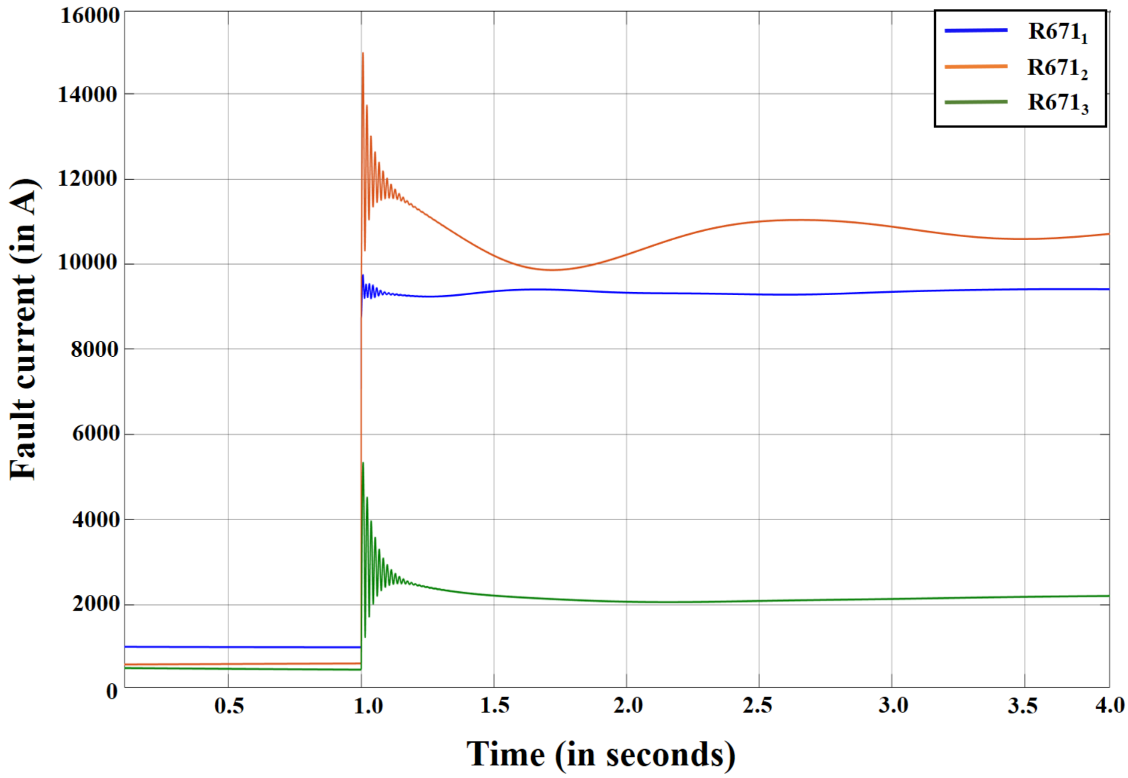

Figure 5.4: Plots for +ve seq fault current magnitudes observed by various relays at Node-671 for Case-1.

observed by all these relays as well the operating time calculated as per Eqn. 5.1 - 5.3, are listed in Table 5.3.

Table 5.3: Proposed relay settings for relays at Node-671

Relays	Observed Fault Current(A)	Operating time(secs)
$R671_2$	10980	2.3
Gen-2 relay	2606	4.3
$R671_1$	9240	2.9
$R671_3$	2366	4.6
$R632_2$	9360	3.3
Gen-3 Relay	2366	5.3

From Table 5.3, it can be observed, that the primary protection relays would ideally operate within 2.3 s and 4.3 s respectively, depending on their pickup currents and TDS values. In case $R671_2$ does not operate as well the associated breaker malfunctions, in the conventional scheme, $R632_2$ and Gen-3 relay would have operated (at 3.3 s and 5.3 s respectively), leading to the lateral load taps of Load-A and B outage. However, due to the proposed logic scheme, $R671_1$ and $R671_3$ acting as secondary protection devices operate earlier (2.9 s and 4.6 s respectively) and isolate the fault. The Load-A and Load-B can still be served from the utility side and Gen-3 side respectively.

Case 2:F2 between node 632 and 671

In this case, a 3-phase bolted fault was applied in the middle of the distribution line between node 632 and 671. In this scenario, the primary protection is provided by $R632_2$ from the utility source end and $R671_1$ from the other end, acting as the relays in primary protection *Set P*. However, if $R671_1$ fails to operate the breaker, according to the proposed logic, $R671_2$ and $R671_3$ can be used to trip the same breaker. As per the proposed scheme, secondary set S for $R671_1$ in primary *Set P* contains $R671_2$ and $R671_3$, and the tertiary *Set T* for $R671_1$ in P would be Gen-2 relay and Gen-3 relay. The fault currents observed by all these relays as well the operating time calculated as per Eqn. 5.2 & 5.3 are listed in Table 5.3. In this case, the primary protection relays would ideally operate within 2.7s and 2.1s, respectively. In the conventional scheme, if $R671_1$ does not pick up and the associated breaker does not trip for F2, Gen-2 relay and Gen-3 relay would have operated, leading to the lateral load taps of Load-B outage. However, due to the proposed logic scheme, $R671_2$ and $R671_3$ acting as secondary protection devices operate earlier (5.3 s and 4.3 s respectively) and isolate the fault.

Table 5.4: Proposed relay settings for relays at Node-671

Relays	Observed Fault Current(A)	Operating time(secs)
$R671_1$	4346	2.7
$R632_2$	10010	2.1
$R671_2$	1818	5.3
$R671_3$	2539	4.3
Gen-2 relay	1818	6.3
Gen-3 Relay	2539	5.0

5.7 Conclusion

A comprehensive decentralized multi-setting adaptive protection scheme for DOCRs in power distribution systems is proposed. The decentralized approach makes this protection scheme practically feasible and easily deployable in the recent future, as it considers zero reliability on extensive communication links over various distribution system nodes. The methodology proposes storing an additional and separate set of pickup current and TDS (Reverse Protection Settings) in the DOCRs in order to provide an additional tier of protection response to fault clearing. These versatile settings correspond to the reverse direction of the DOCRs and need to be coordinated with other relays. The proposed methodology was validated on a modified IEEE 13 node test feeder system built in MATLAB/Simulink. The performance of the proposed protection scheme was evaluated for 3-phase faults at various locations. Such a protection scheme assures superior primary protection in case of loss of signals from the relays involved, along with improved backup protection reducing the area of load outage, and ensuring a higher level of security in the system. However, the technique discussed in this chapter only considered the base topology and do not cater to multiple contingencies of the system. The settings of the protective devices should consider multiple topologies to order to ensure grid resiliency in case of severe weather induced outages. A few such simulation based and analytical approaches are discussed in Chapter 6 & Chapter 7

Chapter 6

K-Medoids Clustering of Setting Groups in Directional Overcurrent Relays for Distribution System Protection

6.1 Details of the publication

Co-authors: Virgilio.A.Centeno

Reference [70]**:** from T. K. Barik and V. A. Centeno, "K - medoids clustering of setting groups in directional overcurrent relays for distribution system protection," in *2020 IEEE Kansas Power and Energy Conference (KPEC)*, July 2020.

6.2 Abstract

Large-scale integration of Distributed Energy Resources (DERs) in power distribution networks has raised concerns for distribution system's protection coordination. Due to the

bi-directional flow of power, Directional Overcurrent Relays (DOCRs) are being widely used in distribution systems. The pickup settings and time dial settings of these DOCRs needs to be modified with changing topologies and added DERs, to ensure proper selectivity and sensitivity towards fault identification and isolation. However, the setting groups that can be stored in DOCRs to accommodate these numerous topologies are limited. The work in this paper discusses the implementation of K-Medoids clustering technique to cluster the numerous grid-connected and islanded topologies of a distribution system based upon the various pickup currents and operating time indices. The testing results generated on a modified IEEE 13 node test feeder system demonstrate the effectiveness of the methodology over prior works.

6.3 Introduction

Traditional distribution system protection relies on the assumption that the distribution system is radial, and the flow of power is unidirectional, i.e., from utility source to consumer end. However, this notion has changed drastically with the addition of Distributed Energy Resources (DERs), and hence, conventional protection schemes need to undergo modifications to correctly identify and isolate faults [12]. With increasing numbers of DERs, the operating scenarios are becoming more complex, resulting in frequent changes in the short-circuit currents flowing through local relays. These scenarios include changes in system topology and the connection status of various DERs in the system. Additionally, with the inclusion of inverter-based generation sources, the short circuit fault MVA of the distribution system has decreased, hence posing a challenge to proper sensitivity of the relays and coordination towards fault clearing. Several adaptive overcurrent (OC) protection schemes [56],[57] were proposed to modify the setting values for local relays by utilizing the high-speed communication networks and employing numerous fault analysis techniques. The changing topology of the system is usually monitored by the Distribution Management System (DMS) at the control center by acquiring the status of circuit breakers as well as the connection status of the various DERs. Based on this information, appropriate settings of the overcurrent relays are calculated online and transmitted back to modern digital relays via communication networks. However, due to multiple tasks at the control center related to monitoring, supervision and control, communication channels may overflow with heavy traffic [71]. Such an action can cause delays in the adaptive protection scheme's response to topology changes. Digital microprocessor-based relays consist of multiple setting group (SG) functionality, which has been one of the basis to design many adaptive schemes in the past [72],[73]. These setting groups may correspond to multiple operating conditions of the system, ensuring proper selectivity and sensitivity of the relay with only one SG being active at one time. Pertaining to numerous possible topologies of the system, suitable relay settings can be computed offline and stored as a separate, distinct setting group. Subsequently, detecting any change in the topology of the network by the DMS, the corresponding SG can be activated on the relay, thus lessening the amount of information to be transmitted back to the relay. The drawback of this method is that the modern commercial relays only allow a limited number of SGs to be stored in them, which is far lesser than the total number of possible system topologies and hence, needs to be classified. Clustering techniques have been used in the past for differentiating healthy and faulty conditions, identifying the fault type, and locating the faulty component of the network [74]-[77]. The work in [4] discusses a K-Means clustering technique to classify possible operating topologies of the network into clusters. However, K-Means technique is highly sensitive to outliers. An extremely large or small data point might result in sub-optimal resultant clustering. In addition, the initial centroid choice might lead to different resultant clusters each time the algorithm is executed. The work presented in this paper puts forth three major contributions:

i) It proposes the implementation of K-Medoids clustering technique using the Partitioning around Medoids (PAM) algorithm [79], which is robust to outliers to categorize the topologies of the system more effectively as compared to previous works;
ii)Additionally, a K-Means ++ algorithm [81] is implemented to initialize the starting medoid positions for producing consistent clustering groups in each execution;
iii) The method is executed considering both pickup current and operating time as the clustering index, to demonstrate the comparison and effectiveness of both approaches.
It should be noted that this work proposes the implementation of K-Medoids clustering technique for selecting only pickup currents for k number of setting groups in a relay. Time dial setting values of the relays would still need to be calculated separately as an optimal relay time coordination problem and can be studied as a part of future work. Section 6.4 explains the layout of the distribution system protection illustrated on a modified IEEE 13 node test feeder system. Section 6.5 discusses the K-Medoids clustering technique using PAM algorithm along with a brief description of K-Means++ algorithm for the initialization of clusters. Section 6.6 describes the testing of the clustering methodology using pickup current and operating time as the clustering index and comparing the results for both scenarios. Lastly, section 6.7 summarizes the work in the paper, outlining the possible scope of future work.

6.4 Test Bench Setup

The work in this paper is validated on a modified IEEE 13 node test feeder system, as shown in Fig. 6.1.Three DERs of 10 MW, 3 MW, and 5 MW were included in the distribution system connected to nodes 633, 675 and 680 respectively, as shown in Fig. 6.1. The direction of operation of the DOCRs (depicted by red boxes in the figure) placed in this model is depicted with an arrow beside each relay. It should be noted that at certain locations of the system, DOCRs might be redundant due to the presence of individual protection schemes of equipment such as transformers and generators. The individual DERs would have their own protection schemes located at the Point of Common Coupling (PCC) in order to protect the equipment from system faults if required. For example, a fault in the line between nodes 671 and 680 would be cleared from the utility source side by the DOCR placed on this line near node 671.

However, to clear the fault from the consumer side, directional overcurrent relays need not be present near node 680 as the protection schemes of the DER can isolate the fault if required. The same holds true also for the transformer between nodes 633 and 634, which would have standard transformer protection schemes to detect any internal or external faults. All these individual equipment's protection devices are depicted as purple boxes in fig. 6.1. This assumption leads to an economical deployment approach of protective relaying in distribution systems. The DOCRs at node 632 are denoted as $R632_1$ and $R632_2$, whereas the DOCRs at node 671 are denoted as $R671_1, R671_2, R671_3$ respectively. This paper would focus on the clustering of the various network topologies in these DOCRs primarily based upon the calculation of near-end faults for each relay for the numerous topologies.

6.5 Clustering Algorithm

Clustering is a technique used to categorize different data items into clusters that share similar features with each other. One of the most widely used and popular technique is the K-Medoids clustering algorithm. K-Medoids technique is less sensitive to outliers and can be made more robust to properly initialize the clusters by incorporating K-Means++ algorithm, as discussed below.

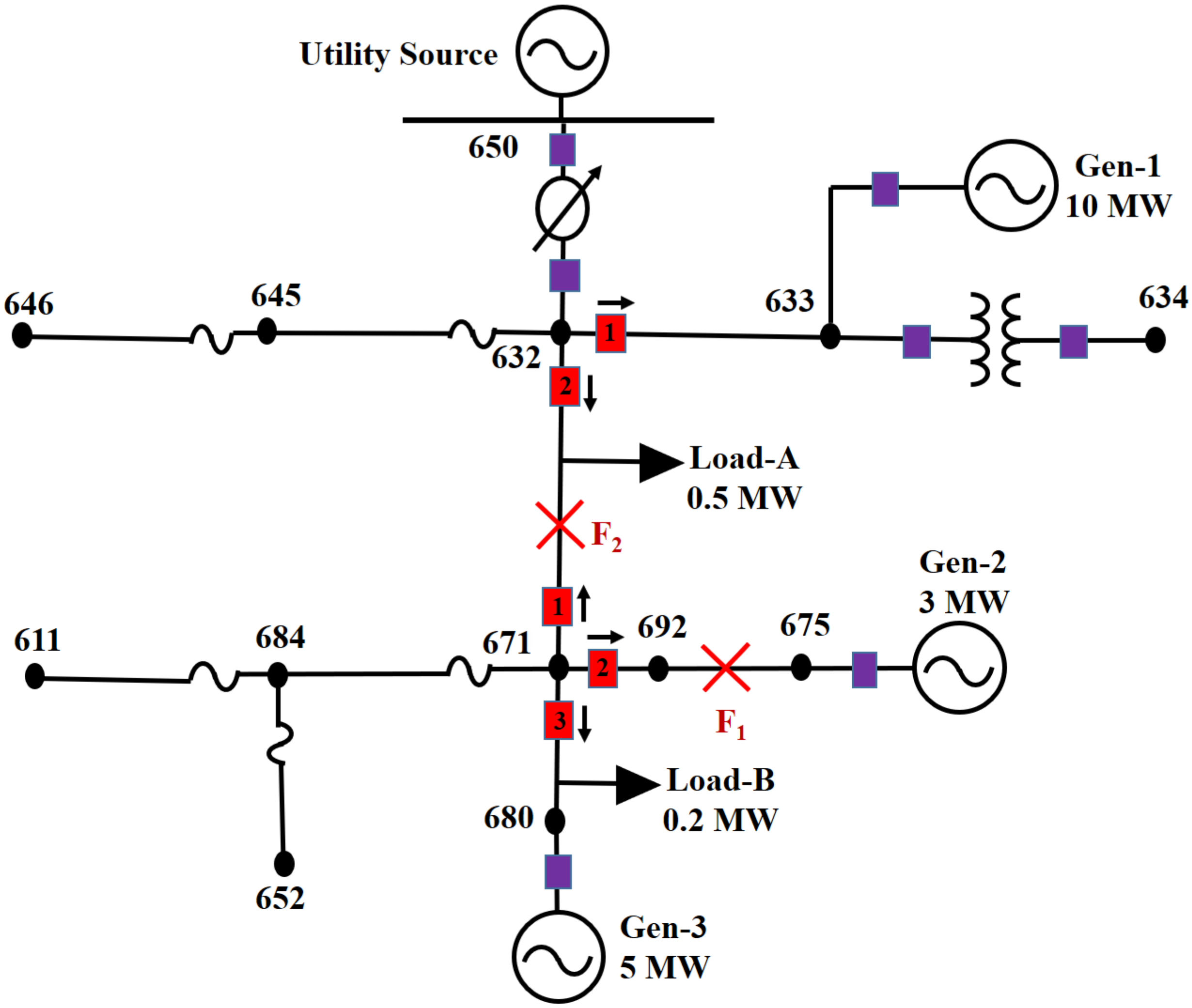

Figure 6.1: Modified IEEE 13 node test feeder system.

6.5.1 K-Medoids PAM Algorithm

Rather than using conventional mean/centroid as used by K-Means technique in prior works [71], K-Medoids technique uses medoids to represent the clusters. The medoid represents a data point in a data set whose average dissimilarity to all the other data points is minimal [80]. It represents the most centrally located data item of the data set. This technique clusters the data set of n objects into k clusters, with the number k known a priori. It is more robust to noise and outliers as compared to K-Means because it minimizes a sum of pairwise dissimilarities (Manhattan distances) instead of a sum of squared Euclidean distances [79],[80]. A commonly used K-Medoids algorithm is the Partitioning Around Medoids (PAM) algorithm, the steps of which are explained below:

1. Specify the total number of data points n in the dataset X as well as the total number of clusters k.

2. Choose k data points as the initial medoids at random.

3. Calculate the Manhattan distances between data points and the medoids and assign each data point to a cluster with the nearest medoid.

$$D_{ij} = \sum_{p=1}^{d} |x_{ip} - m_{jp}|. \tag{6.1}$$

Where,

D_{ij} is the Manhattan distance between datapoint x_i and medoid m_j in d dimensional space. $i = 1, 2, ..., n$ and $j = 1, 2, ..., k$.

4. Once the data points are assigned to k clusters with respective medoids, calculate the cost given by:

$$cost = \sum_{j=1}^{k} \sum_{\forall i: x_j \in C_j} D_{ij} \tag{6.2}$$

Where,

C_j is the j^{th} cluster with m_j as the medoid.

5. For each pair of non-medoid datapoint x_i and selected medoid m_j, first swap x_i with m_j as the medoid and then re-compute the new cost following steps 3 and 4 and finally calculate the total swapping cost S_{ij} given by:

$$S_{ij} = New\ Cost - Original\ Cost \tag{6.3}$$

For each pair of x_i and m_j, if $S_{ij} < 0$, m_j is replaced by x_i, else undo the swap.

6. Repeat steps 3-5 until there is no change of the medoids.

Although PAM works efficiently for small data sets, the performance deteriorates for large data sets. As the data set in the test system used in this work is relatively small, K-Medoids using PAM algorithm is primarily used. However, in the case of large datasets, CLARA (CLustering LARge Applications) algorithm [80] can be used to enhance the performance of the K-Medoids technique. Irrespective of the algorithm used, the focus of the work in this paper is primarily to demonstrate the effectiveness of K-Medoids algorithm in general.
One of the other drawbacks of directly applying K-Medoids clustering technique is that, based upon the initial choice of medoid locations, the method might produce different sub-optimal resultant clustering groups with each execution. To provide similar results in each iteration, the medoids at the beginning can be initialized using the K-Means++ algorithm [81]. The algorithm tries to spread the initial k centroids out so that they are far apart from each other. The following subsection explains the K-Means++ Algorithm.

6.5.2 K-Means++ Algorithm

One of the other drawbacks of simply applying K-Medoids clustering technique is that, based upon the initial choice of medoid locations, the technique might produce different sub-optimal resultant clustering groups with each execution. In order to produce similar results in each iteration, the medoids at the beginning can be initialized using the K-Means++ algorithm. The algorithm tries to spread the initial k centroids out so that they are far apart from each other. The K-Means++ algorithm for choosing these k initial centroids is explained as follows:

1. Arbitrarily select a datapoint from the data set, X as the first centroid c_1.

2. Calculate Euclidean distances from each datapoint to c_1. Denote the distance between c_j and a datapoint x_m as $d(x_m, c_j)$.

3. Randomly choose the next centroid, c_2 from X with probability:

$$Probability_{c_2} = \frac{d^2(x_m, c_1)}{\sum_{j=1}^{n} d^2(x_j, c_1)} \tag{6.4}$$

4. Similarly to choose centroid j:

a. Calculate the distances from each datapoint to each centroid, and assign each datapoint to a cluster based on the closest centroid.

b. For $m = 1, 2, .., n$ and $p = 1, 2, ..., j–1$, randomly select centroid j, c_j from X with probability:

$$Probability_{c_j} = \frac{d^2(x_m, c_p)}{\sum_{\forall h: x_h \in S_p} d^2(x_h, c_p)} \tag{6.5}$$

Where,

S_p is the set of all observations nearest to centroid c_p and x_m belongs to S_p.

5. Repeat step 4 until k centroids are chosen.

The resulting k centroids from the algorithm can then be selected as the initial k medoids for the K-medoids PAM algorithm as discussed before.

6.6 Simulation Testing

6.6.1 Simulink Model Data

The modified IEEE 13 node test feeder model explained earlier is built in MATLAB/Simulink. The fault data for all the five DOCRs (depicted in fig. 6.1), was generated by applying a 3-phase bolted fault in front of each relay. It was noted that the fault data for $R632_1$ and $R632_2$ weren't widely distributed due to their location as well as the placement of DERs nearby. Hence, only the results of $R671_1$, $R671_2$ and $R671_3$ are shown in this section. Various contingencies were simulated for generating the fault data. The grid-connected base case is when the distribution system is connected to the utility source. The case in which the whole distribution system is disconnected from the utility source (632 disconnected from 650) is termed as the islanded base case.

Hereafter, based upon the disconnection of various components of the distribution system such as lines and transformer, numerous topologies were created for generating fault data. Eleven contingencies in the system were considered to generate a total number of 22 separate topologies with node 650 connected and disconnected from the distribution system hence, emulating grid-connected and islanded scenarios. However, based upon different topologies, the normal load current though the relay would also change and needs to be considered for deciding the pickup current in each scenario. Additionally, it should be noted that depending upon specific contingencies, each DOCR might not operate in some particular topologies and pickup currents for these DOCRs would not exist. Hence, various relays have different total number of topologies that are studied for the results. The pickup current for individual relays for the various scenarios was calculated based on Eqn. 5.3 and the operating time was calculated using $TDS = 1$ and I_{fmax} values for each relay and using Eqn. 5.1 & 5.2.

6.6.2 Testing & Results

Firstly, the K-Medoids clustering technique was applied to cluster the various topologies based upon the pickup current. Modern digital relays usually can store 2-6 relay setting groups and hence, for the purpose of study in this work, the number of clusters, k is set equal to 3. The results of the K-Medoids clustering technique based upon pickup current are shown in Fig. 6.2 along with K-Means technique to demonstrate the comparison between both methods. The pickup currents for various topologies for each of the three DOCR are sorted in ascending order and depicted in Fig. 6.2(a)-(c). As can be seen from Fig. 6.2(d)-(i), both the techniques produced varied results. For example, in case of $R671_2$, all the topologies were clustered similarly by both the techniques.

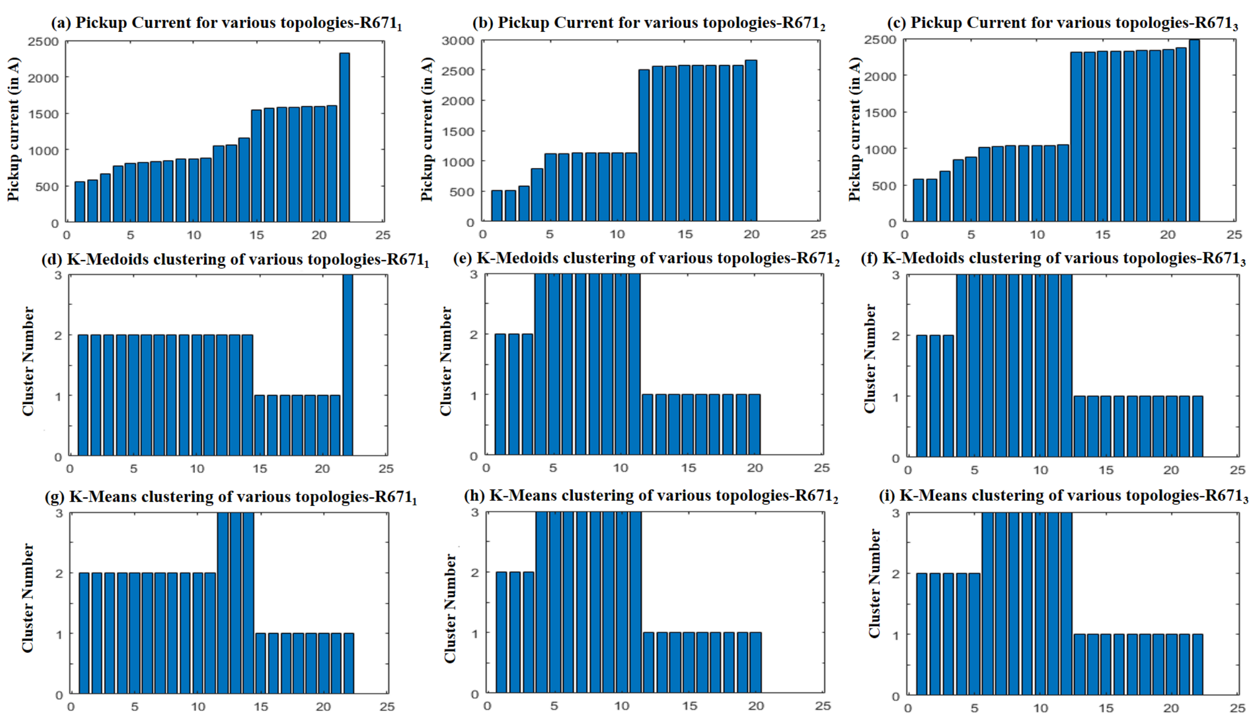

Figure 6.2: Comparison of K-Medoids and K-Means clustering techniques based on pickup currents for various topologies for $R671_1$, $R671_2$ and $R671_3$

However, it can be observed that for topology number 22 (last topology in Fig. 6.2(a)) in case of $R671_1$, the pickup current is 2324 A and K-Means technique clubbed it in a cluster having a lowest value of 1548 A. The difference between these two datapoints is 776 A. This results in a pickup current value (centroid position) of 1674 A. On the contrary, K-medoids technique clustered topologies 1-14 together, where the maximum difference of pickup currents between lowest and highest datapoints in the group is 490 A. Yet the K-Means technique clustered three of these topologies separately as shown in fig. 6.2(g). This analysis shows the effectiveness of K-Medoids techniques and its robustness in the presence of outliers. Therefore, the three setting groups of pickup current values corresponding to the clusters should be set at the medoid positions, which in this case are 1578A, 850A and 2324A respectively. Similar conclusions can also be drawn in the case of $R671_3$ and the clustering of its various topologies.

Furthermore, the K-Medoids technique was applied to the operating time dataset and was compared with K-Means algorithm. Results pertaining to $R671_3$ are only depicted in Fig. 6.3(a)-(c). The topologies arranged in this figure correspond to the topology order for $R671_3$ in Fig. 6.3(c) for better understanding. It can be seen that K-medoids clustered these topologies appropriately as compared to K-Means technique. K-Means technique clustered topologies 1-3 together even if the maximum difference of operating time between any two datapoints in this cluster is 1.3 seconds. However, topologies 4, 5 and 20, 21, 22 are clustered separately even though the maximum difference between cluster 1 and 3 in K-means is 0.7 seconds. It should be noted that grouping of multiple topologies on the basis of operating time of relays doesn't guarantee appropriate clustering. In this case, operating time has been calculated on the basis of $TDS = 1$ for all relays, which might not be the case for various topologies.

Additionally, the operating time of the relays would vary based upon the actual fault current and can't be set as a predetermined fault current value (I_{fmax} in this case) to perform the

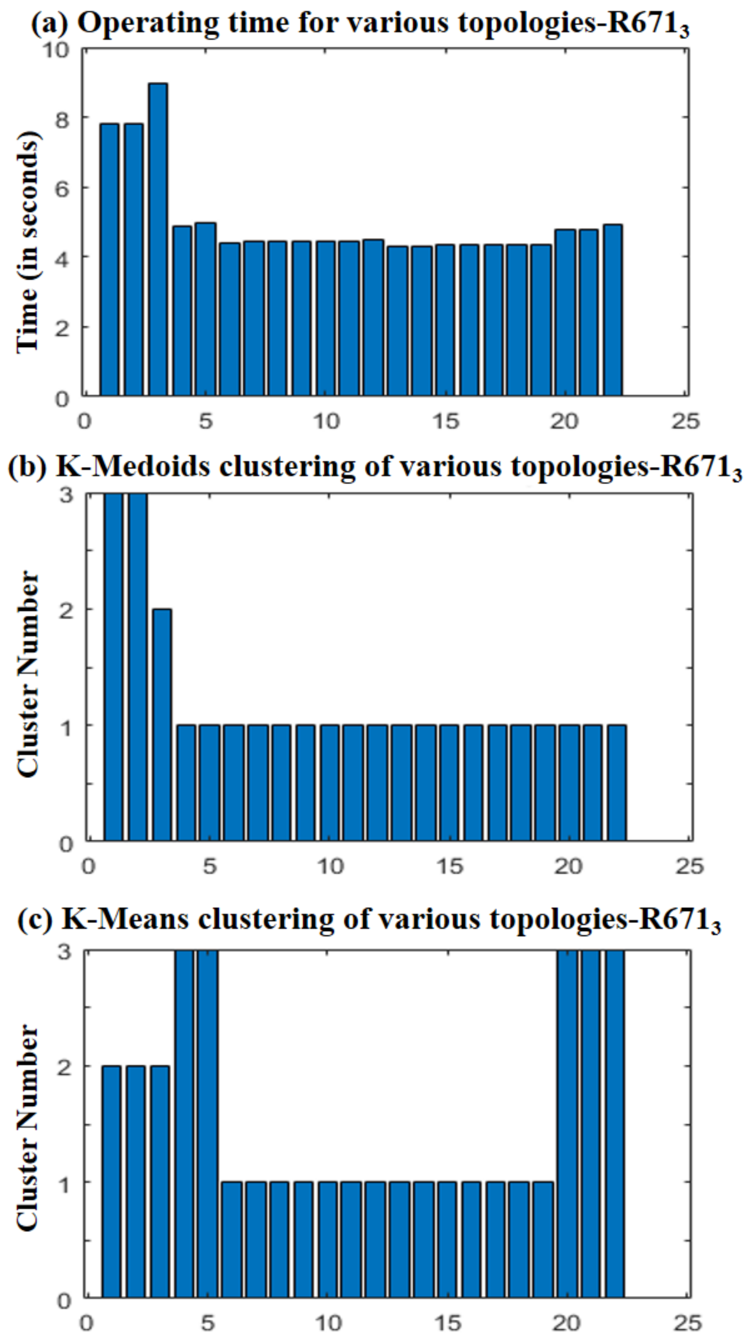

Figure 6.3: Comparison of clustering techniques based on relay operating times for various topologies for $R671_3$

required analysis. Hence, prior offline clustering of topologies based upon operating time is not a suitable option.

Finally, it can be seen in fig. 6.4, that with different iteration, and a different random initial choice of centroids, K-Means clustering can produce different results. However due to the initialization of medoids using K-means++ algorithm, K-Medoids technique produces consistent results with each iteration almost every time. An example showing K-Medoids and K-Means clustering for $R671_1$ with pickup currents as the clustering index is depicted in fig. 6.4(a)-(c). In this figure, it can be observed that K-Medoids produces the same clusters as that of fig. 6.2(d). However, the standard K-Means technique produces different results and hence, can't be relied for deciding the setting groups in the relay.

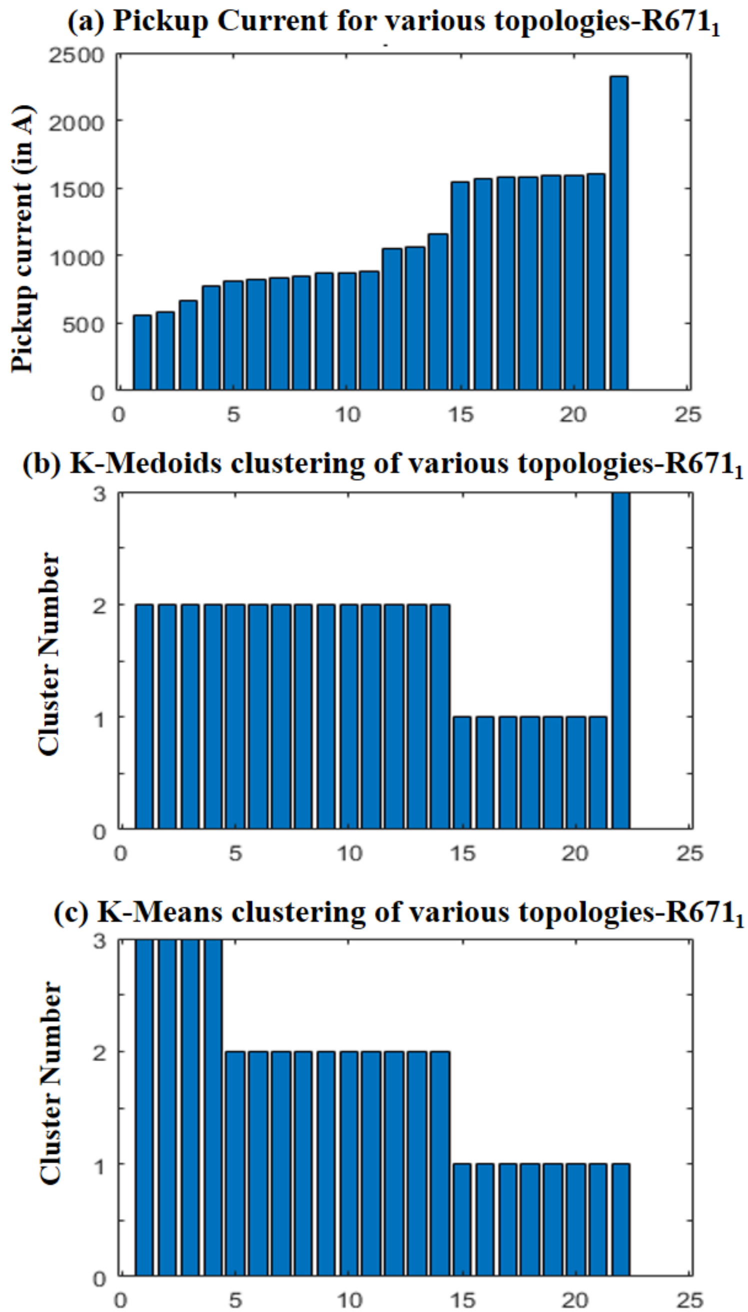

Figure 6.4: Comparison of clustering techniques based on relay pickup current for various topologies for $R671_1$ in a different iteration

6.7 Conclusion

Implementation of K-Medoids clustering technique was proposed to cluster the various topologies of a distribution system in order to store a limited number of SGs in DOCRs for ensuring proper selectivity and sensitivity towards fault identification and clearing. PAM algorithm based K-Medoids technique was adopted and tested on a modified IEEE 13 node test feeder system. The results demonstrate that the implementation of such a technique is robust to outliers in pickup currents and proves to be more efficient than standard K-Means technique. To produce consistent results each time, the initial choice of the medoids is vital and hence, K-Means++ algorithm was incorporated to ensure that the initially chosen medoids are spaced far apart from each other. It was demonstrated that even though operating time is a function of pickup current, clustering based on simply pickup current value produces reliable clusters and helps in ensuring proper coordination among protection devices. Additionally, for a large set of datapoints CLARA algorithm based K-Medoids technique can be implemented if required.

Although such techniques help in assigning settings of the relay catering to multiple topologies, these do not guarantee the most optimal solutions. These methods are simulation based and an analytical approach can be incorporated in order to optimally decide the pick up and TDS setting groups of the relays. Such an analytical approach of solving the optimal relay co-ordination problem is discussed in Chapter 7

Chapter 7

Optimal Relay coordination of Directional Overcurrent relays uisng multiple setting groups

7.1 Details of the publication

Co-authors: Virgilio.A.Centeno

Reference: T. K. Barik and V. A. Centeno, "Optimal Relay coordination of Directional Overcurrent relays using multiple setting groups," (to be submitted).

7.2 Abstract

Large-scale integration of Distributed Energy Resources (DERs) in power distribution networks has raised concerns for distribution system's protection coordination. Due to the bi-directional flow of power, Directional Overcurrent Relays (DOCRs) are being widely used in distribution systems. The pickup settings and time dial settings of these DOCRs needs to be modified with changing topologies and added DERs, to ensure proper selectivity and sensitivity towards fault identification and isolation. The nonlinear DOCR protection coor-

dination model is formulated as a Mixed Integer Linear programming problem (MILP) by linearizing the bilinear terms existing in the original formulation incorporating the multiple setting groups storage functionality of modern microprocessor based relays. McCormick linearization technique is used to achieve this goal. One of the variables in each bilinear term is discretized over its interval into a fixed number of steps. Additionally, multiple topologies are considered to allow a feasible solution of relay settings. The efficacy of the technique is tested for various grid connected and islanded scenarios of a modified IEEE 13 node test feeder system.

7.3 Introduction

Modern power distribution systems have undergone numerous changes over the last two decades with the wide-scale incorporation of Distributed Energy Resources (DERs). Although it has increased the resiliency of the distribution system, it has also posed a multitude of challenges to the conventional protection schemes in place. Traditional distribution systems used to be radial with the unidirectional flow of power, and hence, protection coordination among distribution protection devices was relatively more straightforward. However, with large-scale integration of DERs, conventional protection schemes need to be adaptive in nature to ensure proper selectivity and sensitivity towards fault identification and isolation. Additionally, as the percentage of DER penetration in the system increases, the necessity of an adaptive protection scheme increases as the operating scenarios are becoming more complicated, which may cause the short-circuit currents flowing through local relays to vary frequently. Apart from this, fault current availability in the system dynamically changes in real-time with changes in operating conditions. These conditions primarily refer to changes in the topology or connection status of DERs in the system. One of the widely used primary distribution system protective device is the Directional Overcurrent relay (DOCR). The tripping times of DOCRs are based on two settings viz., time dial settings (TDS) and current pickup setting (Ip). To properly coordinate the DOCRs, their respective TDS and Ip values have to be set optimally so that the fault is isolated in minimum time resulting in no miscoordinations. Such DOCR protection coordination problem can be written as a mathematical optimization problem with the objective of minimizing the primary and backup operating times of DOCRs constrained with time coordination and limit constraints.So, to ensure grid resilency in case a fault occurs in the system, the relays must be optimally set with the protection relay parameters during the planning stage such that, the relay tripping characteristics and the fault characteristics are matched.

Numerous DOCR coordination techniques have been proposed in the past. In [84],[85] ,the authors consider the network as an oriented graph, and simple loop structures are found with the help of a set of minimum number of breakpoints to initiate the coordination process . In [85], the coordination constraints relating to the operating times of primary and backup DOCRs are written as a set of functional dependencies similar to database systems. [87]-[91] develops numerical algorithms in which coordination constraints and parameter limit constraints are considered as inequalities and solved iteratively. Linear programming (LP) based solution techniques are proposed in [92] and [93] in which I_p values are made constant and TDS values being continuous variables are optimally found. This approach does not give the complete global solution to the problem. The operating time being a non-linear function of I_p makes the relay coordination problem inherently a nonlinear programming (NLP) problem. Mixed integer nonlinear programming (MINLP) is proposed in [94] where I_p values are assumed as integer variables and TDS parameters are considered to be continuous and solved using Seeker's algorithm. [95] also formulated a MINLP based DOCR protection coordination model considering discrete steps of Ip settings. In [96], mixed integer linear programming (MILP) based formulation with discrete Ip values is proposed based on relaxing the bilinear variables in terms of linear inequalities. In [97], sequential quadratic programming (SQP) based solution is proposed for DOCR coordination problem with both TDS and Ip as continuous variables. The work in [98] proposes a solution using linear interval programming (ILP) which considers various network topologies to find the best DOCR settings that fit for all scenarios. Quadratically constrained quadratic programming (QCQP) based solution approach is proposed in [99] which obtained the optimal global solution for the DOCR coordination problem irrespective of the initial solution. Naturally inspired optimization algorithms like GA [101], PSO [102], symbiotic organisms search [103], and hybrid heuristic methods like GA-NLP [105], GSASQP [106] have also been used to solve the DOCR optimal coordination problem.

Although the prior works have talked about various formulation of the relay coordination problem (including MILP) [109], to the best of the author's knowledge, none of them include the aspect of multi-setting groups (SGs) storage functionality in the coordination problem. Each SG corresponds to a TDS and I_p value. Multiple SGs increases the chances of convergence of the optimal relay coordination problem when multiple topologies are considered. In such cases, a single optimal SG might not be guaranteed and the problem sometimes might be rendered infeasible. Digital microprocessor-based relays consist of multiple setting group (SG) functionality, which has been one of the basis to design many adaptive schemes in the past [72],[73]. These setting groups may correspond to multiple operating conditions of the system, ensuring proper selectivity and sensitivity of the relay with only one SG being active at one time. Pertaining to numerous possible topologies of the system, suitable relay settings can be computed offline and stored as a separate, distinct setting group. Subsequently, detecting any change in the topology of the network by the DMS, the corresponding SG can be activated on the relay, thus lessening the amount of information to be transmitted back to the relay. The drawback of this method is that the modern commercial relays only allow a limited number of SGs to be stored in them, which is far lesser than the total number of possible system topologies and hence, needs to be classified. These SGs pertaining to various topologies can be decided in two approaches. One approach is implementing a simulation based clustering technique to cluster the various topologies to provide limited number of setting groups in relays. Such clustering techniques have been discussed in [74]-[77]. However, such techniques do not guarantee optimal solutions and primarily focu on I_p setting and not TDS. Another approach is the analytical or numerical approach of solving the relay coordination problem which has been discussed above. The work presented in this paper puts forth two major contributions:

i) It proposes an MILP formulation of the optimal relay coordination problem incorporating multiple setting groups into the problem formulation ;

ii)The problem formulation caters to multiple topologies and due to use of MILP formulation offers certain advantages such as global optimal solution, faster convergence, and exact formulation rather than approximate relaxation in this case.;

Section 7.4 firstly explains the traditional DOCR settings along with the conventional relay coordination problem.Section 7.5 discusses the proposed problem formulation and modified constraints. Section 7.6 describes the testing of the proposed methodology on a modified IEEE 13 node test feeder system. Finally, section 7.7 summarizes the work in the paper, outlining the possible scope of future work.

7.4 Background for relay coordination problem

7.4.1 Traditional DOCR settings

To understand the relay coordination problem in detail, it is highly important to have a better understanding of the DOCR settings. A typical DOCR consists of two elements. The first element is the directional element, which detects the direction of current based upon the relative angle between current and voltage signals fed to the relay with voltage signal acting as the polarizing quantity. The second element is the time overcurrent element, which has two values to be set, which are the Pickup current (I_p) value and Time Dial Setting (TDS). Ip is the minimum current value for which the relay operates. TDS defines the operating time (t) of the relay for each fault current value (I_f) as seen by the relay) and is given as a curve t vs M, where M refers to multiples of pickup current as is calculated as per Eq. 5.1 discussed in Chapter 5. The pickup current referred at the primary side of the Current transformer associated with the relay can be calculated as per Eq. 7.1.

$$I_p = CTR * PS. \tag{7.1}$$

Where,

CTR= Current transformer turn ratio

PS=Plug setting value (Discrete value, may not be integers)

These relays adhere to inverse overcurrent characteristics necessary to ensure protection coordination concerned with the bi-directional nature of the power flow in distribution systems. The relay operating time is a non-linear function of both TDS and I_p and illustrated in Fig. 5.2. The TDS setting is usually asuumed continuous and can be adjusted very minutely.

The time characteristics of overcurrent relay are generally non-linear and can be approximated as per Eq. 5.2. Finally incorporating the plug settings of the relay the operating time equation can be modified as:

$$t = \frac{\alpha * TDS}{\left(\frac{I_f}{CTR*PS}\right)^{\beta} - 1}. \tag{7.2}$$

Where, α, β are constants for IEC standard time overcurrent characteristics for various types of overcurrent relays as shown in Table 5.1. and for this work normal inverse overcurrent relays are used, which have parameters, α=0.14 and β= 0.02.

Now, Eq.7.2 can be reprsented as $t = PT$ for simplicity throughout the document where, $T = TDS$ and,

$$P = \frac{\alpha}{\left(\frac{I_f}{CTR*PS}\right)^{\beta} - 1}. \tag{7.3}$$

Although the conventional relay coordination problem is a nonlinear, non convex problem, it can be linearized without relaxation due to the presence of the PS variable which is normally considered a discrete variable in most OC relays. The total number of PS values in a conventional OC relay(N_{ps}) might range from 12 - 14 different discrete values of pickup current (referred to secondary side) out of which one is selected to determine the pickup setting. It should be noted that these discrete PS values might not hold integer values. A typical 14 PS setting in an OC relay is depicted in Table 7.4.

The pickup current value for a relay is dependent on the fault current the relay can observe as well as the load current (I_{load}) passing through it in normal conditions. The pickup current value has to be a trade-off between both these values. Such an approach ensures proper

Table 7.1: Plug setting values of a typical OC relay

Plug setting index	Pickup current value (in A)
1	1.0
1	1.2
1	1.5
1	2.0
1	2.5
1	3.0
1	3.5
1	4.0
1	5.0
1	6.0
1	7.0
1	8.0
1	10.0
1	12.0

dependability and security characteristics for the relay by setting the value of pickup current somewhere in between with considerable margins from either extreme. Proper protection coordination is achieved by selecting the appropriate time-current curves of these devices based on prior offline short circuit analysis of the system. The TDS of the relays are set for achieving proper protection time coordination. Firstly, the nearest relay acting as a primary protection device would clear any fault in the system. However, if it fails then, the fault should be cleared by a secondary relay acting as backup protection after a certain coordinated time interval (CTI) which is ensured by setting up different TDS for the various relays based on the overcurrent relay characteristics.

7.4.2 Conventional optimal relay coordination problem

The conventional relay coordination problem tries to minimize the overall time of operation of all the primary and backup relays for all possible faults in the system. The optimal PS and TDS settings obtained from solving such an objective function would ensure that the system is recovered from a fault in the least time possible. The conventional relay coordination problem is formulated as:

$$\min \quad \sum_{f=1}^{F} \sum_{i=1}^{N_r} \left(t_{i,f} + \sum_{k=1}^{K_i} t_{i,f}^{k} \right). \tag{7.4}$$

The conventional relay coordination problem depicted in Eq. 7.4 is subjected to the following constraints.

$$t_{i,f}^{k} - t_{i,f} \geq CTI \tag{7.5a}$$

$$I_{p,i}^{min} \leq I_{p,i} \leq I_{p,i}^{max} \tag{7.5b}$$

$$T_{i}^{min} \leq T_{i} \leq T_{i}^{max} \tag{7.5c}$$

$$t_{i}^{min} \leq t_{i,f} \leq t_{i}^{max} \tag{7.5d}$$

$$t_{i}^{min} \leq t_{i,f}^{k} \leq t_{i}^{max} \tag{7.5e}$$

Where,

F= Total number of faults

N_r= Total number of relays

$t_{i,f}$= Operating time of i^{th} primary relay for fault f

$t_{i,f}^{k}$= Operating time of k^{th} backup relay for i^{th} primary relay for fault f

K_i= Set of backup relays for an i^{th} primary relay for fault f

CTI=Coordinated Time Interval between primary and backup relays

7.5 Proposed formulation for coordination problem

The conventional non-linear relay coordination problem can be modified to introduce some additional variables for simplicity. Due to the nature of P in Eq. 7.3 only obtaining discrete values, and due to the choice of one of them being selected at any given time, we can introduce a binary variable vector $\mathbf{y_i} \in \{0,1\}^{N_{ps}}$, otherwise known as the PS selector vector for the i^{th} relay, which can hold only one value of 1, hence selecting that particular PS index for the relay.Another discrete parameter vector $\mathbf{x_i} \in \mathbb{R}^{N_{ps}}$ for the i^{th} relay can be introduced which contains all possible values of $P_{i,j}$ possible for $j = 1, 2..., N_{ps}$. Now Eq. 7.3 for i^{th} relay can be written as:

$$P_i = \mathbf{x_i}^\top \mathbf{y_i} \tag{7.6}$$

Where,

$$\mathbf{y_i}^\top \mathbf{1} = \mathbf{1}, \tag{7.7}$$

$$x_{i,j} = \frac{\alpha}{\left(\frac{I_{i,f}}{CTR_i * PS_{i,j}}\right)^{\beta} - 1} \tag{7.8}$$

And, the operating time for the i^{th} primary relay gets modified into:

$$t_{i,f} = \left(\mathbf{x_i}^\top \mathbf{y_i}\right) T_i \tag{7.9}$$

Similarly, the backup relay timing equations can be modified accordingly. It can be observed from Eq. 7.9 that the operating times is a bilinear term containing a binary variable ($\mathbf{y_i}$) and a continuous variable (T_i). This bilinear term can be linearized using the McCormick linearization technique as discussed in the following subsection.

7.5.1 McCormick Linearization

The McCormick linearization is a commonly used technique for handling products of optimization variables $x_1 x_2 \cdot x_N$ by their linear convex envelopes[110]. However, this relaxation is not necessarily exact, and prior works have disussed about numerous tightening approaches[111]. That being said, the McCormick linearization becomes exact for the special case of bilinear terms involving at least one binary variable which is similar to what is presented in Eq. 7.9. For example, if we consider the constraint $z = xy$, where $x \in \{0, 1\}$ is the binary variable and $y \in [\underline{y}, \bar{y}]$ is a continuous variable. Now, the constraint $z = xy$ can be equivalently expressed by the four linear inequality constraints

$$x\underline{y} \leq z \leq x\bar{y} \tag{7.10a}$$

$$y + (x-1)\bar{y} \leq z \leq y + (x-1)\underline{y} \tag{7.10b}$$

The exactness can be verified by observing that for $x = 1$, constraint (7.10b) yields $z = y$ and (7.10a) holds trivially. When $x = 0$, both (7.10a) and (7.10b) yield $z = 0$. Therefore, the two cases provide $z = xy$. Thus, using McCormick linearization of (7.10), the bilinear products of binary and (bounded) continuous variables in the relay coordination problem explained earlier could very well be handled. Such linearization can be applied to both primary and backup operating times for all the relays in the system.

7.5.2 Incorporating multiple setting groups and multiple topologies

The earlier subsections dealt with a single setting group and a single base topology of the system to list out the constraints of the optimization problem. The next step would be to include multiple topologies and multiple setting groups for each relay. Let $\mathbf{t} \in \{0,1\}^{N_t}$ refer to the topology indicator vector where, N_t refers to the total number of topology scenarios considered. It should be noted that only one entry of this topology indication vector would be set to 1 to indicate that particular topology is under observation. In other words, $t_z = 1$ if the z^{th} topology is under consideration and $z = 1, 2, ..., N_t$. Now instead of having a single setting group we include multiple setting groups and hence two new variables are added to include this aspect. The scalars P_i and T_i for the i^{th} relay discussed in the earlier subsection are replaced by a possible PS vector, $\hat{\mathbf{P}}_\mathbf{i} = [P_1 \;\; P_2....P_{Ng}]^\top$, and a possible TDS vector, $\hat{\mathbf{T}}_\mathbf{i} = [T_1 \;\; T_2....T_{Ng}]^\top$ respectively, where N_g refers to the total allowable setting groups inside the relay(usually in the range of 2-6). The PS selector vector $\mathbf{y_i}$ discussed in the earlier subsection gets replaced by a PS selector matrix $\mathbf{Y_i} \in \{0,1\}^{N_{ps}N_g}$.A separate binary variable SG selector matrix $B_i \in \{0,1\}^{N_t N_g}$ is introduced which would indicate which single setting group is chosen corresponding to a particular topology such that:

$$\mathbf{B_i 1} = \mathbf{1} \tag{7.11}$$

$$\mathbf{Y_i^\top 1} = \mathbf{1}, \tag{7.12}$$

The operating time of the i^{th} relay for topology t gets modified in comparision to eq. 7.9 as:

$$t_{i,f} = \mathbf{t}^\top \mathbf{B_i} \left(\widehat{\mathbf{P}}_\mathbf{i} \odot \widehat{\mathbf{T}}_\mathbf{i} \right) = \mathbf{t}^\top \mathbf{B_i} \left(\mathbf{diag} \left(\mathbf{x_i^\top Y_i} \right) \widehat{\mathbf{T}}_\mathbf{i} \right) \tag{7.13}$$

Additionally, the CTI in this work has been kept as a decision variable rather than a constant value as denoted in prior works. The value of CTI usually varies from [0.2-0.5] seconds and hence can be added as the following constraint which can improve the convergence rate yet without jeopardizing the dependability aspect of relay coordination.

$$CTI_{min} < CTI < CTI_{max} \tag{7.14}$$

In addition to modified constraints, a few changes to some parameters are also introduced in this work. Instead of allowing a constant t_i^{min} and t_i^{max}, research has shown that these values depend upon the allowable values of minimum and maximum PS as depicted in the following equations.

$$t_i^{min} = \frac{\alpha * TDS_i^{min}}{\left(\frac{I_{i,f}^{max}}{CTR_i * PS_i^{min}}\right)^{\beta} - 1} \tag{7.15a}$$

$$t_i^{max} = \frac{\alpha * TDS_i^{max}}{\left(\frac{I_{i,f}^{min}}{CTR_i * PS_i^{max}}\right)^{\beta} - 1} \tag{7.15b}$$

Where,

$$PS_i^{min} = max\left(\frac{2I_{load,i}^{max}}{CTR_i}, PS_{i,old}^{min}\right) \tag{7.16a}$$

$$PS_i^{max} = min\left(\frac{1}{3}\frac{I_{i,f}^{min}}{CTR_i}, PS_{i,old}^{max}\right) \tag{7.16b}$$

The $PS_{i,old}^{min}$ & $PS_{i,old}^{max}$values refer to the minimum and maximum values of PS as depicted in Table.7.4 In order to maintain a balance between security and dependability aspects of the relay coordination issue, it has been found that the pickup current must lie somewhere in between 2 times the load current and one-third of the minimum fault current as seen by the relay. Hence the modifications were made as shown in Eq. 7.5.2-7.15 Finally the modified objective function for the optimal relay coordination incorporating multiple setting groups and multiple topologies is represented as:

$$\min \quad \sum_{t=1}^{N_t} W_f \sum_{f=1}^{F} \sum_{i=1}^{N_r} \left(t_{i,f}^{t} + \sum_{k=1}^{K_i} t_{i,f}^{k,t} \right) \tag{7.17}$$

$$\text{s.to} \quad (7.5), (7.8), (7.11) - (7.14) \tag{7.18}$$

Where, W_f= Weight or probability of the the fault occurrence. Although this value can vary between [0,1], for the sake of simplicity all the faults have been provided with same weight of 1 in this work.

7.6 Testing and Results

7.6.1 Test bench setup

A modified IEEE 13 node test feeder model as shown in fig. is built in MATLAB/Simulink. 8 DOCRs are placed on the system at critical locations (3 phase main feeders and secondary feeders). Three DERs of 10 MW, 3 MW, and 5 MW were included in the distribution system connected to nodes 633,675 and 680 respectively, as shown in Fig. 7.1. The direction of operation of the DOCRs (depicted by red boxes in the figure) placed in this model is depicted with an arrow beside each relay. It should be noted that at certain locations of the system, DOCRs might be redundant due to the presence of individual protection schemes of equipment such as transformers and generators. The individual DERs would have their own protection schemes located at the Point of Common Coupling (PCC) in order to protect the equipment from system faults if required. For example, a fault in the line between nodes 671 and 680 would be cleared from the utility source side by the DOCR placed on this line near node 671.

However, to clear the fault from the consumer side, directional overcurrent relays need not be present near node 680 as the protection schemes of the DER can isolate the fault if required. The same holds true also for the transformer between nodes 633 and 634, which would have standard transformer protection schemes to detect any internal or external faults. All these individual equipment's protection devices are depicted as purple boxes in Fig. 7.1. This assumption leads to an economical deployment approach of protective relaying in distribution systems. For simplicity, the DOCRs at the various nodes are numbered from $R_1 - R_8$ as illustrated in Fig. 7.1.For example the DOCRs at node 671 are denoted as R_4, R_5, R_6 respectively.

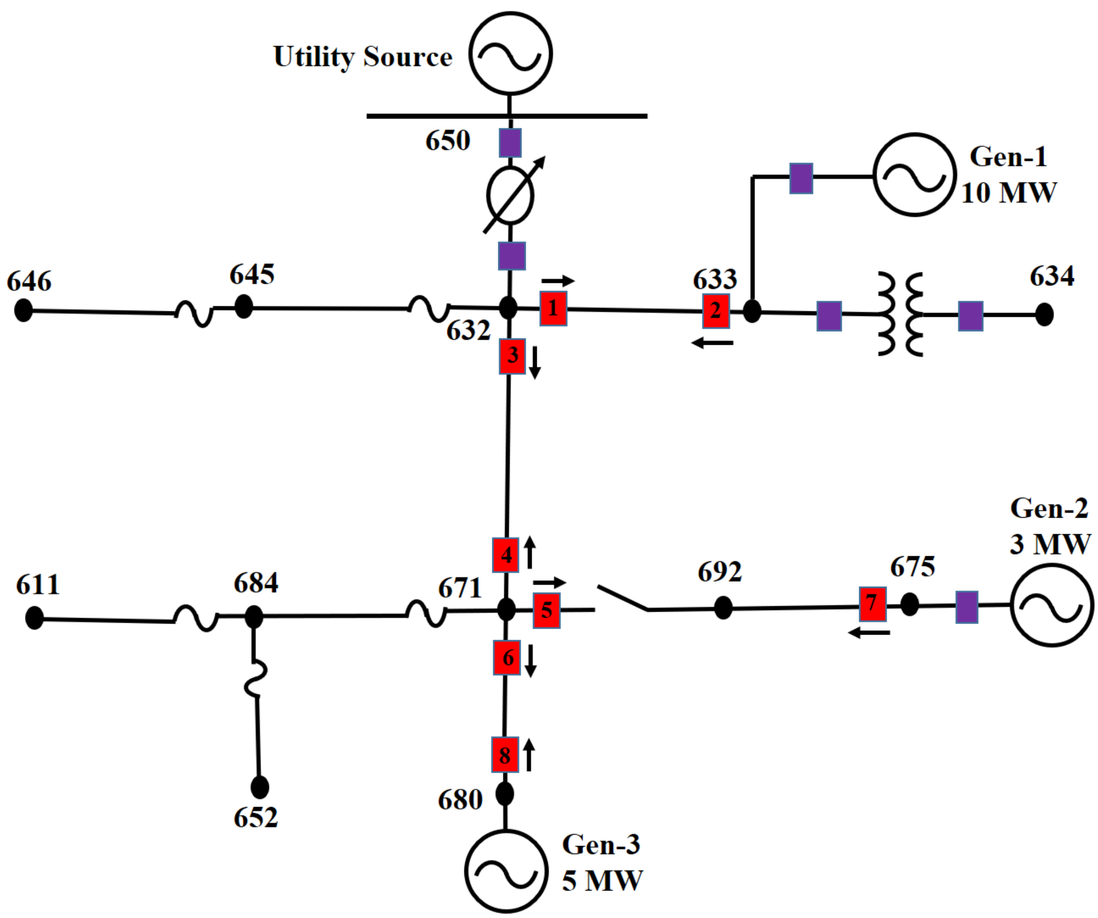

Figure 7.1: Modified IEEE 13 node test feeder system

The fault data for all the eight DOCRs (depicted in Fig. 7.1), was generated by applying a 3-phase bolted fault in front of each relay. Hereafter, based upon the disconnection of various components of the distribution system such as lines and transformer, numerous topologies were created for generating fault data.However, based upon different topologies, the normal load current though the relay would also change and needs to be considered for deciding the pickup current in each scenario. The grid-connected base case is when the distribution system is connected to the utility source. The case in which the whole distribution system is disconnected from the utility source (632 disconnected from 650) is termed as the islanded base case. Six different topologies as depicted in Table 7.2 were generated encapsulating the following conditions:

- Grid Connected and Islanded modes
- Disconnection of vital DERs
- Disconnection of a smaller section with DERs and loads

Table 7.2: Various topologies of the distribution system

Topology index	Description
Top1	Grid connected
Top2	Completely islanded with breaker at node 650 open
Top3	Partially islanded with line recloser at relay 3 position open
Top4	Grid connected with Gen-1 disconnected
Top5	Completely islanded with Gen-1 disconnected
Top6	Grid connected with breaker at relay 5 position open

7.6.2 Results

All tests for solving the proposed optimal relay coordination problem were run using MATLAB-based toolbox YALMIP along with the mixed-integer solver GUROBI; on a 2.2 GHz Intel Core i5-5200U CPU with 8 GB RAM. The number of setting groups(N_g) was set to 2 and the following results were obtained after convergence. It should be noted that although N_g can be increased to higher values. However, increasing the value of N_g comes with the added cost of frequent switching of SGs in the relay for the same number of the topological groups. This kind of frequent operation might not be desirable by the utility during abnormal consitions when there is added burden on the communication network. This type of frequent switching might be only desirable when there is significant reduction of the objective function (OF) value.The difference between OF value with $N_g = 2$ and with $N_g = 3$ was found out to be very small (around 1.5s). Hence 2 setting groups was found to be the best choice in this scenario.

Table 7.3: Assigned setting groups for various relays for each topology, $N_g = 2$

Relay	Top1	Top2	Top3	Top4	Top5	Top6
R1	2	2	1	1	1	1
R2	1	1	2	1	1	1
R3	1	2	2	1	1	1
R4	1	1	2	2	2	1
R5	2	2	2	2	2	1
R6	2	1	1	1	1	1
R7	1	1	2	2	1	1
R8	2	2	1	1	1	1

Table 7.4: Optimal solution for Relay setting groups, $N_g = 2$

Relay name	Relay SG_1		Relay SG_2	
	TDS	PS	TDS	PS
R1	0.3848	14	0.3848	14
R2	0.7339	14	0.2155	1
R3	0.5843	14	0.2696	1
R4	0.4507	11	0.3163	14
R5	0.2937	2	0.3610	14
R6	0.3366	14	0.2356	3
R7	0.4889	8	0.4607	14
R8	0.3419	3	0.5522	9

7.7 Conclusion

A modified MILP formulation of the conventional optimal overcurrent relay coordination incorporating multiple setting groups of the modern DOCRs and catering to multiple topologies was proposed in this document. Using the multi-setting storage functionality of the relays helps in convergence of the classical problem when multiple contingencies are considered. The tests carried out on a modified IEEE 13 node test feeder system provides the appropriate SGs of the relays which can be fed to the respective relays during the planning phase or during regular maintenance. In real-time, sensisng a change in topology, the DMS can communicate with such relays and send a bit to activate necessary SG corresponding to the particular topology. This alleviates the need of solving the optimization problem in real time and sending huge chunks of data over the communication network which normally remains stressed during severe weather induced outage condition. As an extension to the current work, future research could be guided in coordinating fuses with the reclosers in the system to solve the issue of fuse-recloser coordination in the distribution system due to the wide scale integartion of multiple DERs in the system.

Chapter 8

Conclusions

8.1 Summary

The work outlined in this document tackles the modern challenges in protection and control of the distribution system and proposes a comprehensive solution to enhance grid resiliency. The document starts with the a comparative analysis of two of the most common and widely used protective elements in the distribution system protection schemes in Chapter 2. The study was carried out to evaluate the capability of DOC and RP elements to detect various faults and provide an assessment of their functionalities.The work outlined in this chapter concluded that reverse power is not a reliable indicator of fault identification, and the DOC element should be considered instead for feeder protection. The document thereafter continues with a multi-principle islanding detection technique based on 3-phase active power mismatch and ROCOV measurements proposed in Chapter 3. The combination of the two passive techniques produced an NDZ smaller than individual schemes. The proposed method was found to be a viable option in reducing the dependency on the communication-based schemes.

Chapter 4 dealt with a Critical Load Shedding Module (CLSM) to sustain a section of the distribution system upon islanding in real-time by maintaining load generation power balance. The study was done with the consideration of making the technique practically implementable with minimum cost addition. The methodology was based upon analyzing voltage sensitivities calculated by retrieving measurements from AMIs deployed in the system to assign priority levels of the critical loads in real-time to prevent voltage and frequency collapse during islanding. The module would ensure lesser outages of the load, along with serving the maximum amount of load within the service restoration period. A comprehensive decentralized multi-setting adaptive protection scheme for DOCRs in power distribution systems was proposed in Chapter 5. The decentralized approach makes this protection scheme practically feasible and easily deployable in the recent future, as it considers zero reliability on extensive communication links over various distribution system nodes and aims to mimic peer-to-peer communication. The methodology proposes storing an additional and separate set of pickup current and TDS (Reverse Protection Settings) in the DOCRs in order to provide an additional tier of protection response to fault clearing. However, such techniques did not cater to multiple topologies and simply considered the base topology of the system. The settings of the protective devices should consider multiple topologies to order to ensure grid resiliency in case of severe weather induced outages. Hence a few modified approaches were studied and implemented in Chapter 6 & Chapter 7.

Chapter 6 proposed the implementation of PAM algorithm based K-Medoids clustering technique to cluster the various topologies of a distribution system in order to store a limited number of SGs in DOCRs for ensuring proper selectivity and sensitivity towards fault identification and clearing. The results demonstrate that the implementation of such a technique is robust to outliers in pickup currents and proves to be more efficient than standard K-Means technique which have been discussed in prior works. To produce consistent results each time, the initial choice of the medoids is vital and hence, K-Means++ algorithm was incorporated to ensure that the initially chosen medoids are spaced far apart from each other. .
Although such techniques help in assigning settings of the relay catering to multiple topologies, these do not guarantee the most optimal solutions. These methods are simulation

based and an analytical approach can be incorporated in order to optimally decide the pick up and TDS setting groups of the relays. Such an analytical approach of solving the optimal relay co-ordination problem was discussed in Chapter 7 where the optimal relay coordination problem was formulated as a MILP problem incorporating multiple setting groups and catering multiple topologies.

8.2 Main Contributions

The different works proposed in this document present some novel contributions: As the work presented in Chapter 3 relies on the local measurements at the PCC, the multi-principle islanding detection technique can be easily deployable with no additional infrastructural cost and zero dependency on communication networks. The combination of the two passive techniques produced an NDZ smaller than individual schemes.

The CLSM module discussed in Chapter 4 presents a QV based load shedding technique which is primarily used in transmission systems in the past. This research work implements and proves the efficacy of such an algorithm in distribution networks too. Additionally, incorporating generator low voltage ride through contraints, the proposed CLSM provides a novel technique to effectively sustain an island upon its occurrence encapsulating the severity of the event to decide the load shedding wait interval dynamically in real-time.

The adaptive protection scheme discussed in Chapter 5 puts forth three major improvements over the traditional protection schemes: i) The technique proposes storing of versatile setting groups inside the relays which can mimic the peer-to-peer communication scenario without actual usage of extensive communication links between various distribution system nodes, thus making the proposed scheme easily implementable and deployable; ii) The proposed relay settings makes the primary protection logic more robust in case of loss of trip signal generated by the primary protection relay; iii) The proposed scheme also reduces the area of power outage as a part of improved secondary backup protection, ensuring a greater number of loads which can be served with uninterrupted power.

The implementation of K-medoids clustering technique of fault currents for various topologies discussed in Chapter 6 also puts forth three major contributions: i) It proposes the implementation of K-Medoids clustering technique using the Partitioning around Medoids (PAM) algorithm [12], which is robust to outliers to categorize the topologies of the system more effectively as compared to previous works; ii)Additionally, a K-Means ++ algorithm [14] is implemented to initialize the starting medoid positions for producing consistent clustering groups in each execution; iii) The method is executed considering both pickup current and operating time as the clustering index, to demonstrate the comparison and effectiveness of both approaches.

And finally, the contributions of the work presented in Chapter 7 include: i) A MILP formulation of the optimal relay coordination problem incorporating multiple setting groups for the first time to the best of the author's knowledge, into the problem formulation ; ii)The problem formulation caters to multiple topologies and due to use of MILP formulation offers certain advantages such as global optimal solution, faster convergence, and exact formulation rather than approximate relaxation in this case.

8.3 Future Work

Although the works discussed in this document outlined major issues in the protection and control aspects of the distribution system, some of the potential avenues and scope of future work include: Additional comparative studies and analyses between other critical distribution system protective devices can be carried out to help future researchers to have a better comprehensive knowledge of the distribution protection system. The multi-principle islanding detection technique studied in Chapter 3 can be further expanded for a system with more percentage of inverter-based distributed generation as their penetration in the system is increasing substantially. Additionally, the possibility of integrating other islanding detection schemes in conjunction or as a backup to the proposed logic can also be researched.

In continuation of the work outlined in Chapter 4, a comprehensive load and generation shedding module for catering both positive and negative ROCOF scenarios can be researched in the future. Additionally assigning criticality levels to the loads can be modified to incorporate the real time assessment of the severance of the islanding situation. Although the work outlined in Chapter 6 was implemented for a substantial data set, the algorithm can cater for a large set of datapoints by implementing CLARA algorithm based K-Medoids technique if required.

Chapter 7 deals with the MILP formulation of the optimal relay coordination using multiple setting group storage functionalities in modern DOC relays. However, future research could be guided in coordinating fuses with the reclosers in the system to solve the issue of fuse-recloser coordination in the distribution system due to the wide scale integartion of multiple DERs in the system.

Bibliography

[1] P. Naisani, D. Tholomier, T. Yip, and G. Lloyd, "Protection of distributed generation (dg) interconnection," pp. 1 – 17, 05 2010.

[2] J. Simms and G. Johnson, "Protection considerations for installation of distributed energy resources," pp. 289–301, 05 2015.

[3] T. M. Masaud and R. D. Mistry, "Fault current contribution of renewable distributed generation: An overview and key issues," in *2016 IEEE Conference on Technologies for Sustainability (SusTech)*, pp. 229–234, 2016.

[4] D. Costello, M. Moon, and G. Bow, "Use of directional elements at the utility-industrial interface," vol. 2005, pp. 261 – 276, 05 2005.

[5] C. Mozina, "Interconnect protection of dispersed generators," vol. 2, pp. 709 – 723 vol.2, 02 2001.

[6] A. Ukil, B. Deck, and V. H. Shah, "Current-only directional overcurrent protection for distribution automation: Challenges and solutions," *IEEE Transactions on Smart Grid*, vol. 3, no. 4, pp. 1687–1694, 2012.

[7] J. Mulhausen, J. Schaefer, M. Mynam, A. Guzman, and M. Donolo, "Anti-islanding today, successful islanding in the future," pp. 1 – 8, 05 2010.

[8] R. Anne, F. Basha, R. Palaniappan, K. Oliver, and M. Thompson, "Reliable generator islanding detection for industrial power consumers with on-site generation," *IEEE Transactions on Industry Applications*, vol. 2015, pp. 1–1, 01 2015.

[9] K. Rajamani and U. Hambarde, “Islanding and load shedding schemes for captive power plants,” *IEEE Transactions on Power Delivery*, vol. 14, no. 3, pp. 805–809, 1999.

[10] T. K. Barik, K. M. Phelps, J. J. Petti, and F. Velez-Cedeno, “A comparative study of the reliability of reverse power and directional overcurrent elements for distribution level fault identification,” in *2018 Grid of the Future colloquia*, pp. 1–5, 2018.

[11] T. K. Barik, K. M. Phelps, J. J. Petti, and F. Velez-Cedeno, “A multi-principle passive islanding detection technique for power distribution systems,” in *2019 IEEE Power Energy Society General Meeting (PESGM)*, pp. 1–5, 2019.

[12] “IEEE standard for interconnection and interoperability of distributed energy resources with associated electric power systems interfaces,” *IEEE Std 1547-2018 (Revision of IEEE Std 1547-2003)*, pp. 1–138, 2018.

[13] “IEEE application guide for ieee std 1547(tm), IEEE standard for interconnecting distributed resources with electric power systems,” *IEEE Std 1547.2-2008*, pp. 1–217, 2009.

[14] Y. H. Cheng, K. Chen, C. Yin, J. Zhang, and L. B. Bai, “An improved active islanding detection method applying to multi-inverter power system,” in *2015 IEEE International Conference on Applied Superconductivity and Electromagnetic Devices (ASEMD)*, pp. 561–562, 2015.

[15] Z. Guo, “A harmonic current injection control scheme for active islanding detection of grid-connected inverters,” in *2015 IEEE International Telecommunications Energy Conference (INTELEC)*, pp. 1–5, 2015.

[16] P. Gupta, R. S. Bhatia, and D. K. Jain, “Average absolute frequency deviation value

based active islanding detection technique," *IEEE Transactions on Smart Grid*, vol. 6, no. 1, pp. 26–35, 2015.

[17] L. A. C. Lopes and Y. Zhang, "Islanding detection assessment of multi-inverter systems with active frequency drifting methods," *IEEE Transactions on Power Delivery*, vol. 23, no. 1, pp. 480–486, 2008.

[18] D. Reigosa, F. Briz, C. B. Charro, P. Garcia, and J. M. Guerrero, "Active islanding detection using high-frequency signal injection," *IEEE Transactions on Industry Applications*, vol. 48, no. 5, pp. 1588–1597, 2012.

[19] A. Yafaoui, B. Wu, and S. Kouro, "Improved active frequency drift anti-islanding detection method for grid connected photovoltaic systems," *IEEE Transactions on Power Electronics*, vol. 27, no. 5, pp. 2367–2375, 2012.

[20] H. Karimi, A. Yazdani, and R. Iravani, "Negative-sequence current injection for fast islanding detection of a distributed resource unit," *IEEE Transactions on Power Electronics*, vol. 23, no. 1, pp. 298–307, 2008.

[21] L. Yu, D. Zhang, and J. He, "Active islanding detection method for multi-inverter in power distribution system," in *2017 IEEE Conference on Energy Internet and Energy System Integration (EI2)*, pp. 1–5, 2017.

[22] S. Salman, D. King, and G. Weller, "New loss of mains detection algorithm for embedded generation using rate of change of voltage and changes in power factors," in *2001 Seventh International Conference on Developments in Power System Protection (IEE)*, pp. 82–85, 2001.

[23] B. Guha, R. J. Haddad, and Y. Kalaani, "A novel passive islanding detection tech-

nique for converter-based distributed generation systems," in *2015 IEEE Power Energy Society Innovative Smart Grid Technologies Conference (ISGT)*, pp. 1–5, 2015.

[24] N. Liu, C. Diduch, L. Chang, and J. Su, "A reference impedance-based passive islanding detection method for inverter-based distributed generation system," *IEEE Journal of Emerging and Selected Topics in Power Electronics*, vol. 3, no. 4, pp. 1205–1217, 2015.

[25] S. Nikolovski, H. R. Baghaee, and D. Mlakić, "Islanding detection of synchronous generator-based dgs using rate of change of reactive power," *IEEE Systems Journal*, vol. 13, no. 4, pp. 4344–4354, 2019.

[26] A. M. I. Mohamad and Y. A.-R. I. Mohamed, "Impedance-based analysis and stabilization of active dc distribution systems with positive feedback islanding detection schemes," *IEEE Transactions on Power Electronics*, vol. 33, no. 11, pp. 9902–9922, 2018.

[27] N. Liu, A. Aljankawey, C. Diduch, L. Chang, and J. Su, "Passive islanding detection approach based on tracking the frequency-dependent impedance change," *IEEE Transactions on Power Delivery*, vol. 30, no. 6, pp. 2570–2580, 2015.

[28] J. Mulhausen, J. Schaefer, M. Mynam, A. Guzmán, and M. Donolo, "Anti-islanding today, successful islanding in the future," in *2010 63rd Annual Conference for Protective Relay Engineers*, pp. 1–8, 2010.

[29] F.-S. Pai and S.-J. Huang, "A detection algorithm for islanding-prevention of dispersed consumer-owned storage and generating units," *IEEE Transactions on Energy Conversion*, vol. 16, no. 4, pp. 346–351, 2001.

[30] J. Yang, J. Yuan, and S. Lin, "The study on island detection for distributed power

combining power line zero-crossing communication technology," in *2017 7th IEEE International Conference on Electronics Information and Emergency Communication (ICEIEC)*, pp. 304–307, 2017.

[31] T. K. Barik and V. A. Centeno, "Dynamic prioritization of critical loads for sustaining power distribution systems upon islanding," in *2020 IEEE Power Energy Society Innovative Smart Grid Technologies Conference (ISGT)*, pp. 1–5, 2020.

[32] H. Gao, Y. Chen, Y. Xu, and C.-C. Liu, "Resilience-oriented critical load restoration using microgrids in distribution systems," *IEEE Transactions on Smart Grid*, vol. 7, no. 6, pp. 2837–2848, 2016.

[33] B. Chen, C. Chen, J. Wang, and K. L. Butler-Purry, "Sequential service restoration for unbalanced distribution systems and microgrids," *IEEE Transactions on Power Systems*, vol. 33, no. 2, pp. 1507–1520, 2018.

[34] W. Gu, W. Liu, J. Zhu, B. Zhao, Z. Wu, Z. Luo, and J. Yu, "Adaptive decentralized under-frequency load shedding for islanded smart distribution networks," *IEEE Transactions on Sustainable Energy*, vol. 5, no. 3, pp. 886–895, 2014.

[35] A. Parizad, H. Khoshkhoo, S. Dehghan, and R. Moradtalab, "An intelligent load and generation shedding procedure in an islanded network using a smart power management system," in *2017 Smart Grid Conference (SGC)*, pp. 1–12, 2017.

[36] Y. Tofis, S. Timotheou, and E. Kyriakides, "Minimal load shedding using the swing equation," *IEEE Transactions on Power Systems*, vol. 32, no. 3, pp. 2466–2467, 2017.

[37] T. Shekari, A. Gholami, F. Aminifar, and M. Sanaye-Pasand, "An adaptive wide-area load shedding scheme incorporating power system real-time limitations," *IEEE Systems Journal*, vol. 12, no. 1, pp. 759–767, 2018.

[38] C. P. Reddy, S. Chakrabarti, and S. C. Srivastava, "A sensitivity-based method for under-frequency load-shedding," *IEEE Transactions on Power Systems*, vol. 29, no. 2, pp. 984–985, 2014.

[39] J. Tang, J. Liu, F. Ponci, and A. Monti, "Adaptive load shedding based on combined frequency and voltage stability assessment using synchrophasor measurements," *IEEE Transactions on Power Systems*, vol. 28, no. 2, pp. 2035–2047, 2013.

[40] Q. Zhou, Z. Li, Q. Wu, and M. Shahidehpour, "Two-stage load shedding for secondary control in hierarchical operation of islanded microgrids," *IEEE Transactions on Smart Grid*, vol. 10, no. 3, pp. 3103–3111, 2019.

[41] M. Karimi, P. Wall, H. Mokhlis, and V. Terzija, "A new centralized adaptive underfrequency load shedding controller for microgrids based on a distribution state estimator," *IEEE Transactions on Power Delivery*, vol. 32, no. 1, pp. 370–380, 2017.

[42] T. K. Barik, A. Schmitt, K. D. Jones, and V. Centeno, "Empirical determination of voltage phasor angle deviation threshold for synchrophasor-based substation topology estimation," in *2017 North American Power Symposium (NAPS)*, pp. 1–5, 2017.

[43] K. D. Jones, J. S. Thorp, and R. M. Gardner, "Three-phase linear state estimation using phasor measurements," in *2013 IEEE Power Energy Society General Meeting*, pp. 1–5, 2013.

[44] C. Qian, Z. Wang, and J. Zhang, "A new algorithm of topology analysis based on pmu information," in *2010 5th International Conference on Critical Infrastructure (CRIS)*, pp. 1–5, 2010.

[45] M. Farrokhabadi and L. Vanfretti, "Phasor-assisted automated topology processing for state estimators," in *2013 IEEE Electrical Power Energy Conference*, pp. 1–8, 2013.

[46] L. Mili, G. Steeno, F. Dobraca, and D. French, "A robust estimation method for topology error identification," *IEEE Transactions on Power Systems*, vol. 14, no. 4, pp. 1469–1476, 1999.

[47] A. M. Sasson, S. T. Ehrmann, P. Lynch, and L. S. Van Slyck, "Automatic power system network topology determination," *IEEE Transactions on Power Apparatus and Systems*, vol. PAS-92, no. 2, pp. 610–618, 1973.

[48] M. Prais and A. Bose, "A topology processor that tracks network modifications," *IEEE Transactions on Power Systems*, vol. 3, no. 3, pp. 992–998, 1988.

[49] P. Yehsakul and I. Dabbaghchi, "A topology-based algorithm for tracking network connectivity," *IEEE Transactions on Power Systems*, vol. 10, no. 1, pp. 339–346, 1995.

[50] M. Zhou, V. Centeno, J. Thorp, and A. Phadke, "An alternative for including phasor measurements in state estimators," *IEEE Transactions on Power Systems*, vol. 21, no. 4, pp. 1930–1937, 2006.

[51] A. Phadke and J. Thorp, *Synchronized Phasor Measurements and Their Applications.* 01 2008.

[52] T. K. Barik and V. A. Centeno, "Decentralized multi-setting adaptive distribution protection scheme for directional overcurrent relays," in *2020 IEEE Kansas Power and Energy Conference (KPEC)*, pp. 1–6, 2020.

[53] N. Hatziargyriou, *Microgrids: Architectures and Control.* 01 2014.

[54] M. A. Zamani, A. Yazdani, and T. S. Sidhu, "A communication-assisted protection strategy for inverter-based medium-voltage microgrids," *IEEE Transactions on Smart Grid*, vol. 3, no. 4, pp. 2088–2099, 2012.

[55] M. E. Elkhatib and A. Ellis, “Communication-assisted impedance-based microgrid protection scheme,” in *2017 IEEE Power Energy Society General Meeting*, pp. 1–5, 2017.

[56] T. S. Ustun and R. H. Khan, “Multiterminal hybrid protection of microgrids over wireless communications network,” *IEEE Transactions on Smart Grid*, vol. 6, no. 5, pp. 2493–2500, 2015.

[57] M. H. Cintuglu, T. Ma, and O. A. Mohammed, “Protection of autonomous microgrids using agent-based distributed communication,” *IEEE Transactions on Power Delivery*, vol. 32, no. 1, pp. 351–360, 2017.

[58] Z. Liu, C. Su, H. K. Høidalen, and Z. Chen, “A multiagent system-based protection and control scheme for distribution system with distributed-generation integration,” *IEEE Transactions on Power Delivery*, vol. 32, no. 1, pp. 536–545, 2017.

[59] S. Shen, H. Wang, K. Jiang, L. Zhu, C. Gan, P. N. Markham, Y. Liu, and B. He, “Regional area protection scheme for modern distribution system,” *IEEE Transactions on Smart Grid*, vol. 10, no. 5, pp. 5416–5426, 2019.

[60] S. Horowitz and A. Phadke, “Power system relaying / stanley h. horowitz, arun g. phadke,” *SERBIULA (sistema Librum 2.0)*, 05 2021.

[61] A. Warrington, *Protective Relays Their Theory and Practice: Volume Two.* 01 1978.

[62] P. Mahat, Z. Chen, B. Bak-Jensen, and C. L. Bak, “A simple adaptive overcurrent protection of distribution systems with distributed generation,” *IEEE Transactions on Smart Grid*, vol. 2, no. 3, pp. 428–437, 2011.

[63] V. Telukunta, J. Pradhan, A. Agrawal, M. Singh, and S. G. Srivani, “Protection chal-

lenges under bulk penetration of renewable energy resources in power systems: A review," *CSEE Journal of Power and Energy Systems*, vol. 3, no. 4, pp. 365–379, 2017.

[64] M. Y. Shih, A. Conde, Z. Leonowicz, and L. Martirano, "An adaptive overcurrent coordination scheme to improve relay sensitivity and overcome drawbacks due to distributed generation in smart grids," *IEEE Transactions on Industry Applications*, vol. 53, no. 6, pp. 5217–5228, 2017.

[65] S. Dambhare, S. A. Soman, and M. C. Chandorkar, "Adaptive current differential protection schemes for transmission-line protection," *IEEE Transactions on Power Delivery*, vol. 24, no. 4, pp. 1832–1841, 2009.

[66] Z. Bo, "Adaptive non-communication protection for power lines bo scheme. ii. the instant operation approach," *IEEE Transactions on Power Delivery*, vol. 17, no. 1, pp. 92–96, 2002.

[67] E. Orduna, F. Garces, and E. Handschin, "Algorithmic-knowledge-based adaptive coordination in transmission protection," *IEEE Transactions on Power Delivery*, vol. 18, no. 1, pp. 61–65, 2003.

[68] J. Kumar, S. Venkata, and M. Damborg, "Adaptive transmission protection: concepts and computational issues," *IEEE Transactions on Power Delivery*, vol. 4, no. 1, pp. 177–185, 1989.

[69] J. Ma, W. Ma, X. Wang, and Z. Wang, "A new adaptive voltage protection scheme for distribution network with distributed generations," *Canadian Journal of Electrical and Computer Engineering*, vol. 36, no. 4, pp. 142–151, 2013.

[70] T. K. Barik and V. A. Centeno, "K - medoids clustering of setting groups in directional

overcurrent relays for distribution system protection," in *2020 IEEE Kansas Power and Energy Conference (KPEC)*, pp. 1–6, 2020.

[71] M. Ojaghi and V. Mohammadi, "Use of clustering to reduce the number of different setting groups for adaptive coordination of overcurrent relays," *IEEE Transactions on Power Delivery*, vol. 33, no. 3, pp. 1204–1212, 2018.

[72] M. Khederzadeh, "Adaptive setting of protective relays in microgrids in grid-connected and autonomous operation," in *11th IET International Conference on Developments in Power Systems Protection (DPSP 2012)*, pp. 1–4, 2012.

[73] A. K. Pradhan and G. Joos, "Adaptive distance relay setting for lines connecting wind farms," *IEEE Transactions on Energy Conversion*, vol. 22, no. 1, pp. 206–213, 2007.

[74] Y. Zhang, M. D. Ilic, and O. Tonguz, "Application of support vector machine classification to enhanced protection relay logic in electric power grids," in *2007 Large Engineering Systems Conference on Power Engineering*, pp. 31–38, 2007.

[75] J. Faiz, S. Lotfi-fard, and S. H. Shahri, "Prony-based optimal bayes fault classification of overcurrent protection," *IEEE Transactions on Power Delivery*, vol. 22, no. 3, pp. 1326–1334, 2007.

[76] M. Farhadi and O. A. Mohammed, "A new protection scheme for multi-bus dc power systems using an event classification approach," in *2015 IEEE Industry Applications Society Annual Meeting*, pp. 1–7, 2015.

[77] Y. Zhang, J. Ma, J. Zhang, and Z. Wang, "Fault diagnosis based on cluster analysis theory in wide area backup protection system," in *2009 Asia-Pacific Power and Energy Engineering Conference*, pp. 1–4, 2009.

[78] Y. Wang, J. Jian, X. Zeng, and S. Liu, "Grounding faulted feeder protection in neutral noneffectively grounded distribution system based on hierarchical clustering technique," in *2011 International Conference on Advanced Power System Automation and Protection*, vol. 3, pp. 2128–2133, 2011.

[79] L. Kaufmann and P. Rousseeuw, "Clustering by means of medoids," *Data Analysis based on the L1-Norm and Related Methods*, pp. 405–416, 01 1987.

[80] L. Kaufman and P. Rousseeuw, *Finding Groups in Data: An Introduction to Cluster Analysis.* 09 2009.

[81] D. Arthur and S. Vassilvitskii, "K-means++: The advantages of careful seeding," vol. 8, pp. 1027–1035, 01 2007.

[82] M. Kezunovic, *Fundamentals of Power System Protection*, pp. 787–803. 12 2005.

[83] J.-H. Teng, "Unsymmetrical short-circuit fault analysis for weakly meshed distribution systems," *IEEE Transactions on Power Systems*, vol. 25, no. 1, pp. 96–105, 2010.

[84] V. Bapeswara Rao and K. Sankara Rao, "Computer aided coordination of directional relays: determination of break points," *IEEE Transactions on Power Delivery*, vol. 3, no. 2, pp. 545–548, 1988.

[85] Q. Yue, F. Lu, W. Yu, and J. Wang, "A novel algorithm to determine minimum break point set for optimum cooperation of directional protection relays in multiloop networks," *IEEE Transactions on Power Delivery*, vol. 21, no. 3, pp. 1114–1119, 2006.

[86] L. Jenkins, H. Khincha, S. Shivakumar, and P. Dash, "An application of functional dependencies to the topological analysis of protection schemes," *IEEE Transactions on Power Delivery*, vol. 7, no. 1, pp. 77–83, 1992.

[87] M. Ezzeddine, R. Kaczmarek, and U. Iftikhar, “Coordination of directional overcurrent relays using a novel method to select their settings,” *Generation, Transmission Distribution, IET*, vol. 5, pp. 743–750, 07 2011.

[88] A. Mahari and H. Seyedi, “An analytic approach for optimal coordination of overcurrent relays,” *IET Generation Transmission Distribution*, vol. 7, p. 674–680, 06 2013.

[89] D. Birla, R. P. Maheshwari, and H. O. Gupta, “An approach to tackle the threat of sympathy trips in directional overcurrent relay coordination,” *IEEE Transactions on Power Delivery*, vol. 22, no. 2, pp. 851–858, 2007.

[90] V. Prasad, K. Prakaso Rao, and A. Subba Rao, “Coordination of directional relays without generating all circuits,” *IEEE Transactions on Power Delivery*, vol. 6, no. 2, pp. 584–590, 1991.

[91] R. Mohammadi, H. A. Abyaneh, H. M. Rudsari, S. H. Fathi, and H. Rastegar, “Overcurrent relays coordination considering the priority of constraints,” *IEEE Transactions on Power Delivery*, vol. 26, no. 3, pp. 1927–1938, 2011.

[92] A. Urdaneta, H. Restrepo, S. Marquez, and J. Sanchez, “Coordination of directional overcurrent relay timing using linear programming,” *IEEE Transactions on Power Delivery*, vol. 11, no. 1, pp. 122–129, 1996.

[93] B. Chattopadhyay, M. Sachdev, and T. Sidhu, “An on-line relay coordination algorithm for adaptive protection using linear programming technique,” *IEEE Transactions on Power Delivery*, vol. 11, no. 1, pp. 165–173, 1996.

[94] T. Amraee, “Coordination of directional overcurrent relays using seeker algorithm,” *IEEE Transactions on Power Delivery*, vol. 27, no. 3, pp. 1415–1422, 2012.

[95] H. Zeienldin, E. El-Saadany, and M. Salama, "A novel problem formulation for directional overcurrent relay coordination," in *2004 Large Engineering Systems Conference on Power Engineering (IEEE Cat. No.04EX819)*, pp. 48–52, 2004.

[96] Y. Damchi, M. Dolatabadi, and H. Mashhadi, "Milp approach for optimal coordination of directional overcurrent relays in interconnected power systems," *Electric Power Systems Research*, vol. 158, pp. 267–274, 05 2018.

[97] D. Birla, R. Maheshwari, and H. Gupta, "A new nonlinear directional overcurrent relay coordination technique, and banes and boons of near-end faults based approach," *IEEE Transactions on Power Delivery*, vol. 21, no. 3, pp. 1176–1182, 2006.

[98] A. S. Noghabi, H. R. Mashhadi, and J. Sadeh, "Optimal coordination of directional overcurrent relays considering different network topologies using interval linear programming," *IEEE Transactions on Power Delivery*, vol. 25, no. 3, pp. 1348–1354, 2010.

[99] V. A. Papaspiliotopoulos, G. N. Korres, and N. G. Maratos, "A novel quadratically constrained quadratic programming method for optimal coordination of directional overcurrent relays," *IEEE Transactions on Power Delivery*, vol. 32, no. 1, pp. 3–10, 2017.

[100] K. A. Saleh, H. H. Zeineldin, A. Al-Hinai, and E. F. El-Saadany, "Optimal coordination of directional overcurrent relays using a new time–current–voltage characteristic," *IEEE Transactions on Power Delivery*, vol. 30, no. 2, pp. 537–544, 2015.

[101] F. Razavi, H. Abyaneh, M. Al-Dabbagh, R. Mohammadi, and H. Torkaman, "A new comprehensive genetic algorithm method for optimal overcurrent relays coordination," *Electric Power Systems Research*, vol. 78, pp. 713–720, 04 2008.

[102] M. M. Mansour, S. F. Mekhamer, and N. El-Kharbawe, "A modified particle swarm optimizer for the coordination of directional overcurrent relays," *IEEE Transactions on Power Delivery*, vol. 22, no. 3, pp. 1400–1410, 2007.

[103] A. Datta, D. Saha, and P. Das, "Optimal coordination of directional overcurrent relays in power systems using symbiotic organism search (sos) optimization technique," *IET Generation, Transmission Distribution*, vol. 10, 06 2016.

[104] A. Korashy, S. Kamel, A.-R. Youssef, and F. Jurado, "Modified water cycle algorithm for optimal direction overcurrent relays coordination," *Applied Soft Computing*, vol. 74, pp. 10–25, 01 2019.

[105] P. P. Bedekar and S. R. Bhide, "Optimum coordination of directional overcurrent relays using the hybrid ga-nlp approach," *IEEE Transactions on Power Delivery*, vol. 26, no. 1, pp. 109–119, 2011.

[106] J. Radosavljević and M. Jevtic, "Hybrid gsa-sqp algorithm for optimal coordination of directional overcurrent relays," *IET Generation Transmission Distribution*, vol. 10, p. 1928 – 1937, 05 2016.

[107] S. Srinivas and K. Swarup, "A hybrid ga — interval linear programming implementation for microgrid relay coordination considering different fault locations," pp. 785–790, 12 2017.

[108] G. Benmouyal, M. Meisinger, J. Burnworth, W. Elmore, K. Freirich, P. Kotos, P. Leblanc, P. Lerley, J. McConnell, J. Mizener, J. de Sa, R. Ramaswami, M. Sachdev, W. Strang, J. Waldron, S. Watansiriroch, and S. Zocholl, "IEEE standard inverse-time characteristic equations for overcurrent relays," *IEEE Transactions on Power Delivery*, vol. 14, pp. 868 – 872, 08 1999.

[109] S. T. P. Srinivas and K. Shanti Swarup, “A new mixed integer linear programming formulation for protection relay coordination using disjunctive inequalities,” *IEEE Power and Energy Technology Systems Journal*, vol. 6, no. 2, pp. 104–112, 2019.

[110] G. P. McCormick, “Computability of global solutions to factorable nonconvex programs: Part I – Convex underestimating problems,” *Mathematical Programming*, vol. 10, pp. 147–175, Dec 1976.

[111] H. Nagarajan, M. Lu, E. Yamangil, and R. Bent, “Tightening McCormick relaxations for nonlinear programs via dynamic multivariate partitioning,” in *Principles and Practice of Constraint Programming*, pp. 369–387, Springer, 2016.